



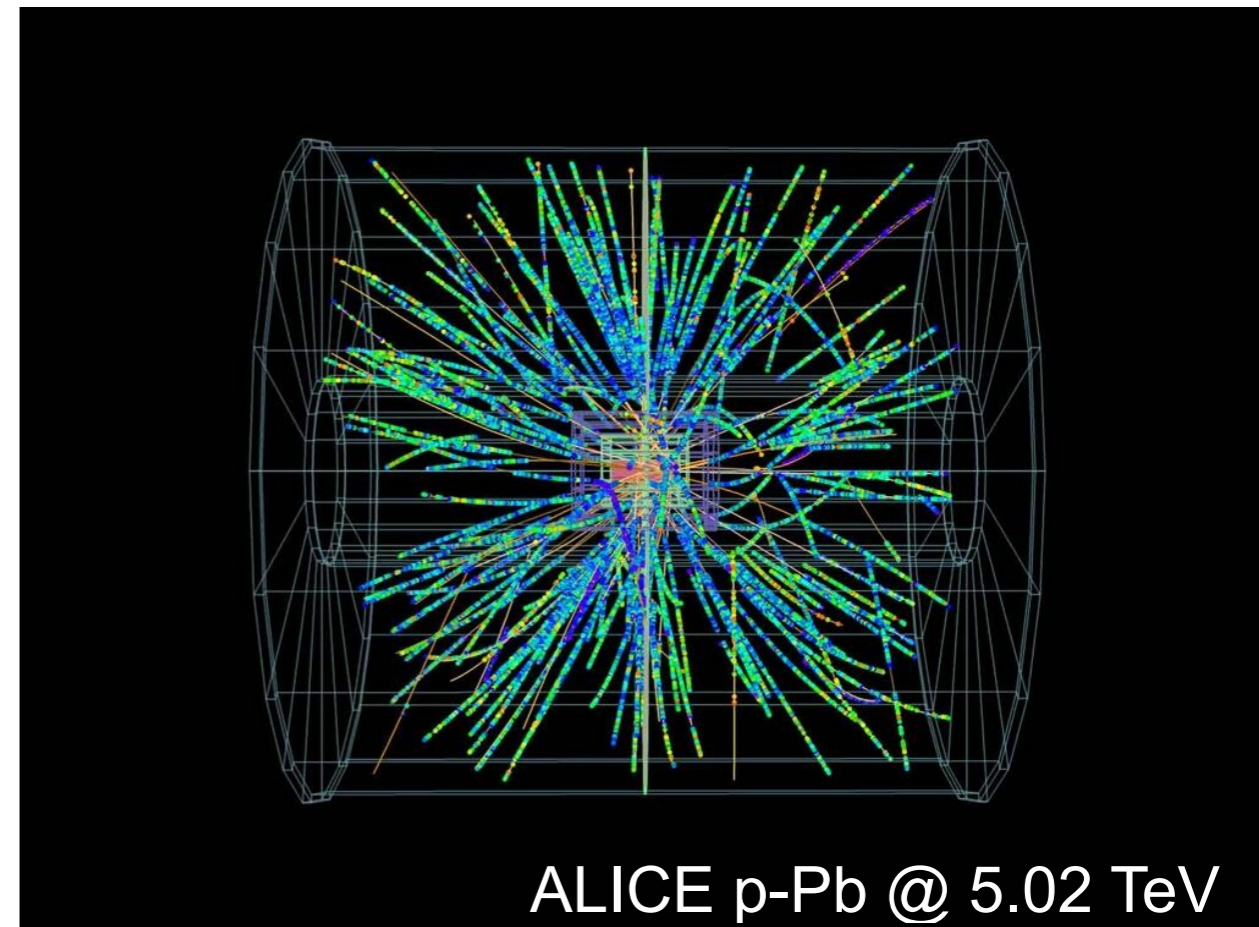
Phenomena in p-Pb collisions at the LHC

(ALICE, ATLAS, CMS, LHCb)

A. Kalweit, *CERN*

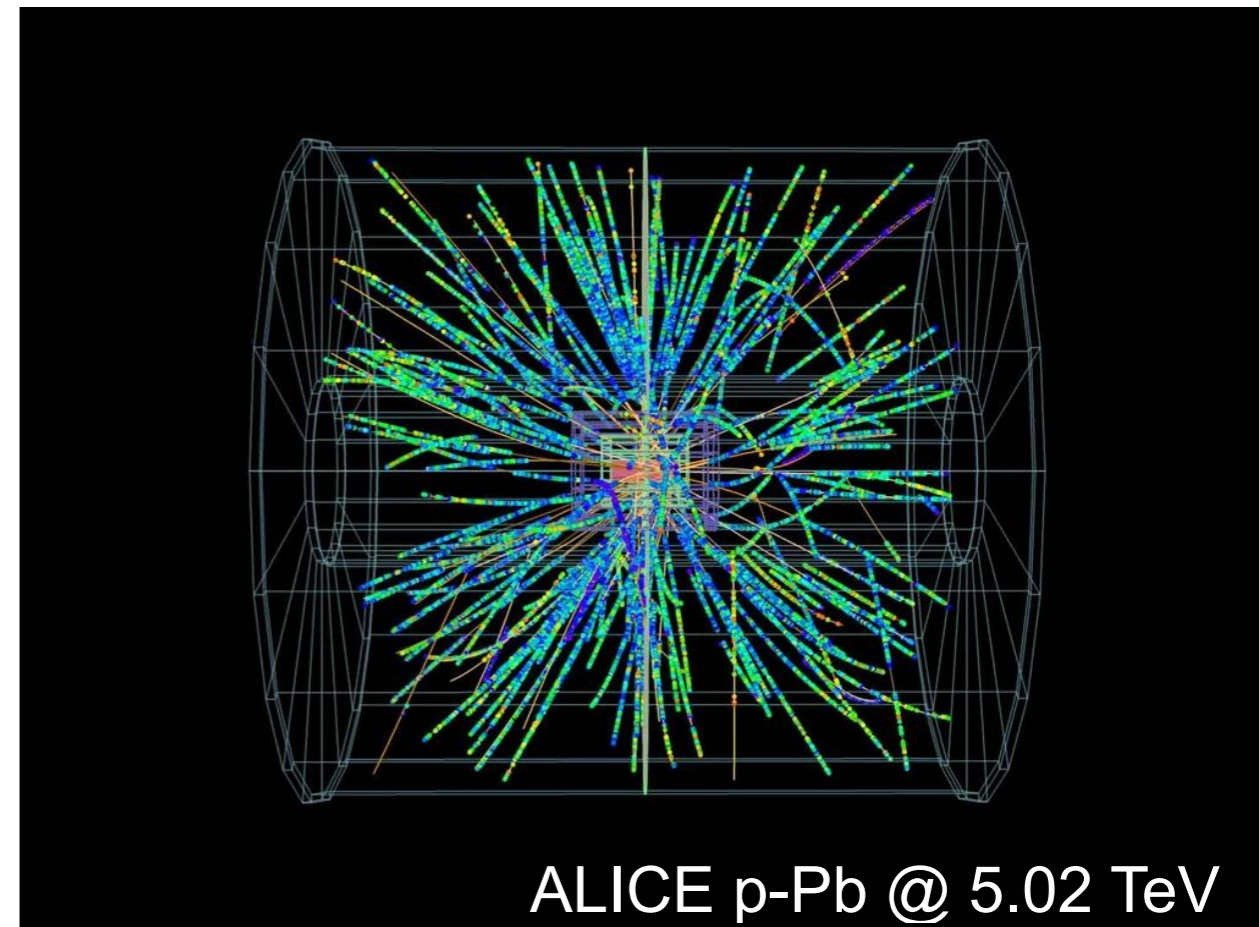
p-Pb running at the LHC

- September 2012 pilot run
 - 4h data taking
 - μb^{-1} per experiment
- January 2013 production run
 - 3 weeks data taking
 - 35 nb^{-1} delivered to ATLAS, CMS, and ALICE (1.6 nb^{-1} to LHCb)
 - beam reversal (p-Pb \leftrightarrow Pb-p)
- 4 TeV proton beam on 1.57 TeV/nucleon Pb beam
 - center of mass energy of 5.02 TeV per nucleon pair
 - center of mass per nucleon pair shifted by $\Delta y = 0.465$ in the direction of the proton beam



p-Pb running at the LHC

- September 2012 pilot run
 - 4h data taking
 - μb^{-1} per experiment
- January 2013 production run
 - 3 weeks data taking
 - 35 nb^{-1} delivered to ATLAS, CMS, and ALICE (1.6 nb^{-1} to LHCb)
 - beam reversal (p-Pb \leftrightarrow Pb-p)
- 4 TeV proton beam on 1.57 TeV/nucleon Pb beam
 - center of mass energy of 5.02 TeV per nucleon pair
 - center of mass per nucleon pair shifted by $\Delta y = 0.465$ in the direction of the proton beam



Many more interesting results from this data set are available than what can be presented in 20min. Only a biased selection can be shown in this talk...



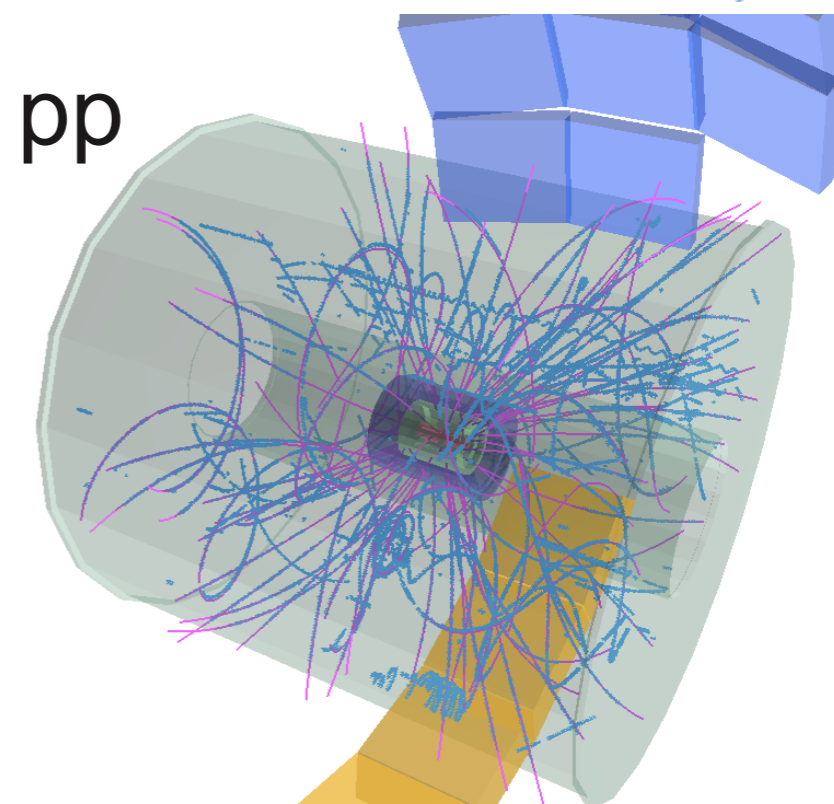
Why do we investigate p-Pb collisions?

- Traditional idea: reference for Pb-Pb collisions in order to investigate *cold nuclear matter effects*.
- However, the data turned out to be very interesting in itself:
 - Do we observe *collective effects* in a small system such as p-Pb collisions? Is there *hot matter* in local thermal equilibrium created?
 - Do we observe an *enhancement* of high- p_T particles with respect to pp collisions while we see a *suppression* in Pb-Pb collisions?
 - What can we learn from heavy flavor and electroweak bosons?

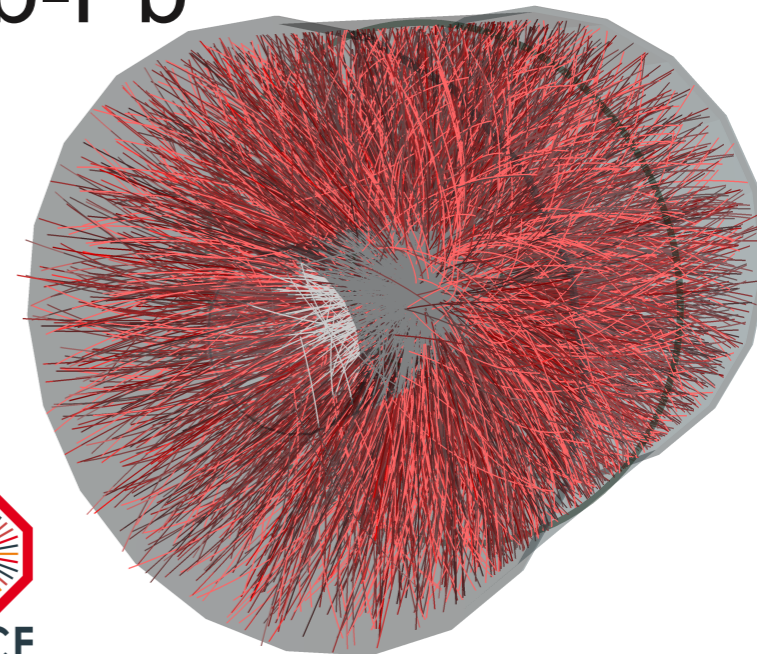
Collectivity and approach to equilibrium

Introduction — collectivity

- It is important to distinguish between
 - a *system of individual particles* and
 - a *medium* in which individual degrees of freedom do not matter anymore and we can apply thermodynamic concepts.
- Thermodynamic concepts are typically used for systems with large number of particles ($> 10^4$) particles in *local thermal equilibrium*.
 - central (0-5%) Pb-Pb collisions (LHC): $dN_{ch}/d\eta \approx 1600$
 - high mult. (0-5%) p-Pb collisions (LHC): $dN_{ch}/d\eta \approx 45$
 - pp collisions (LHC): $dN_{ch}/d\eta \approx 6$
- Lifetime of the system must be long enough so that equilibrium can be established by several (simulations about 3-6) interactions between its constituents.

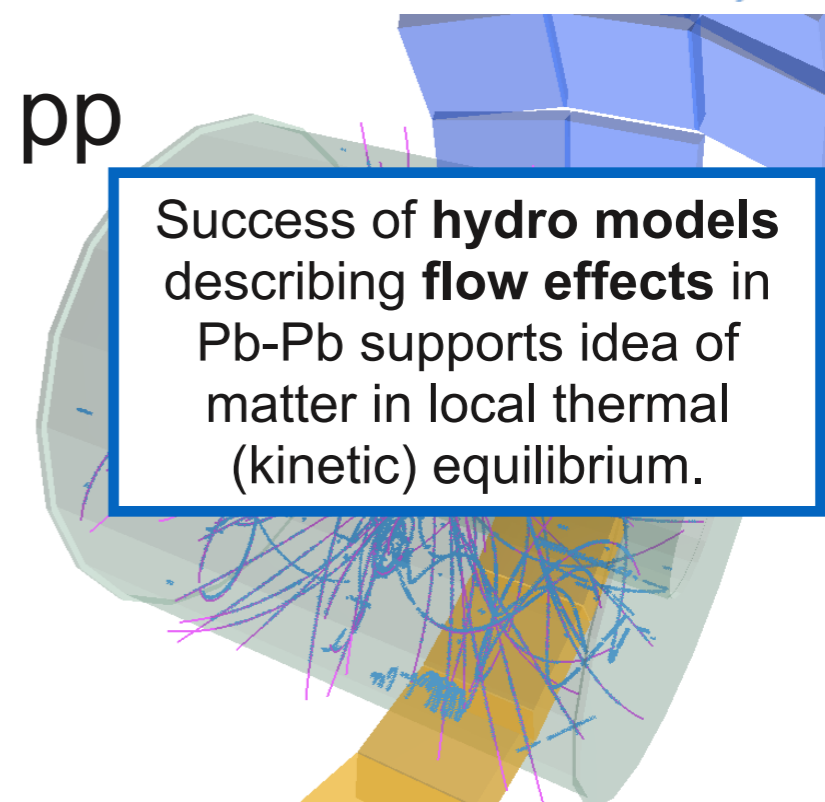


Pb-Pb

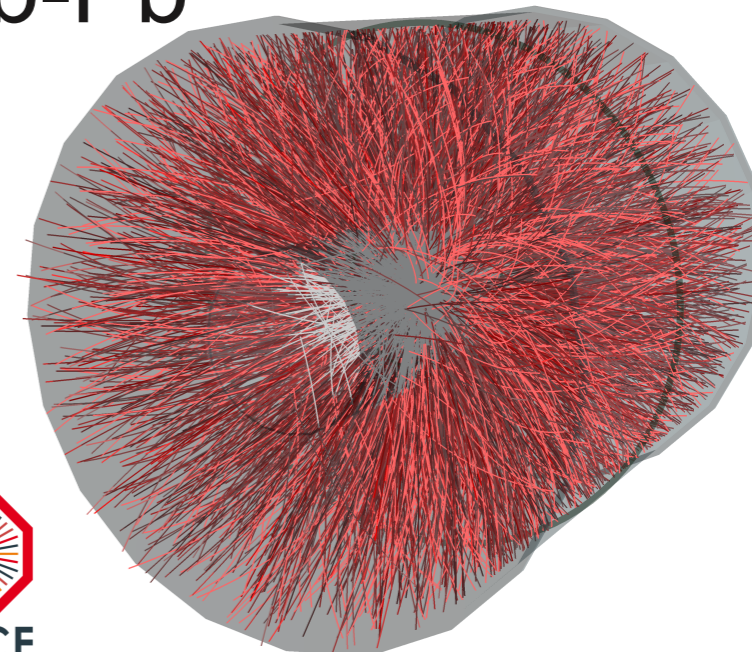


Introduction — collectivity

- It is important to distinguish between
 - a *system of individual particles* and
 - a *medium* in which individual degrees of freedom do not matter anymore and we can apply thermodynamic concepts.
- Thermodynamic concepts are typically used for systems with large number of particles ($> 10^4$) particles in *local thermal equilibrium*.
 - central (0-5%) Pb-Pb collisions (LHC): $dN_{ch}/d\eta \approx 1600$
 - high mult. (0-5%) p-Pb collisions (LHC): $dN_{ch}/d\eta \approx 45$
 - pp collisions (LHC): $dN_{ch}/d\eta \approx 6$
- Lifetime of the system must be long enough so that equilibrium can be established by several (simulations about 3-6) interactions between its constituents.



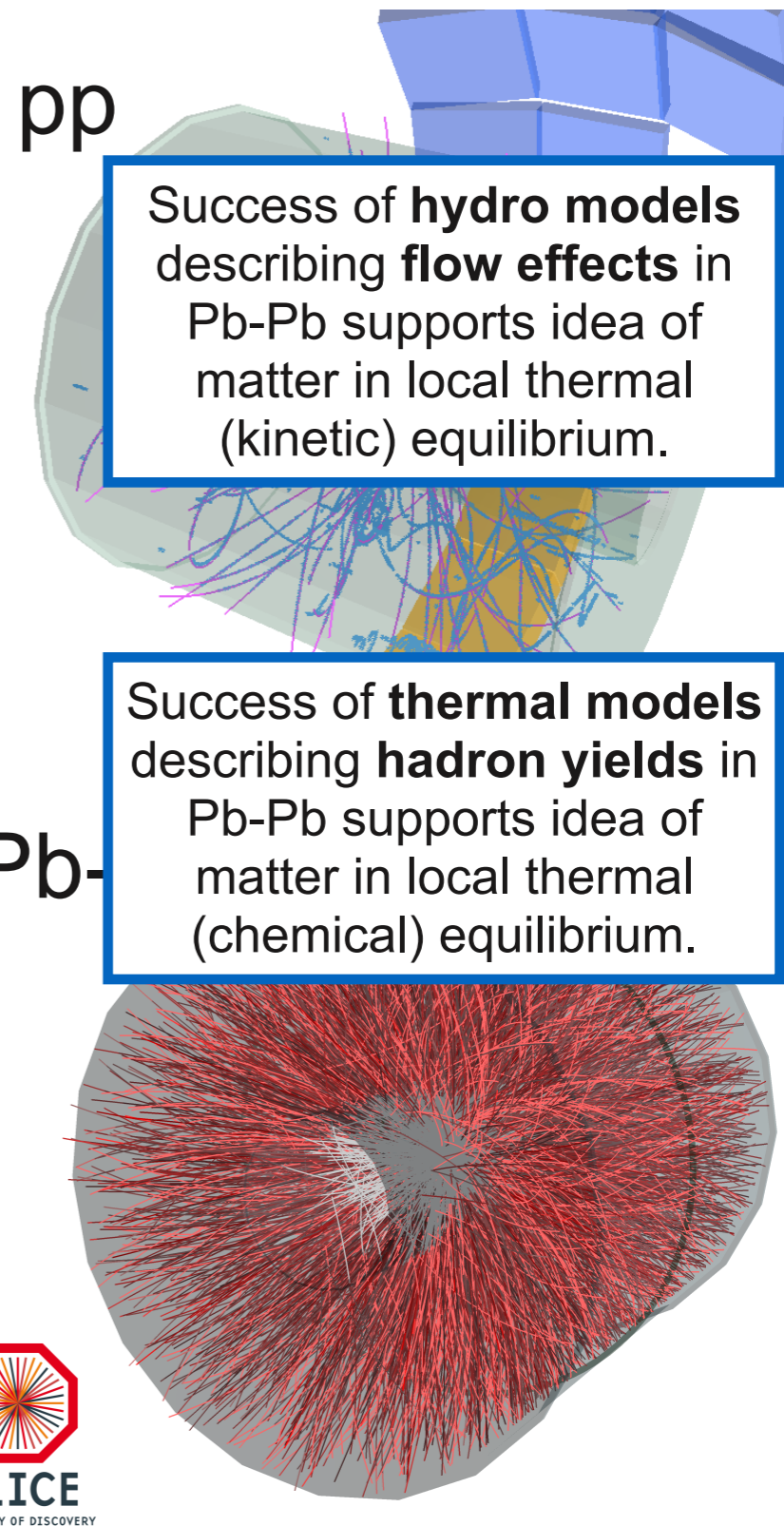
Pb-Pb



ALICE
A JOURNEY OF DISCOVERY

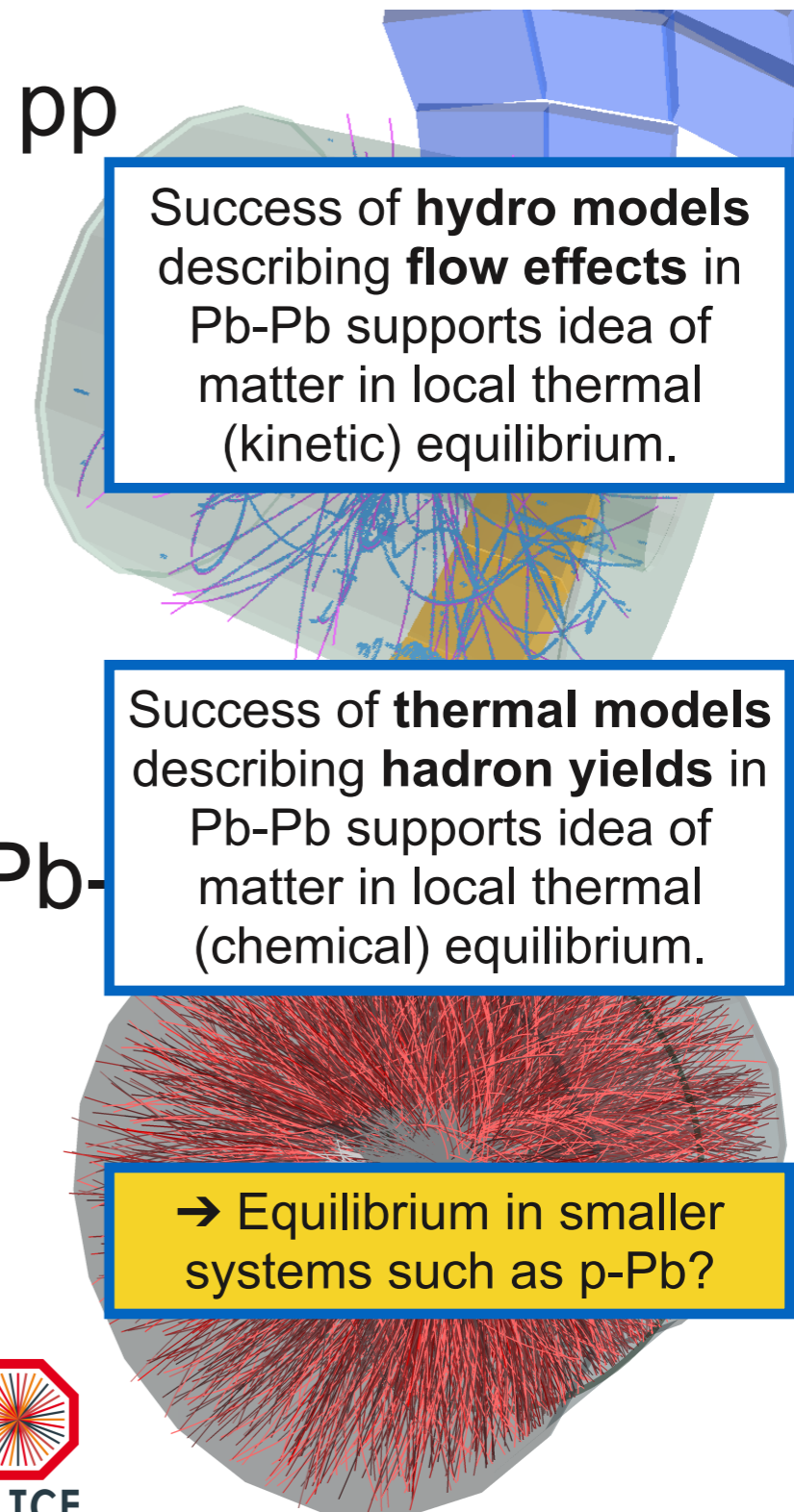
Introduction — collectivity

- It is important to distinguish between
 - a *system of individual particles* and
 - a *medium* in which individual degrees of freedom do not matter anymore and we can apply thermodynamic concepts.
- Thermodynamic concepts are typically used for systems with large number of particles ($> 10^4$) particles in *local thermal equilibrium*.
 - central (0-5%) Pb-Pb collisions (LHC): $dN_{ch}/d\eta \approx 1600$
 - high mult. (0-5%) p-Pb collisions (LHC): $dN_{ch}/d\eta \approx 45$
 - pp collisions (LHC): $dN_{ch}/d\eta \approx 6$
- Lifetime of the system must be long enough so that equilibrium can be established by several (simulations about 3-6) interactions between its constituents.



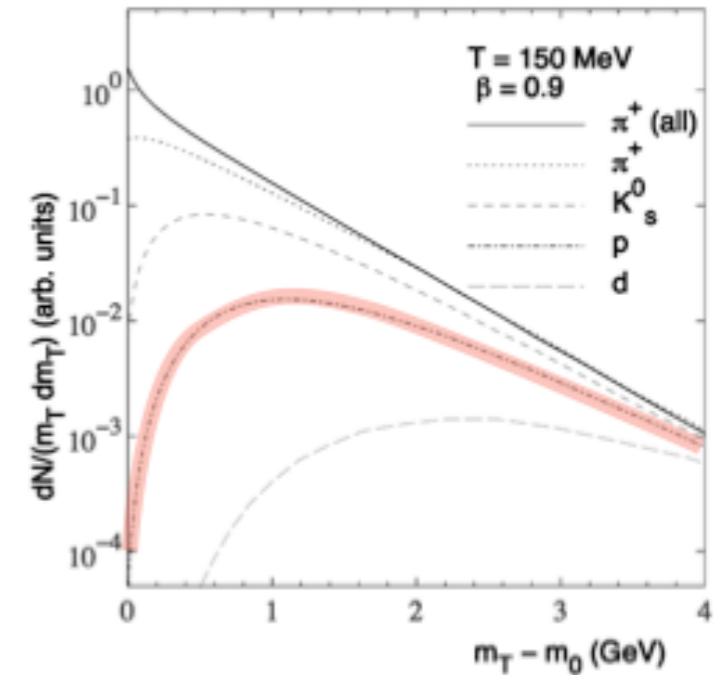
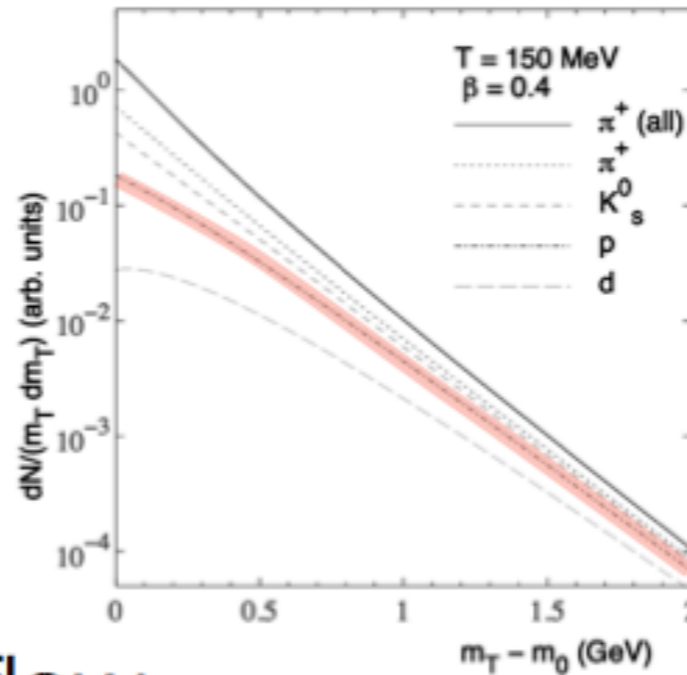
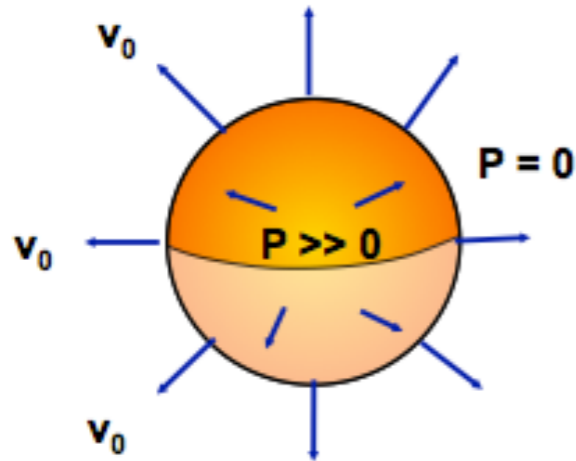
Introduction — collectivity

- It is important to distinguish between
 - a *system of individual particles* and
 - a *medium* in which individual degrees of freedom do not matter anymore and we can apply thermodynamic concepts.
- Thermodynamic concepts are typically used for systems with large number of particles ($> 10^4$) particles in *local thermal equilibrium*.
 - central (0-5%) Pb-Pb collisions (LHC): $dN_{ch}/d\eta \approx 1600$
 - high mult. (0-5%) p-Pb collisions (LHC): $dN_{ch}/d\eta \approx 45$
 - pp collisions (LHC): $dN_{ch}/d\eta \approx 6$
- Lifetime of the system must be long enough so that equilibrium can be established by several (simulations about 3-6) interactions between its constituents.



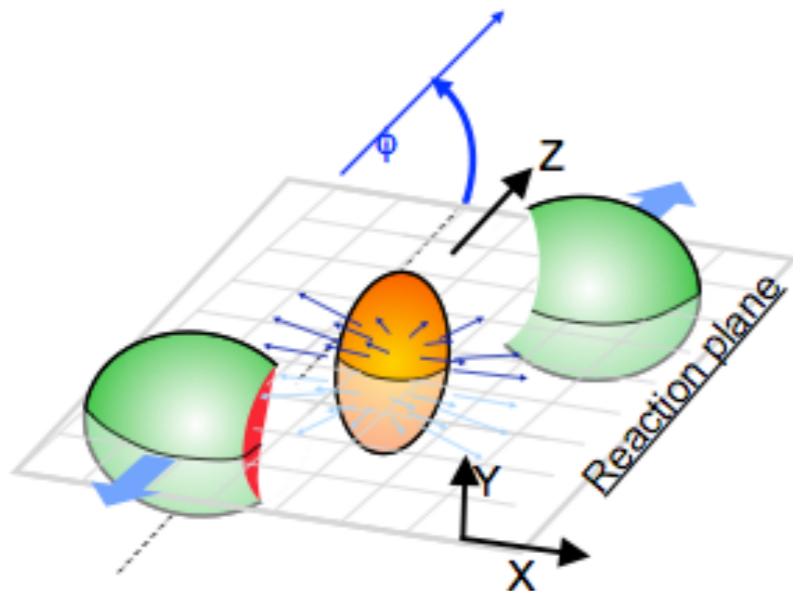
Radial and elliptic flow

Isotropic radial flow

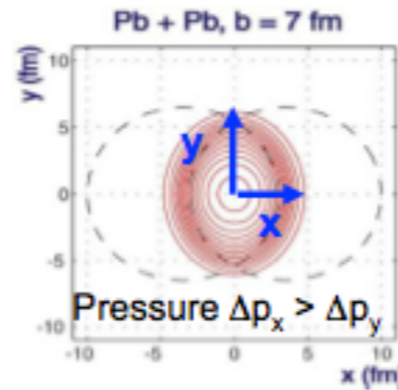


Anisotropic (elliptic) flow

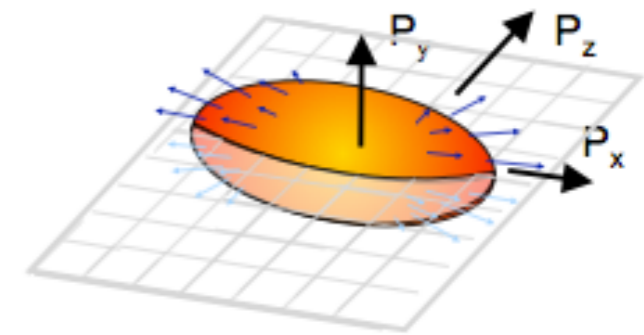
Spatial deformation



Azimuthal (φ) pressure gradients



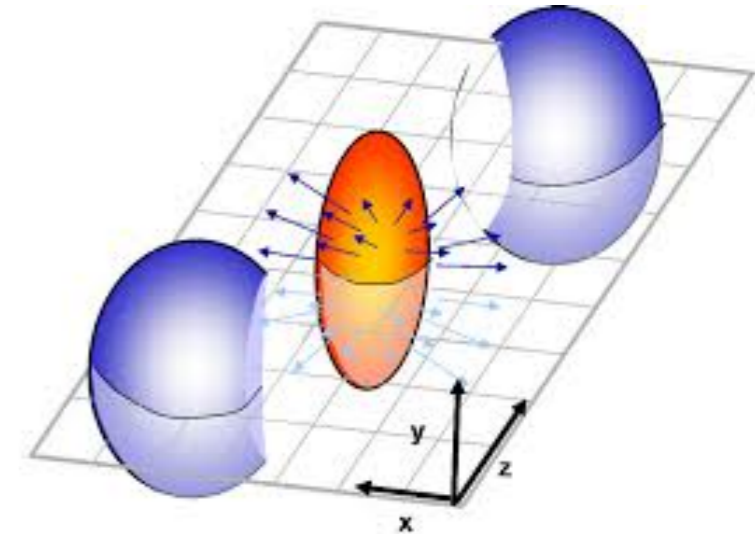
[hep-ph/0407360]
Anisotropic particle density



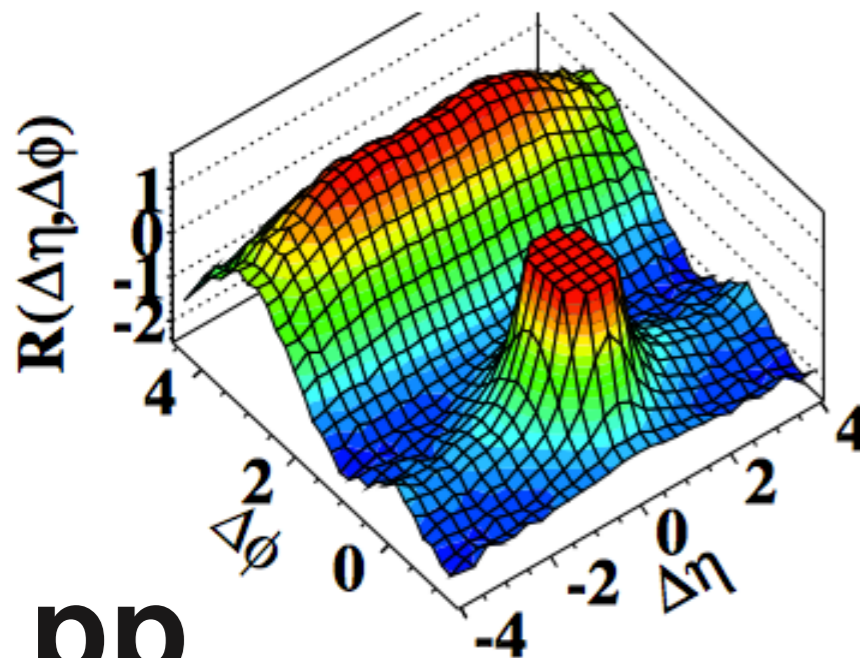
$$\frac{dN}{d\varphi} \propto 1 + 2v_1 \cos[\varphi - \Psi_1] + 2v_2 \cos[2(\varphi - \Psi_2)] + 2v_3 \cos[3(\varphi - \Psi_3)] + \dots$$

Angular correlations and double ridge (1)

- Di-Hadron correlations study anisotropies in the particle production on event-by-event basis.
- In Pb-Pb collisions, they are associated with elliptic flow resulting from the *hydrodynamical expansion* of the system and the initial collision geometry.

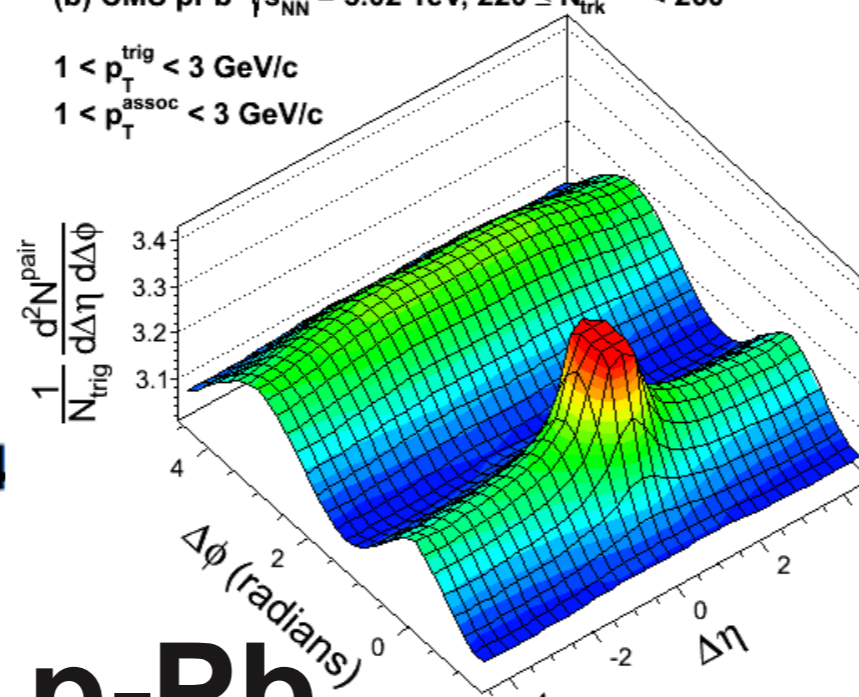


[1009.4122]

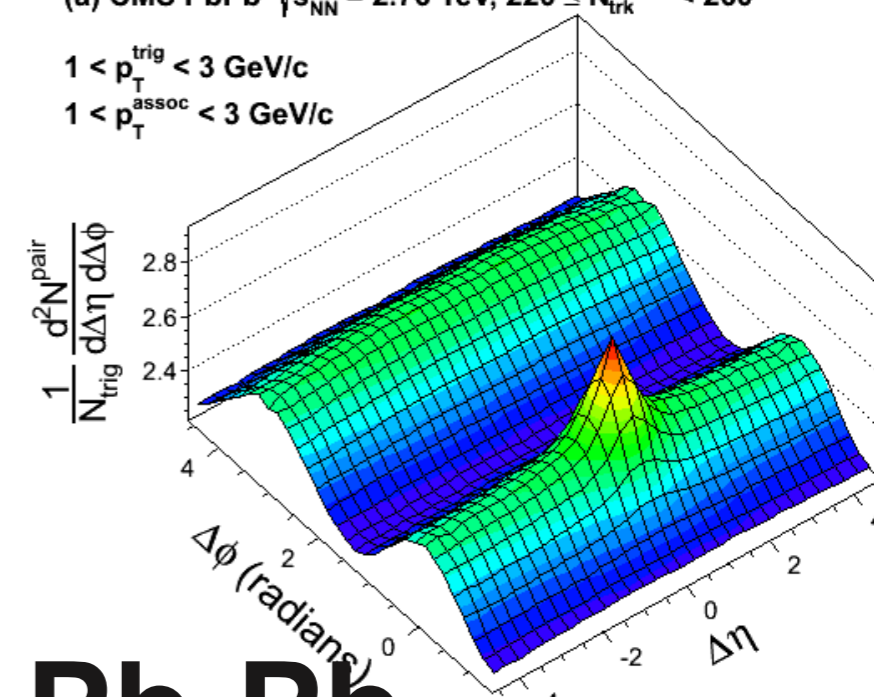
(d) CMS $N \geq 110$, $1.0 \text{ GeV}/c < p_T < 3.0 \text{ GeV}/c$ 

pp

[1210.5482]

(b) CMS pPb $\sqrt{s_{NN}} = 5.02 \text{ TeV}$, $220 \leq N_{\text{trk}}^{\text{offline}} < 260$
 $1 < p_T^{\text{trig}} < 3 \text{ GeV}/c$
 $1 < p_T^{\text{assoc}} < 3 \text{ GeV}/c$


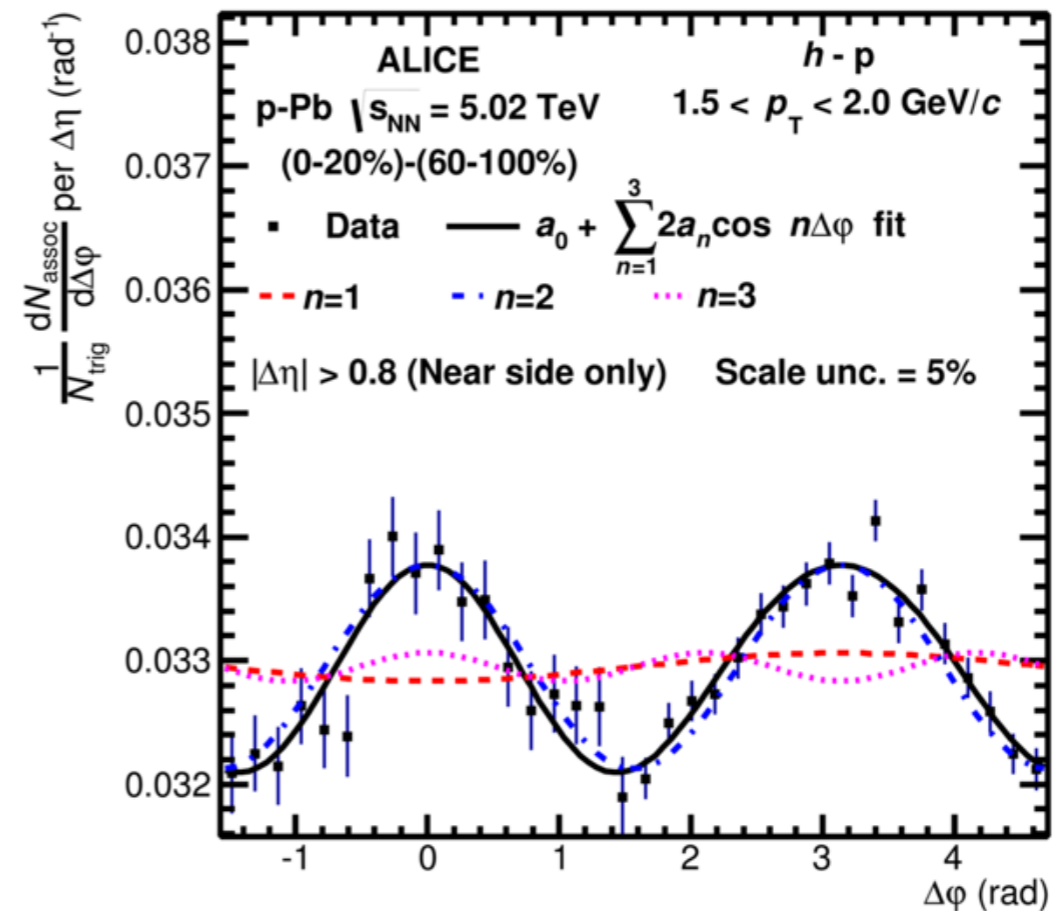
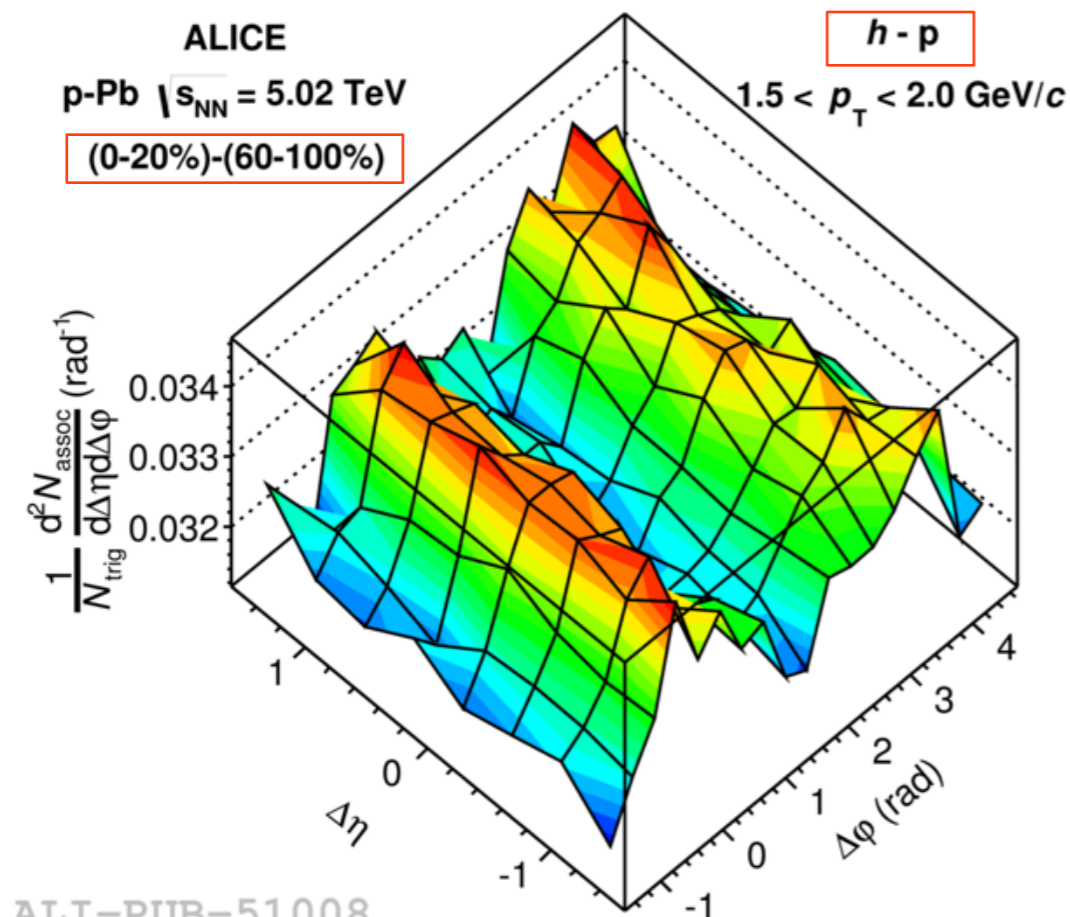
p-Pb

(a) CMS PbPb $\sqrt{s_{NN}} = 2.76 \text{ TeV}$, $220 \leq N_{\text{trk}}^{\text{offline}} < 260$
 $1 < p_T^{\text{trig}} < 3 \text{ GeV}/c$
 $1 < p_T^{\text{assoc}} < 3 \text{ GeV}/c$


Pb-Pb

Angular correlations and double ridge (2)

- Triggered further measurements from ATLAS, CMS, ALICE...
- From the high-multiplicity yield subtract the jet yield obtained in low-multiplicity events (no ridge) → double ridge.
- Correlations of non-identified and also identified particles.
- Azimuthal projection is decomposed into Fourier components: v_2 and v_3 dominant

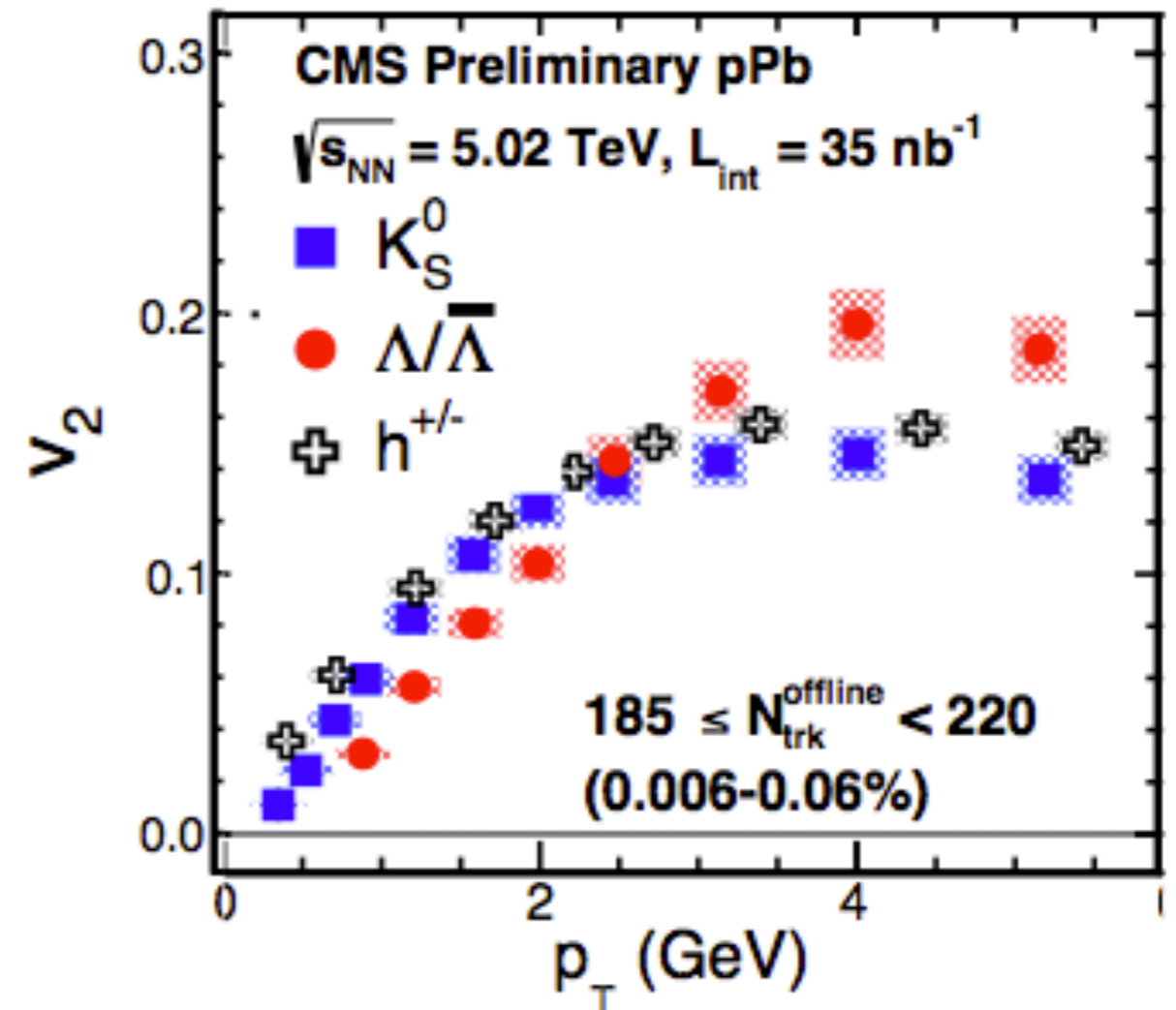
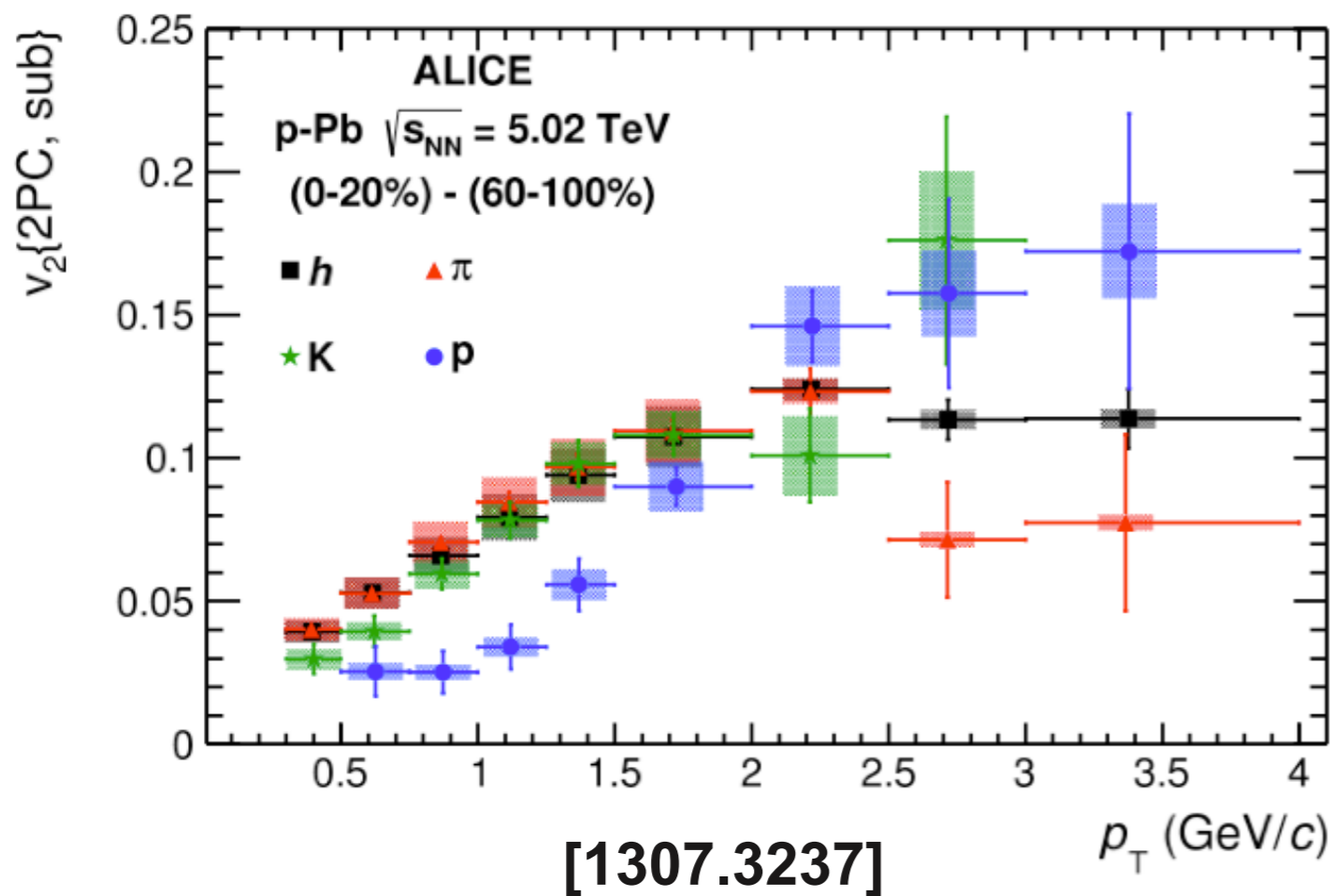


[1307.3237]

Angular correlations and double ridge (3)

- Mass ordering observed by ALICE and CMS
→ reminiscent of Pb-Pb phenomenology
- as expected from hydrodynamic behavior: $p = \beta\gamma \cdot m$

[CMS-HIN-14-002]

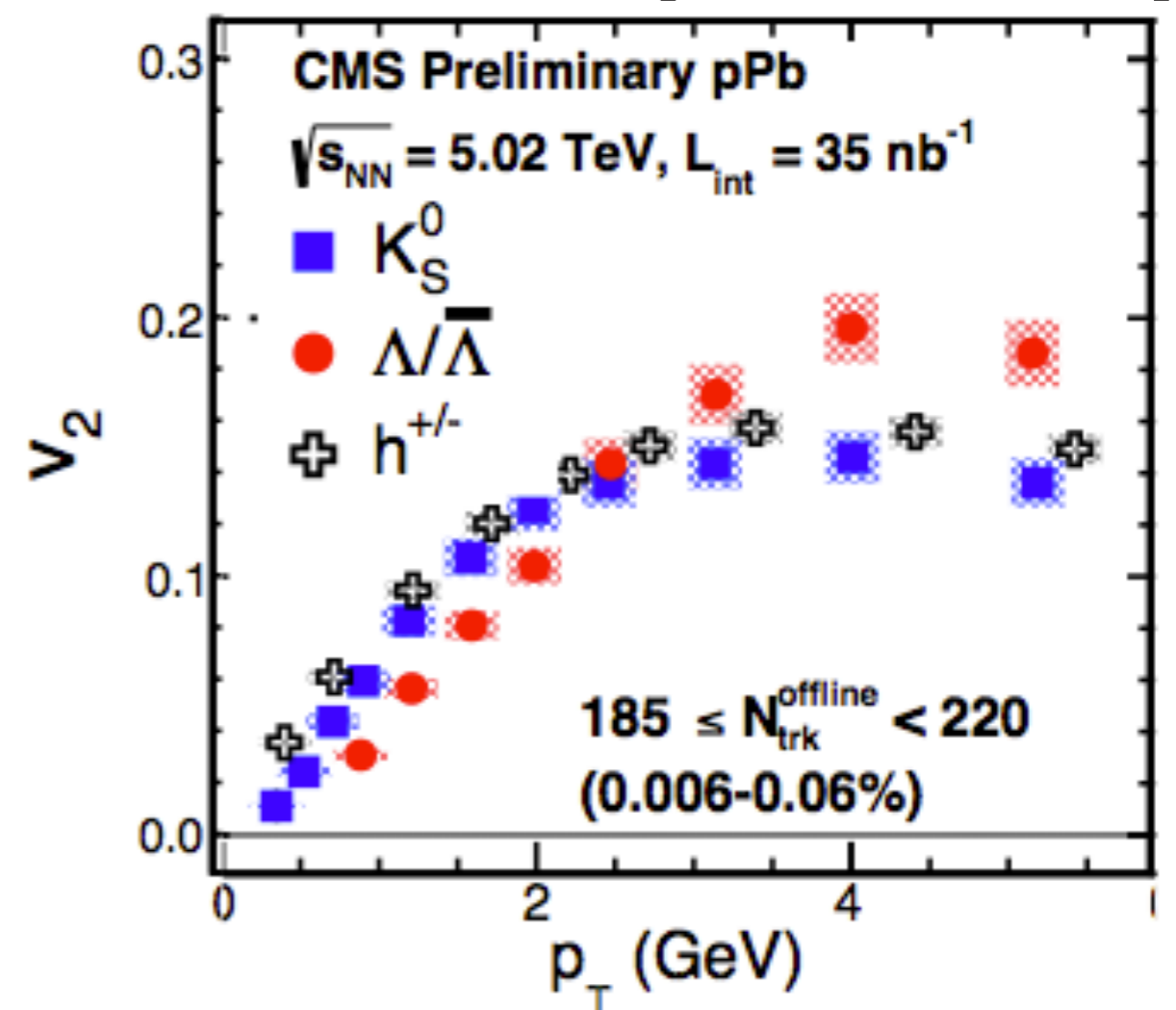
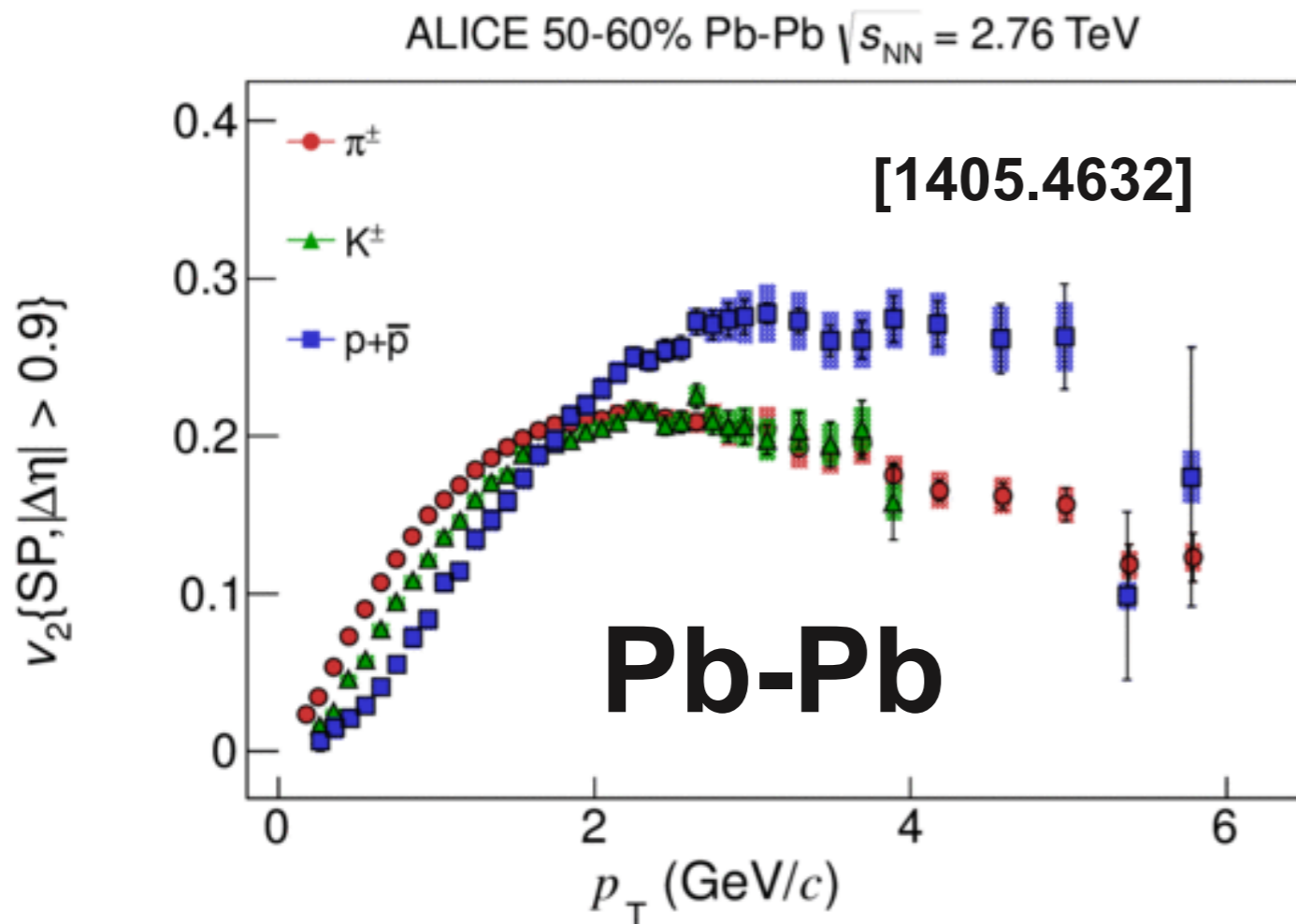


CMS: no subtraction of peripheral events!

Angular correlations and double ridge (3)

- Mass ordering observed by ALICE and CMS
→ reminiscent of Pb-Pb phenomenology
- as expected from hydrodynamic behavior: $p = \beta\gamma \cdot m$

[CMS-HIN-14-002]



CMS: no subtraction of peripheral events!



Multiparticle correlations

- Confirms the previous picture with an alternative method.
- v_2 stays large when calculated with multi-particle correlations (different sensitivity to non-flow effects!).
- $c_2\{4\} < 0$ above $N_{ch} > 80 \rightarrow v_2$ becomes real

$$\langle 2 \rangle = \langle e^{in(\phi_1 - \phi_2)} \rangle$$

$$\langle 4 \rangle = \langle e^{in(\phi_1 + \phi_2 - \phi_3 - \phi_4)} \rangle$$

$$c_n\{2\} = \langle \langle 2 \rangle \rangle$$

$$c_n\{4\} = \langle \langle 4 \rangle \rangle - 2\langle \langle 2 \rangle \rangle^2$$

$$c_n\{6\} = \langle \langle 6 \rangle \rangle - 9\langle \langle 4 \rangle \rangle \langle \langle 2 \rangle \rangle + 12\langle \langle 2 \rangle \rangle^3$$

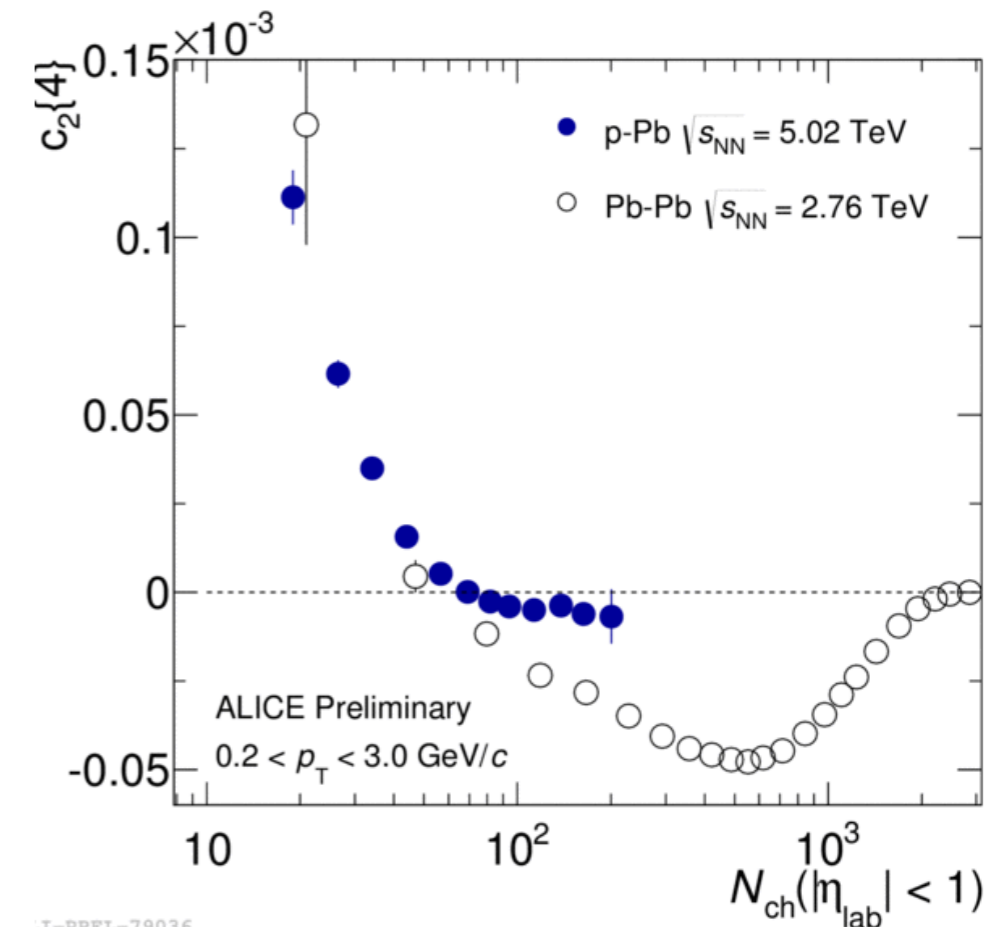
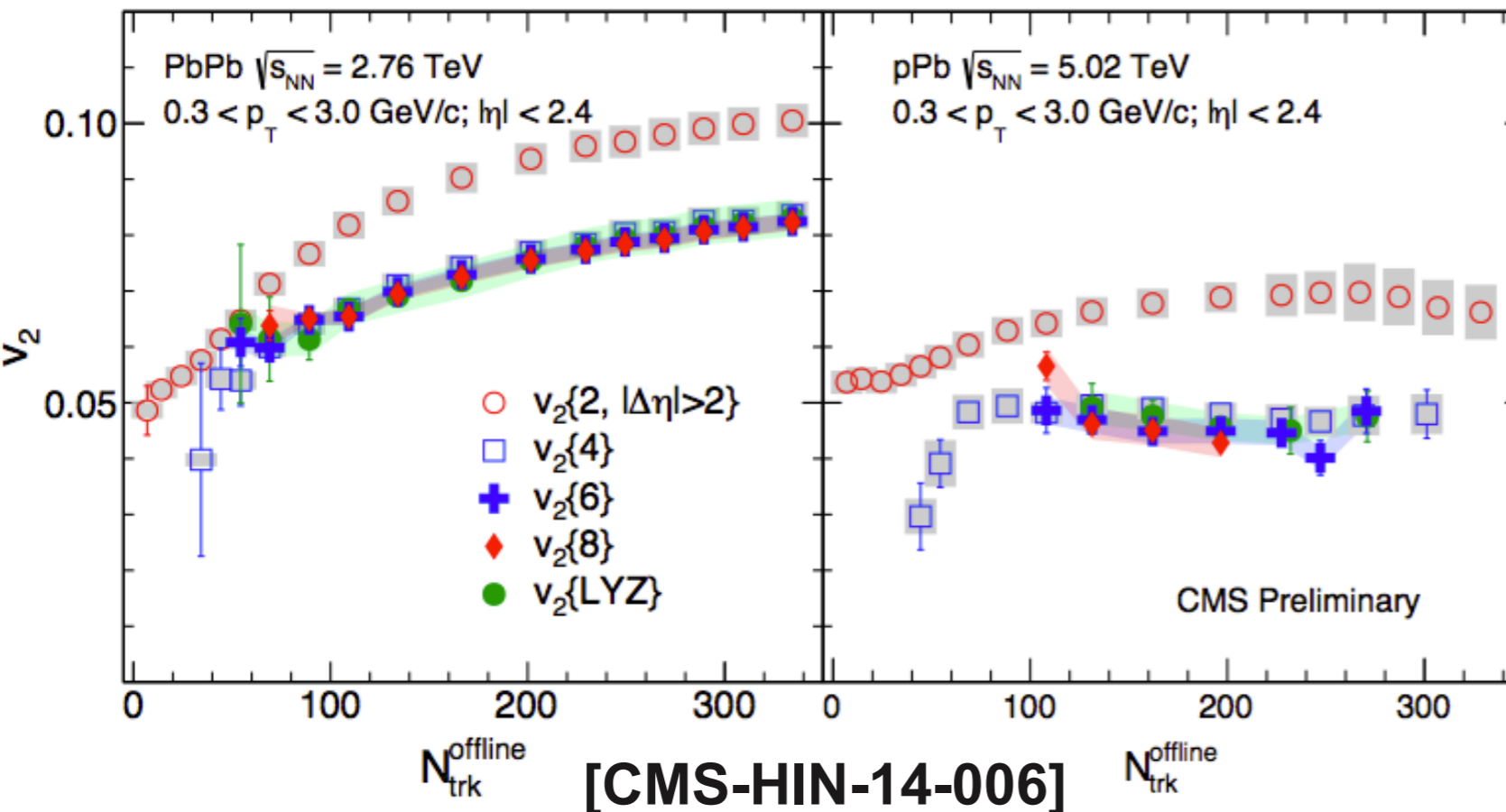
$$v_n\{2\} = \sqrt{c_n\{2\}}$$

$$v_n\{4\} = \sqrt[4]{-c_n\{4\}}$$

$$v_n\{6\} = \sqrt[6]{\frac{1}{4}c_n\{6\}}$$

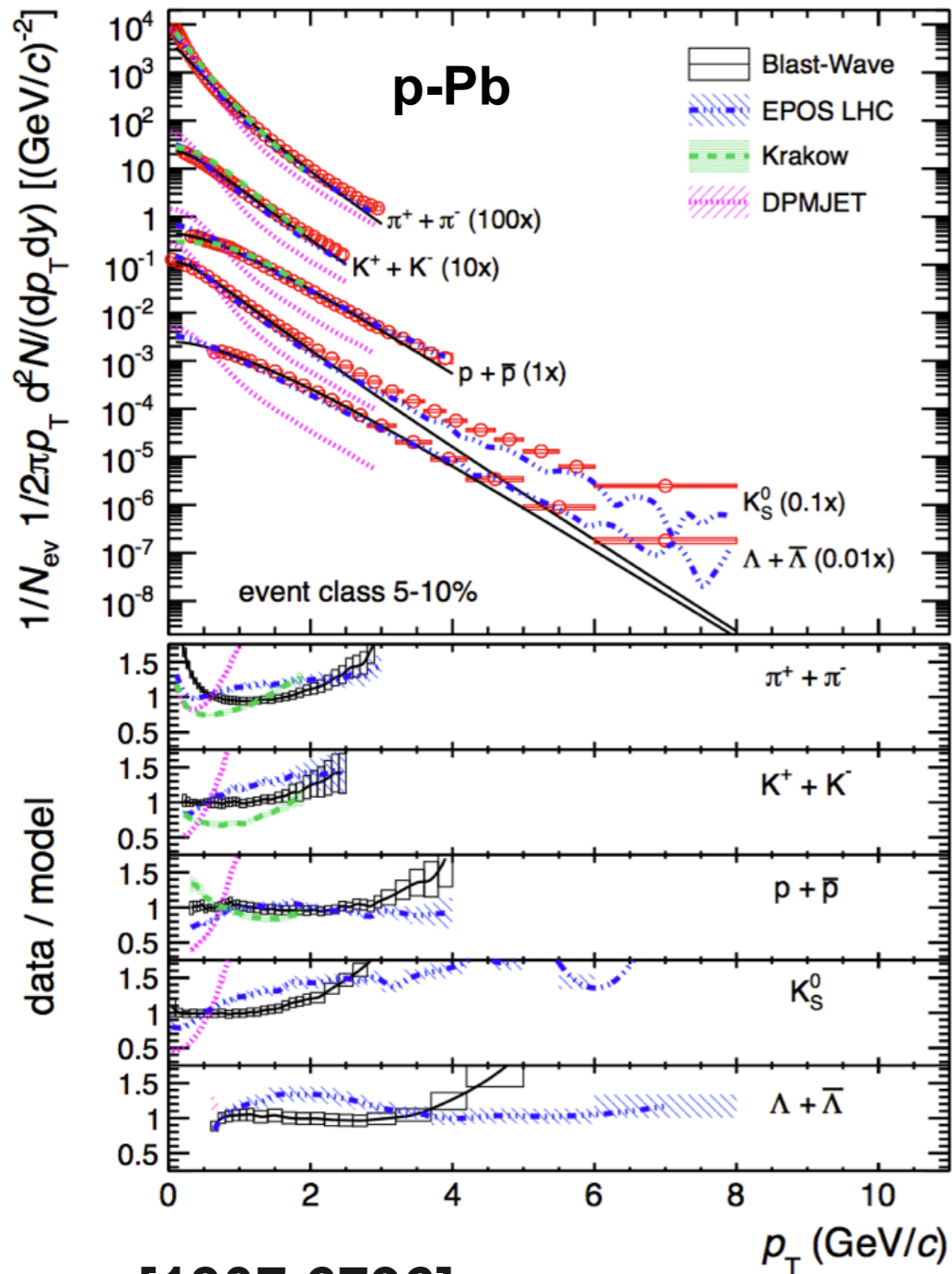
Pb-Pb

p-Pb



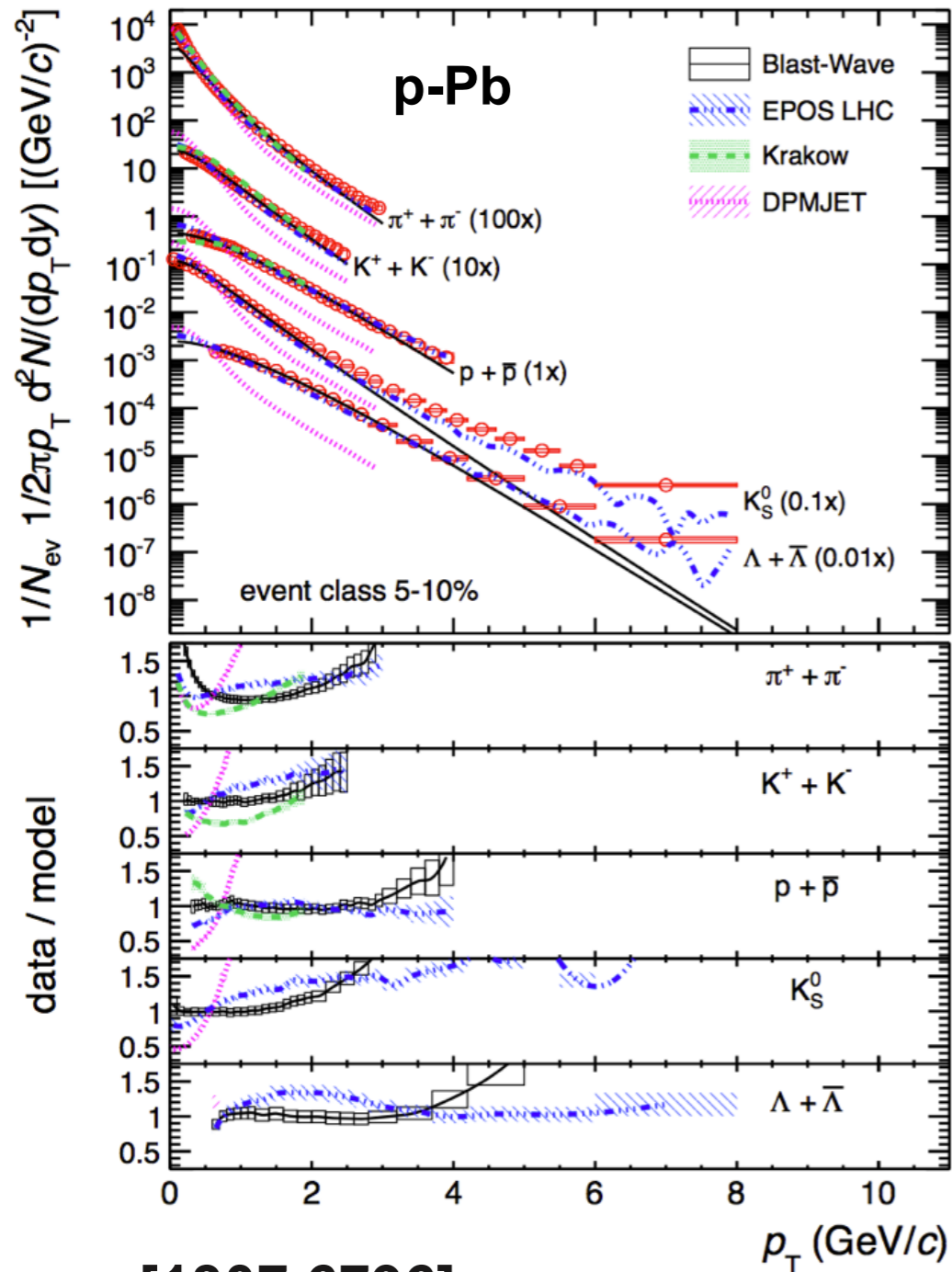
.I-PREL-79036

p_T -Spectra — radial flow?



[1307.6796]

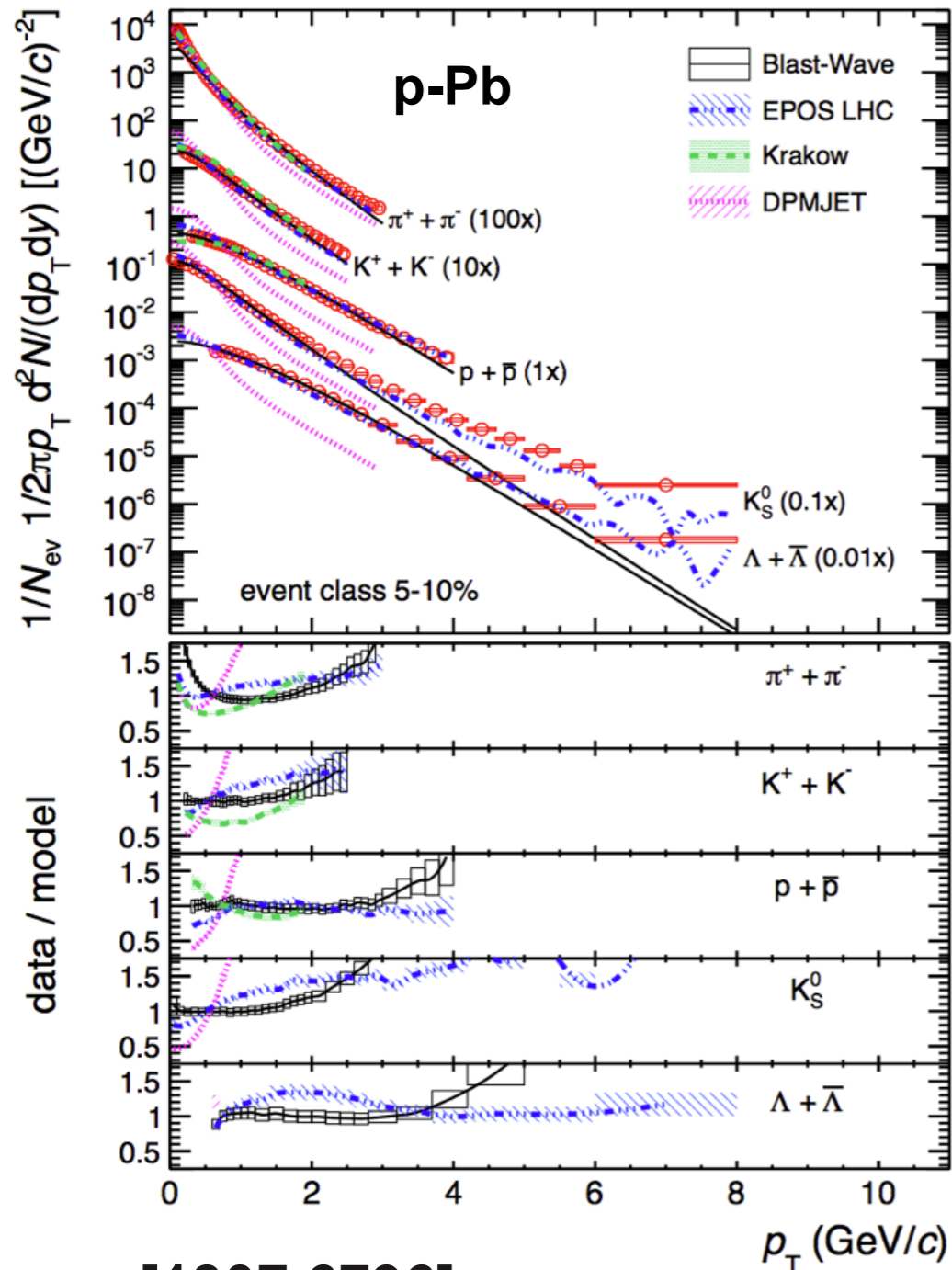
p_T -Spectra — radial flow?



[1307.6796]

Hydrodynamic models (EPOS, Krakow) show a better agreement than QCD inspired models (DPMJET).

p_T -Spectra — radial flow?

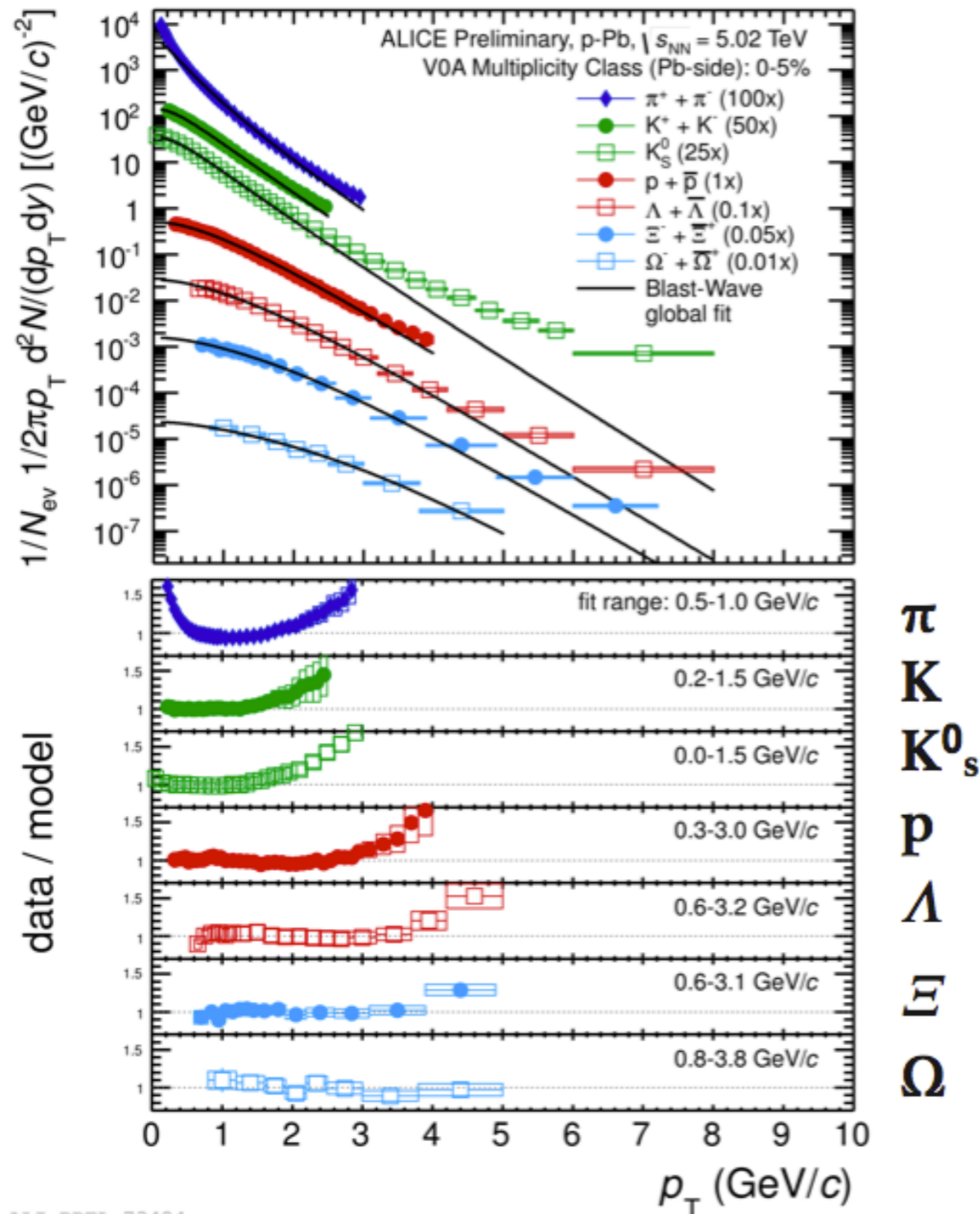


[1307.6796]

Hydrodynamic models (EPOS, Krakow) show a better agreement than QCD inspired models (DPMJET).

A combined blast-wave fit to the data (**simplified hydro model** $\rightarrow T_{kin}, \beta$) gives a reasonable description.

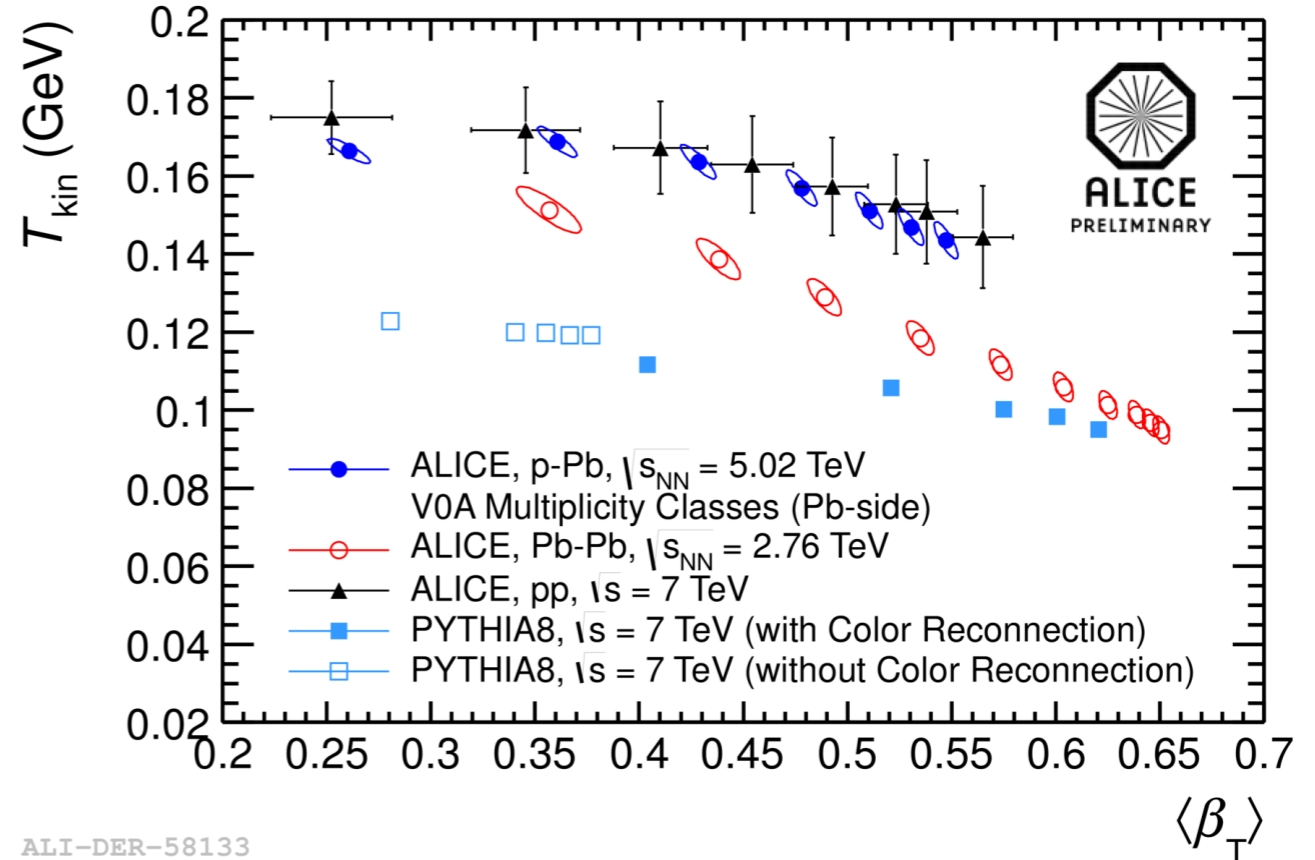
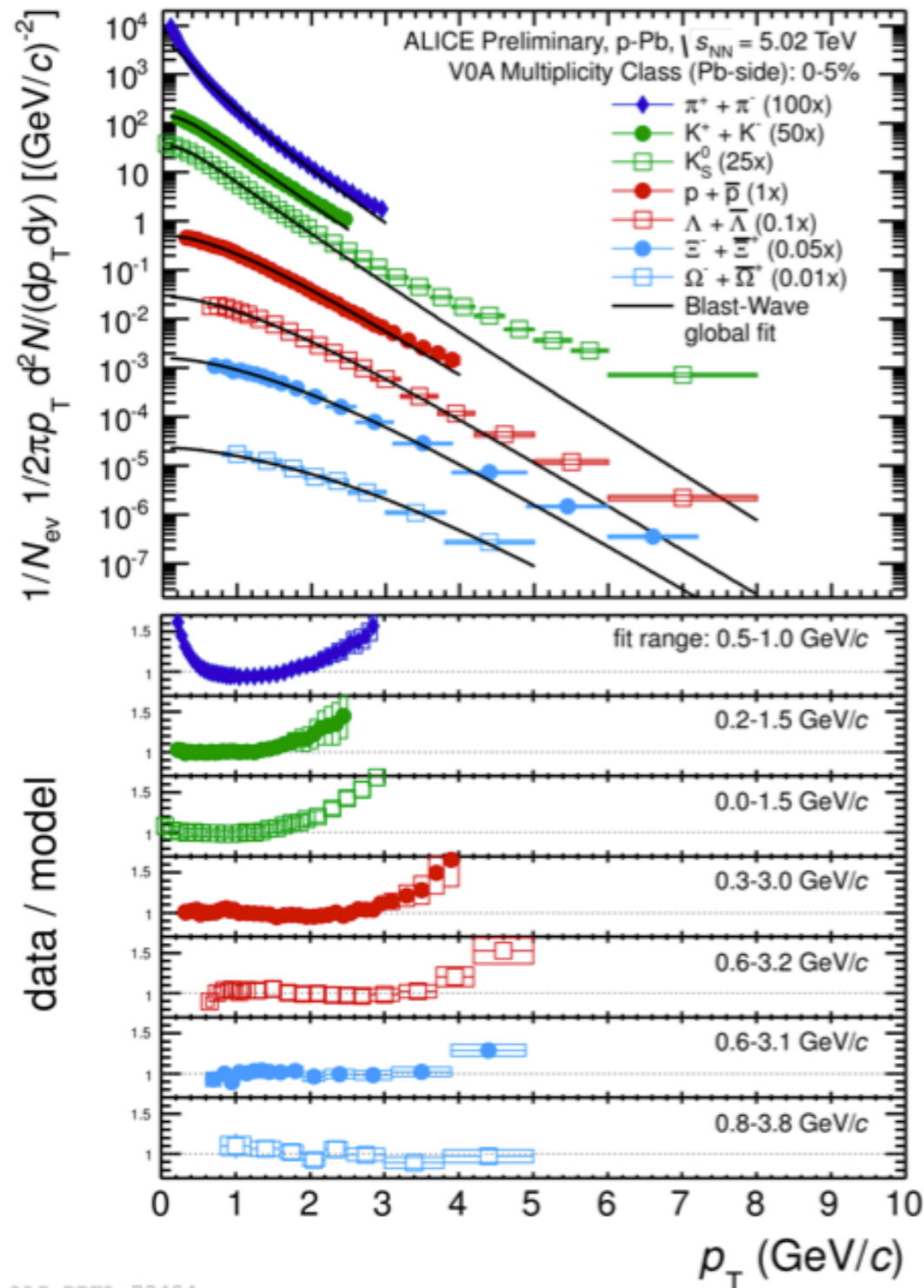
p_T -Spectra — radial flow?



Hydrodynamic models (EPOS, Krakow) show a better agreement than QCD inspired models (DPMJET).

A combined blast-wave fit to the data (**simplified hydro model** $\rightarrow T_{kin}, \beta$) gives a reasonable description.

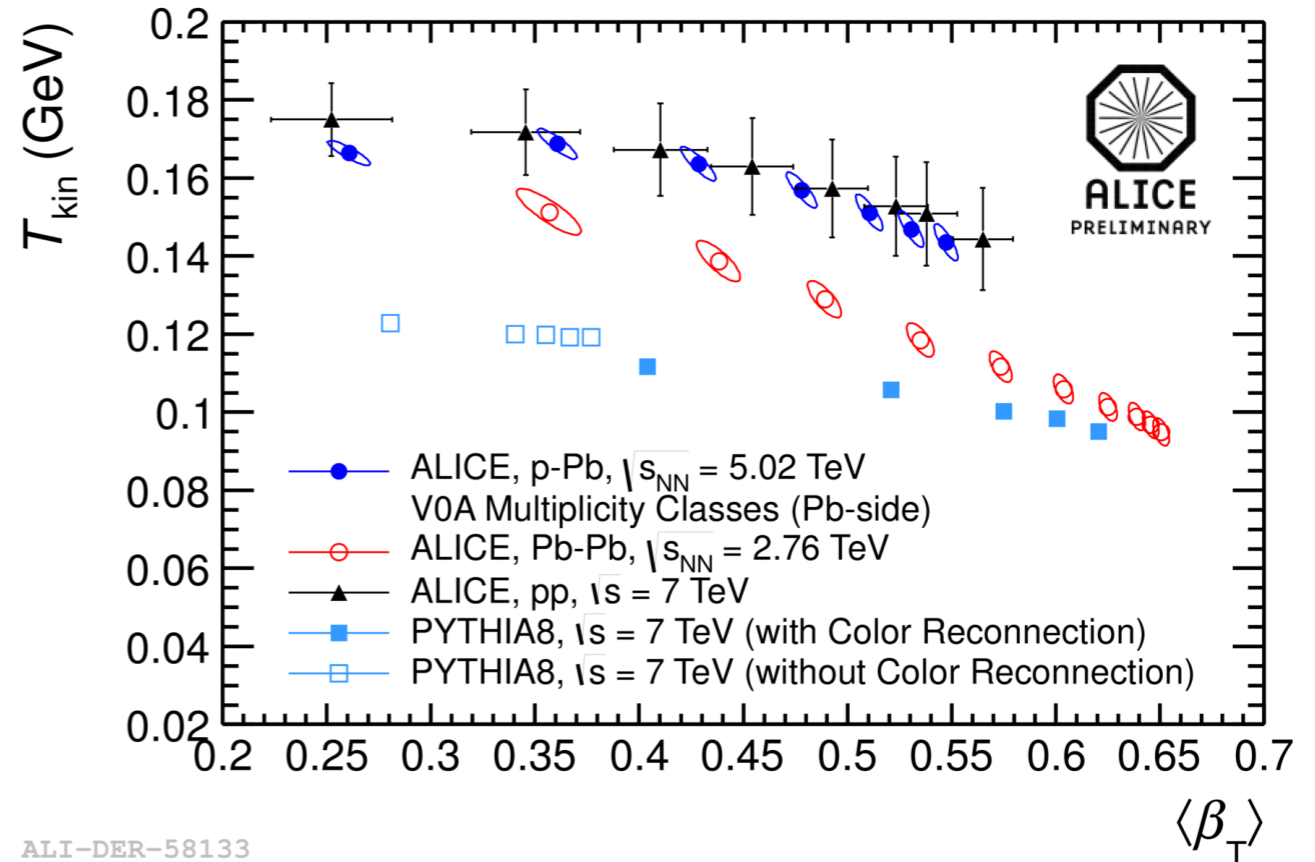
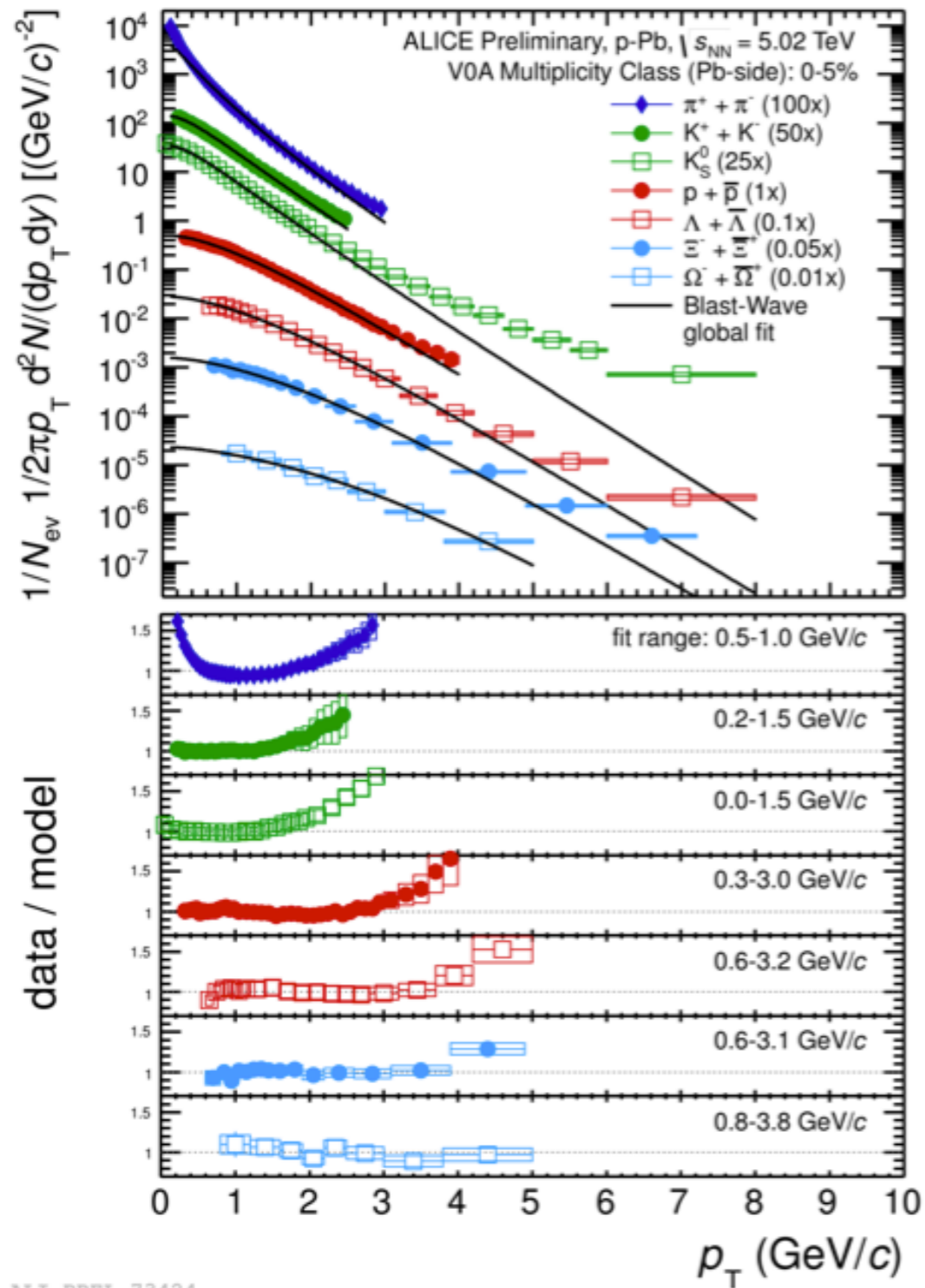
p_T -Spectra — radial flow?



Hydrodynamic models (EPOS, Krakow) show a better agreement than QCD inspired models (DPMJET).

A combined blast-wave fit to the data (**simplified hydro model** $\rightarrow T_{kin}, \beta$) gives a reasonable description.

p_T -Spectra — radial flow?



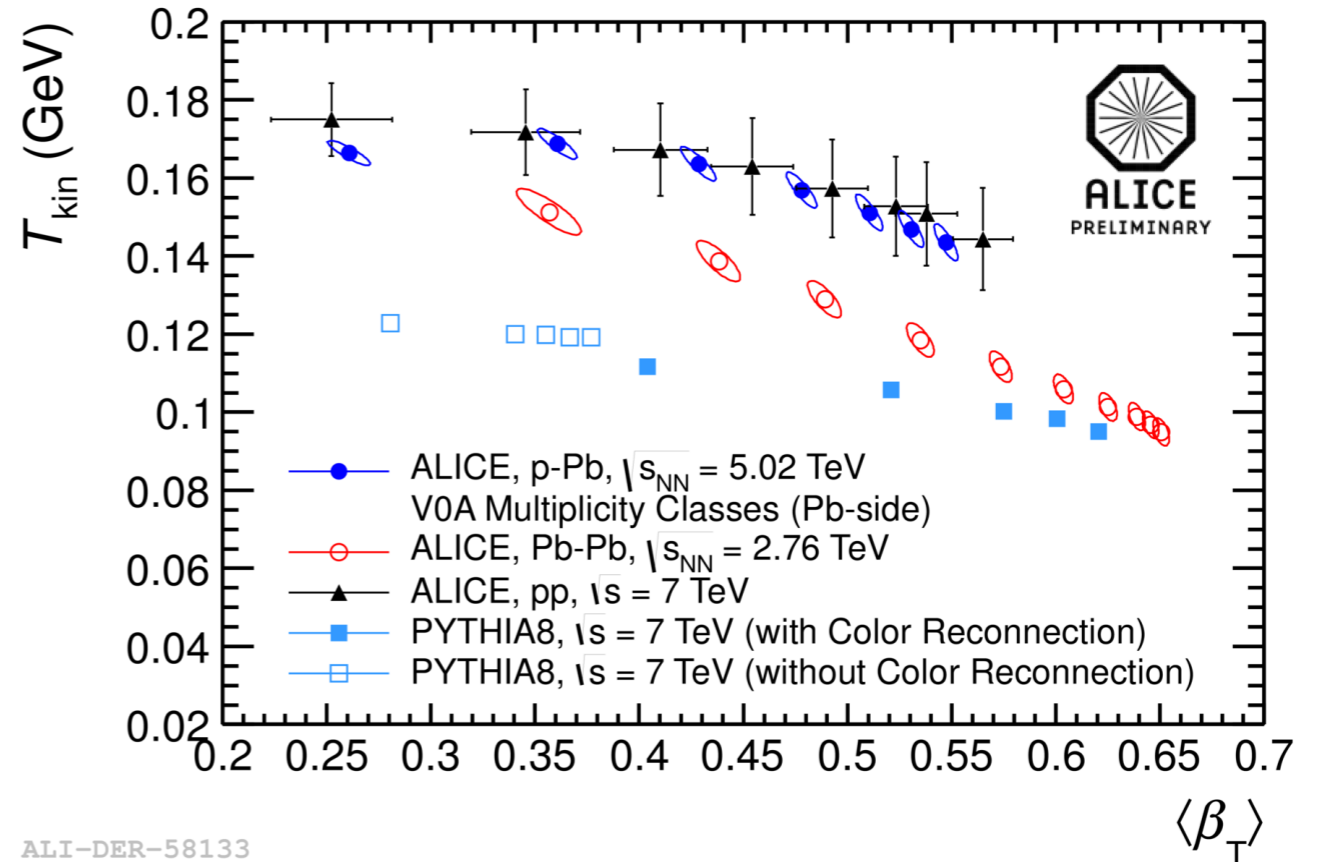
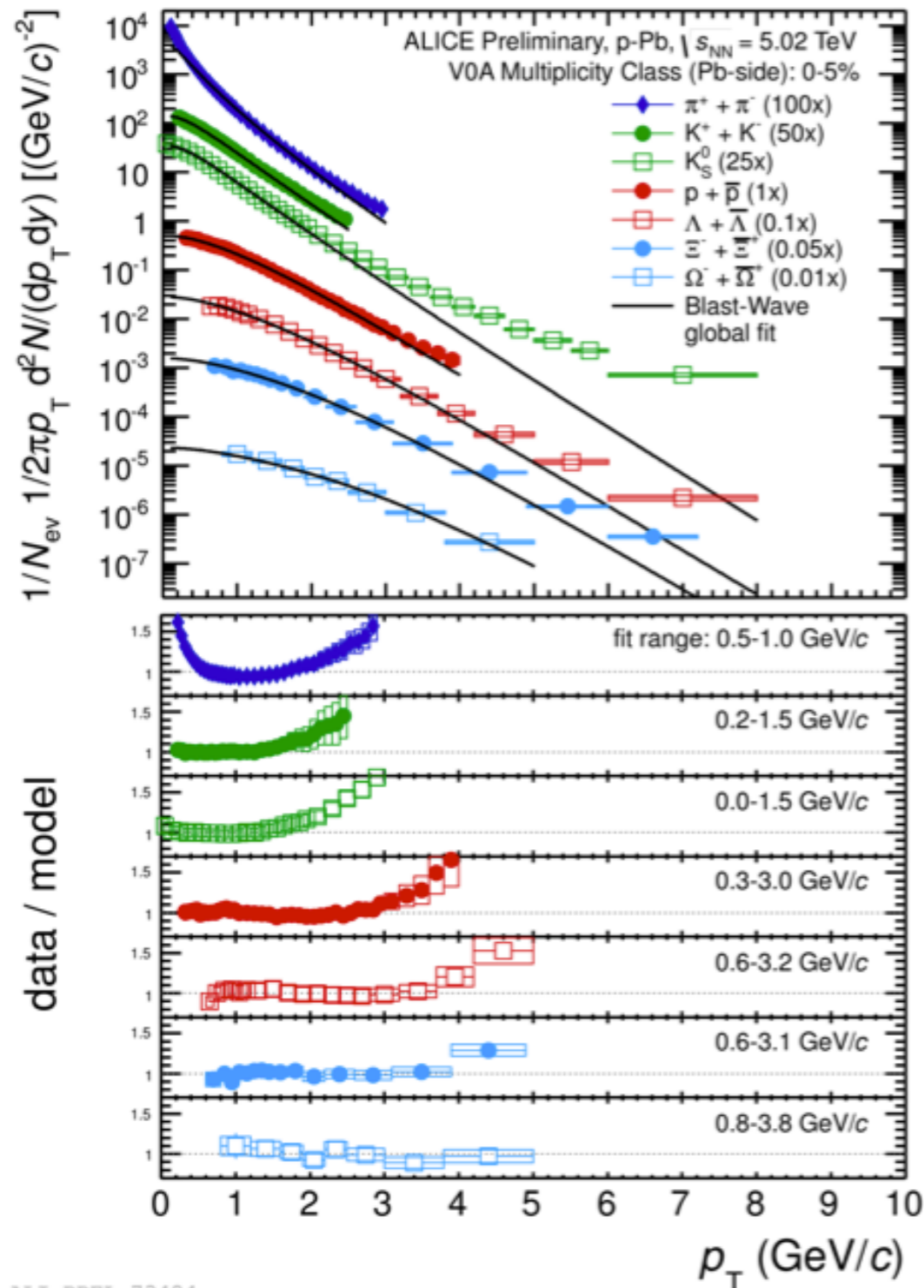
π
 K
 K^0_s
 p
 Λ
 Ξ
 Ω

Hydrodynamic models (EPOS, Krakow) show a better agreement than QCD inspired models (DPMJET).

p-Pb and Pb-Pb data follow the same trend \rightarrow consistent with a collective expansion.

A combined blast-wave fit to the data (**simplified hydro model** $\rightarrow T_{kin}, \beta$) gives a reasonable description.

p_T -Spectra — radial flow?



π
 K
 K^0_s
 p
 Λ
 Ξ
 Ω

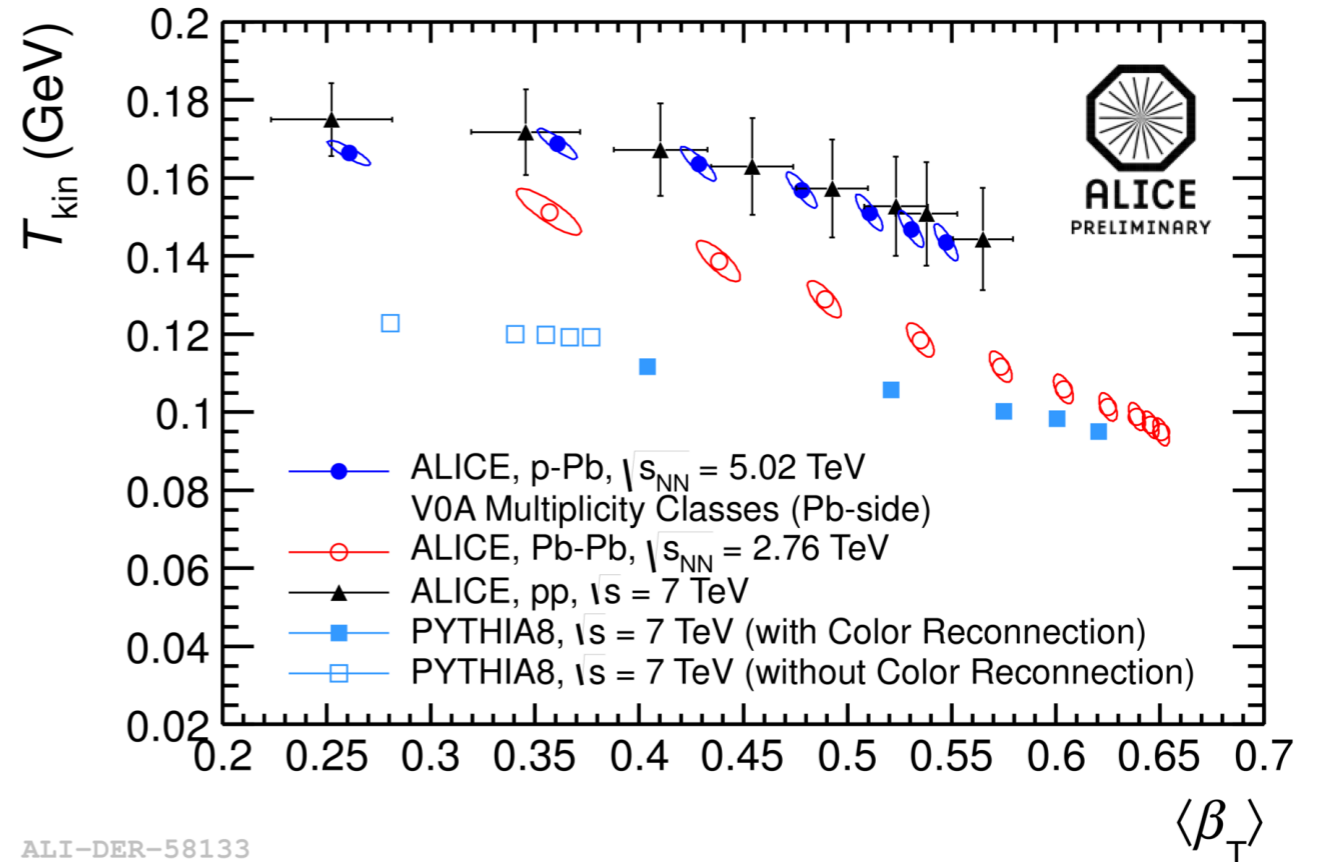
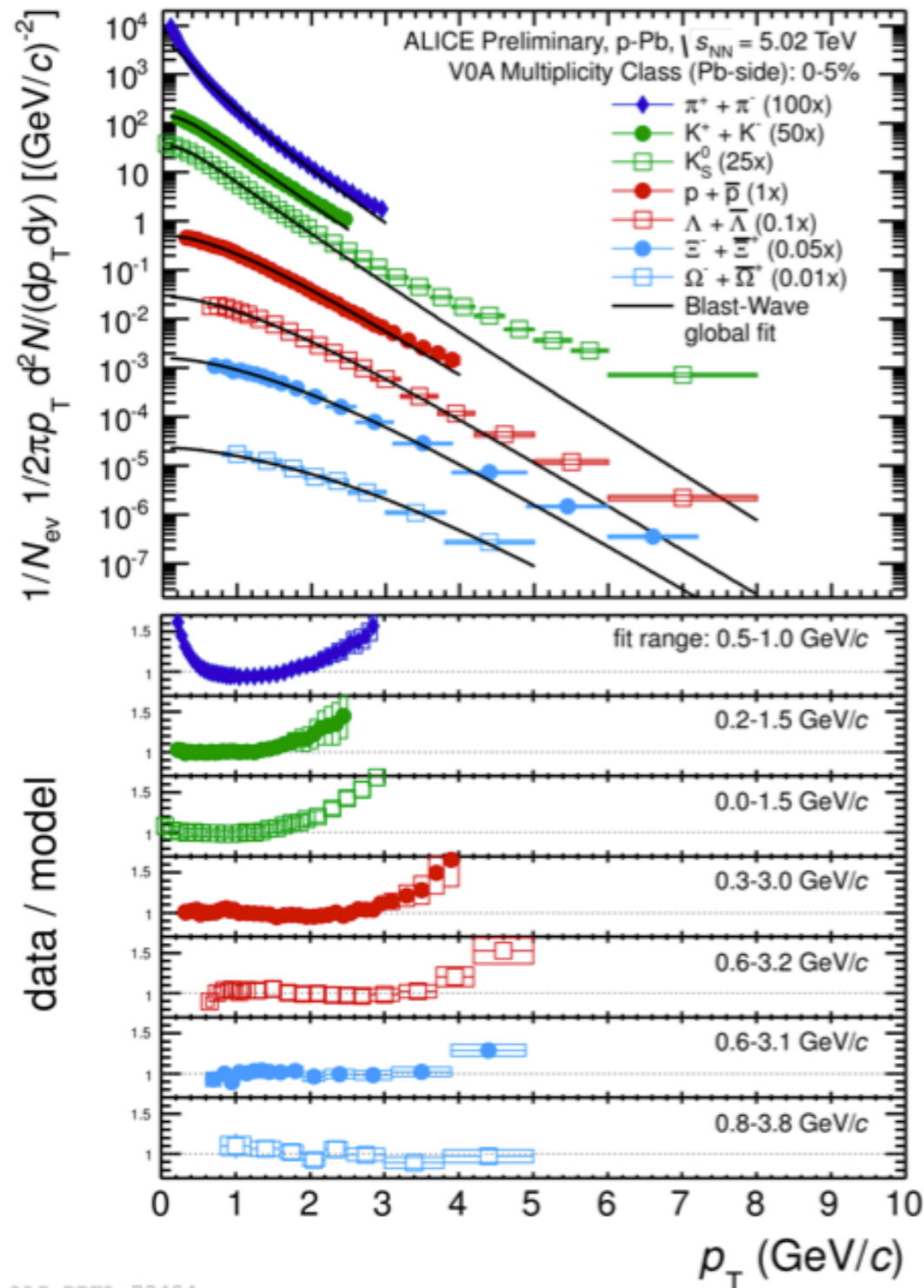
Hydrodynamic models (EPOS, Krakow) show a better agreement than QCD inspired models (DPMJET).

A combined blast-wave fit to the data (**simplified hydro model** $\rightarrow T_{kin}, \beta$) gives a reasonable description.

p-Pb and Pb-Pb data follow the same trend \rightarrow consistent with a collective expansion.

PYTHIA 8 with color reconnection shows a similar trend (without hydrodynamic flow).

p_T -Spectra — radial flow?



π
 K
 K^0_s
 p
 Λ
 Ξ
 Ω

Hydrodynamic models (EPOS, Krakow) show a better agreement than QCD inspired models (DPMJET).

A combined blast-wave fit to the data (**simplified hydro model** $\rightarrow T_{kin}, \beta$) gives a reasonable description.

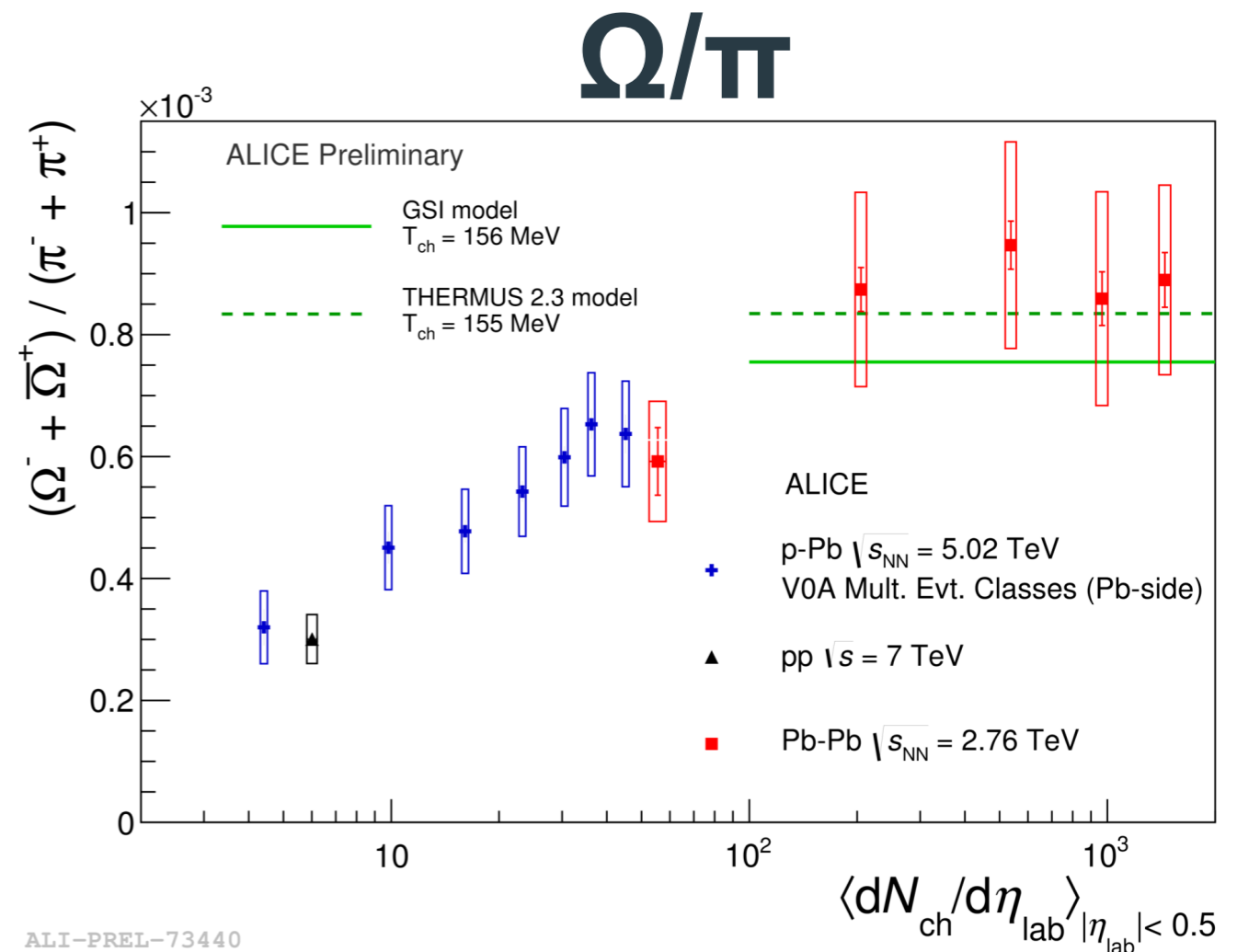
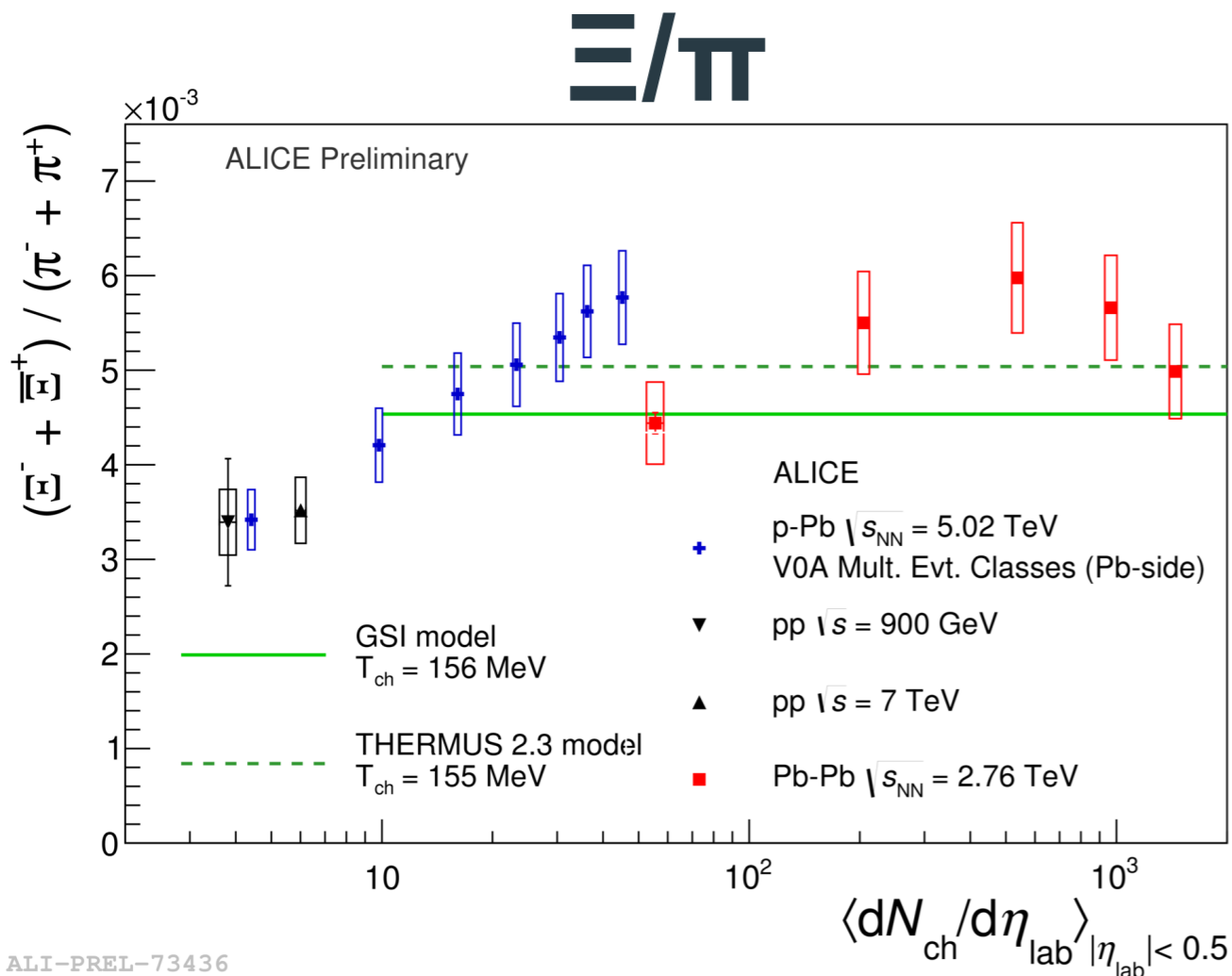
p-Pb and Pb-Pb data follow the same trend \rightarrow consistent with a collective expansion.

PYTHIA 8 with color reconnection shows a similar trend (without hydrodynamic flow).

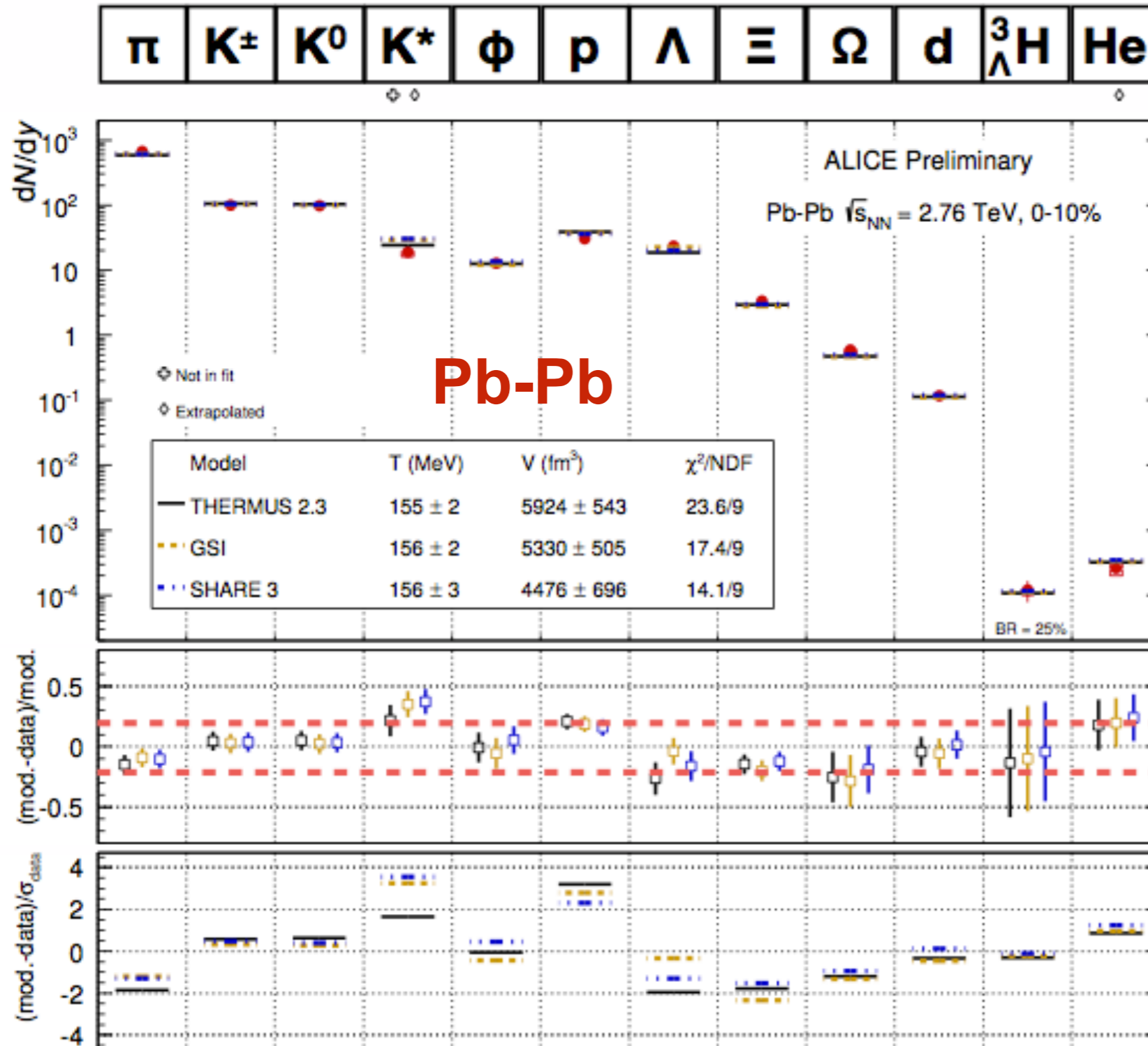
Other effects can mimic flow-like patterns! And also pp data shows a similar trend..

Particle yields and chemical equilibrium (1)

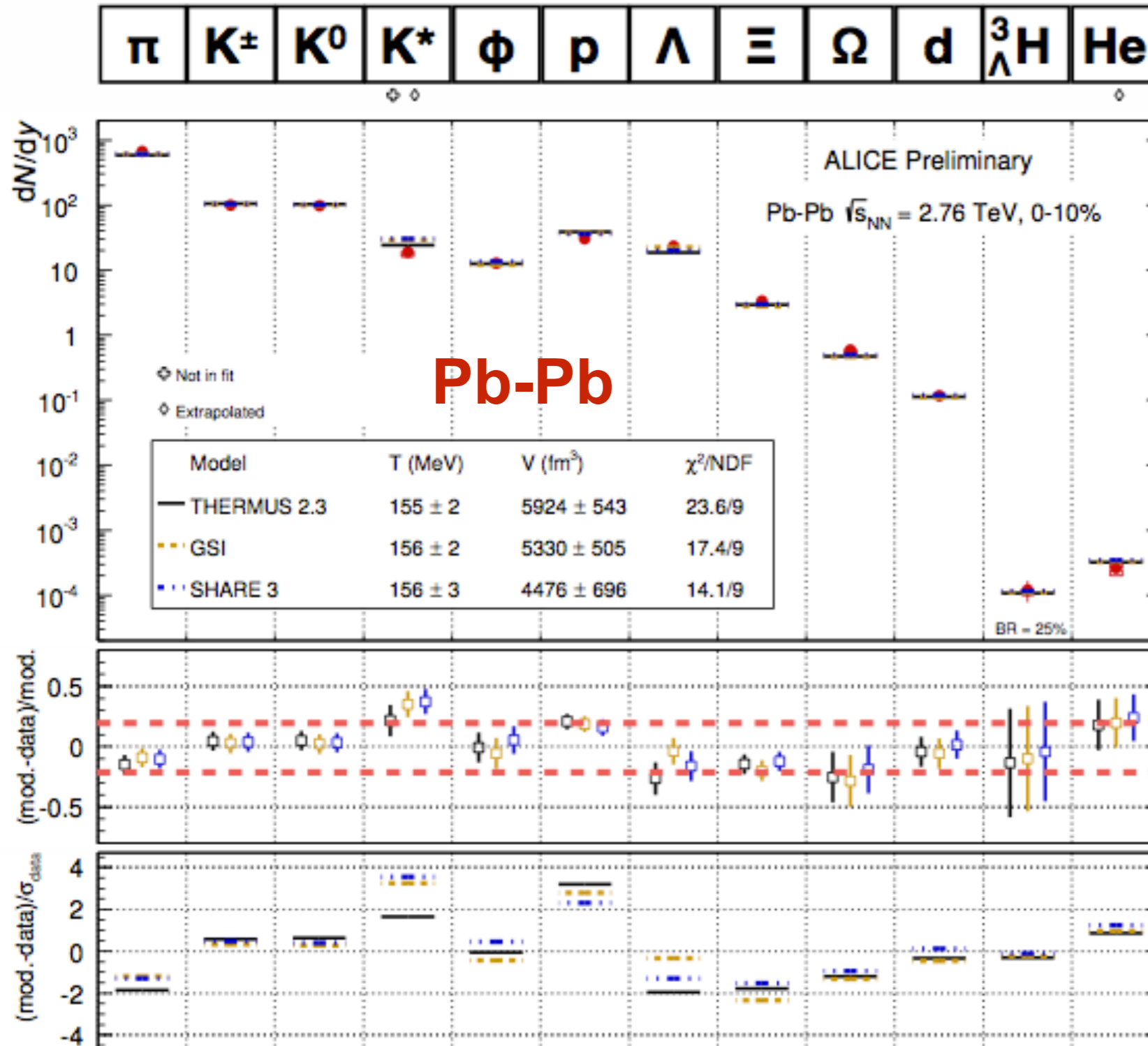
- Multi-strange particles are of particular interest as their production rate is sensitive to the system size.
- In high multiplicity p-Pb collisions similar values as in central Pb-Pb collisions are observed for Ξ (dss), not quite for Ω (sss).



Particle yields and chemical equilibrium (2)

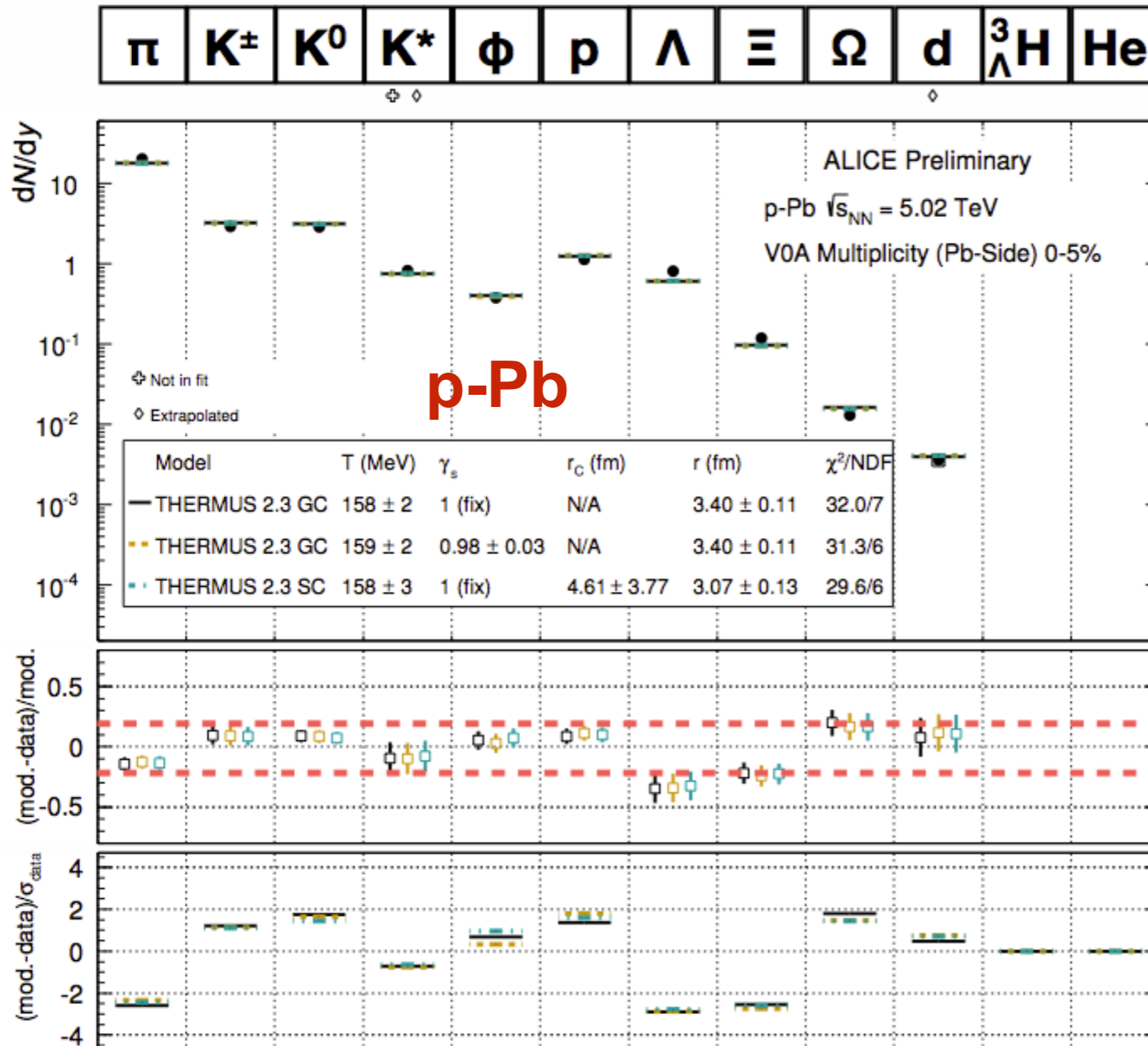


Particle yields and chemical equilibrium (2)



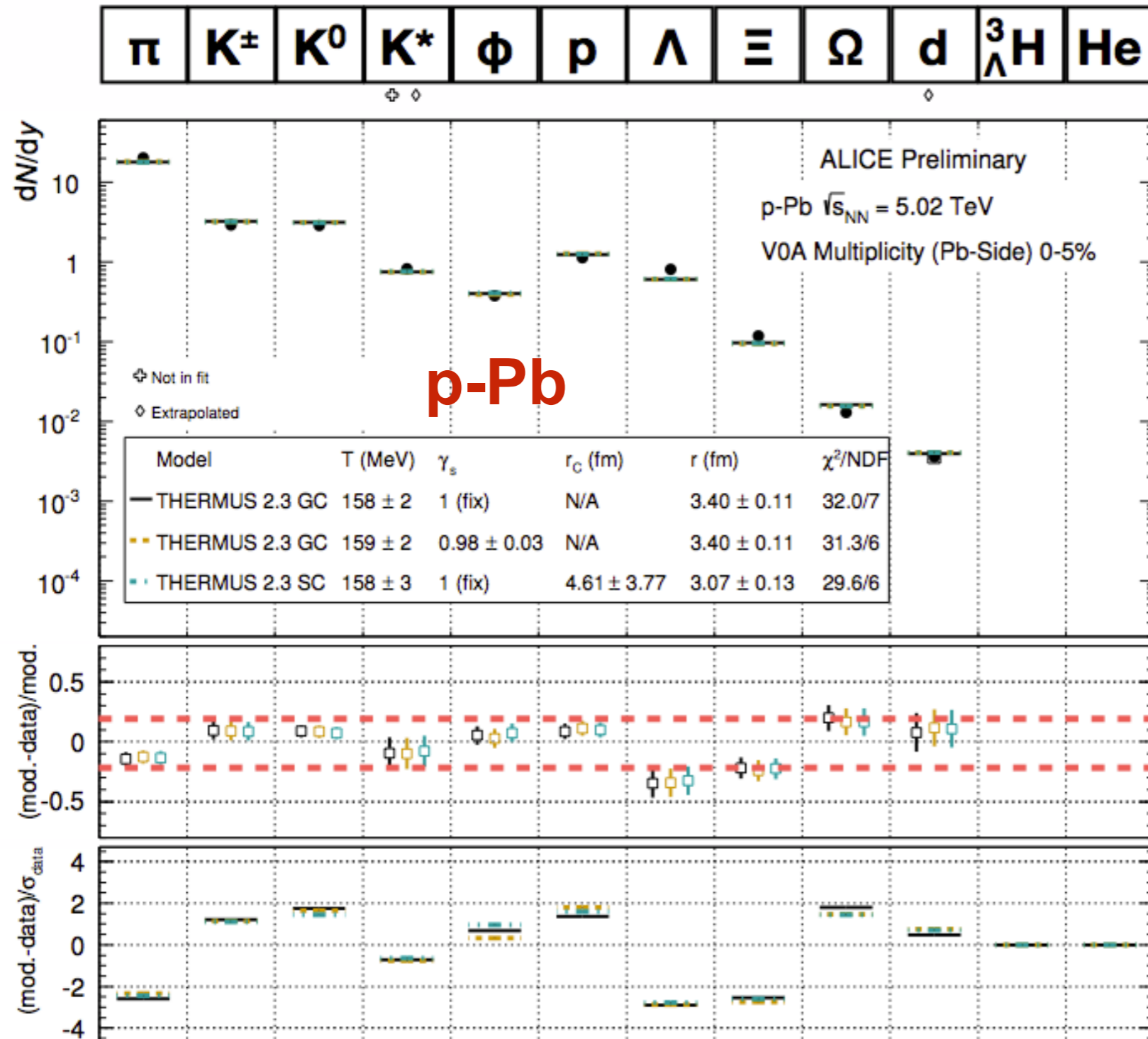
In heavy-ion collisions, chemical equilibrium is typically verified with a *thermal fit* in which all particle yields are described with the same chemical freeze-out temperature $T_{ch} \approx 160$ MeV.

Particle yields and chemical equilibrium (2)



In heavy-ion collisions, chemical equilibrium is typically verified with a *thermal fit* in which all particle yields are described with the same chemical freeze-out temperature $T_{ch} \approx 160$ MeV.

Particle yields and chemical equilibrium (2)



In heavy-ion collisions, chemical equilibrium is typically verified with a *thermal fit* in which all particle yields are described with the same chemical freeze-out temperature $T_{ch} \approx 160$ MeV.

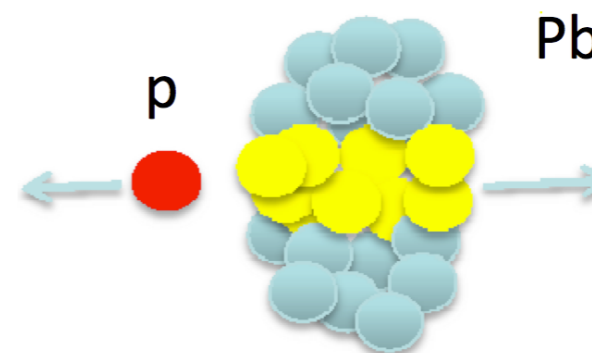
Works in 1st order also in p-Pb collisions, however, the χ^2/n_{dof} is slightly worse: ≈ 5 instead of ≈ 2 , mainly due to multi-strange particles.

High p_T and jets

What is the R_{pA} ?

- Modification of the spectral shape due to nuclear effects is quantified based on the *nuclear modification factor*:

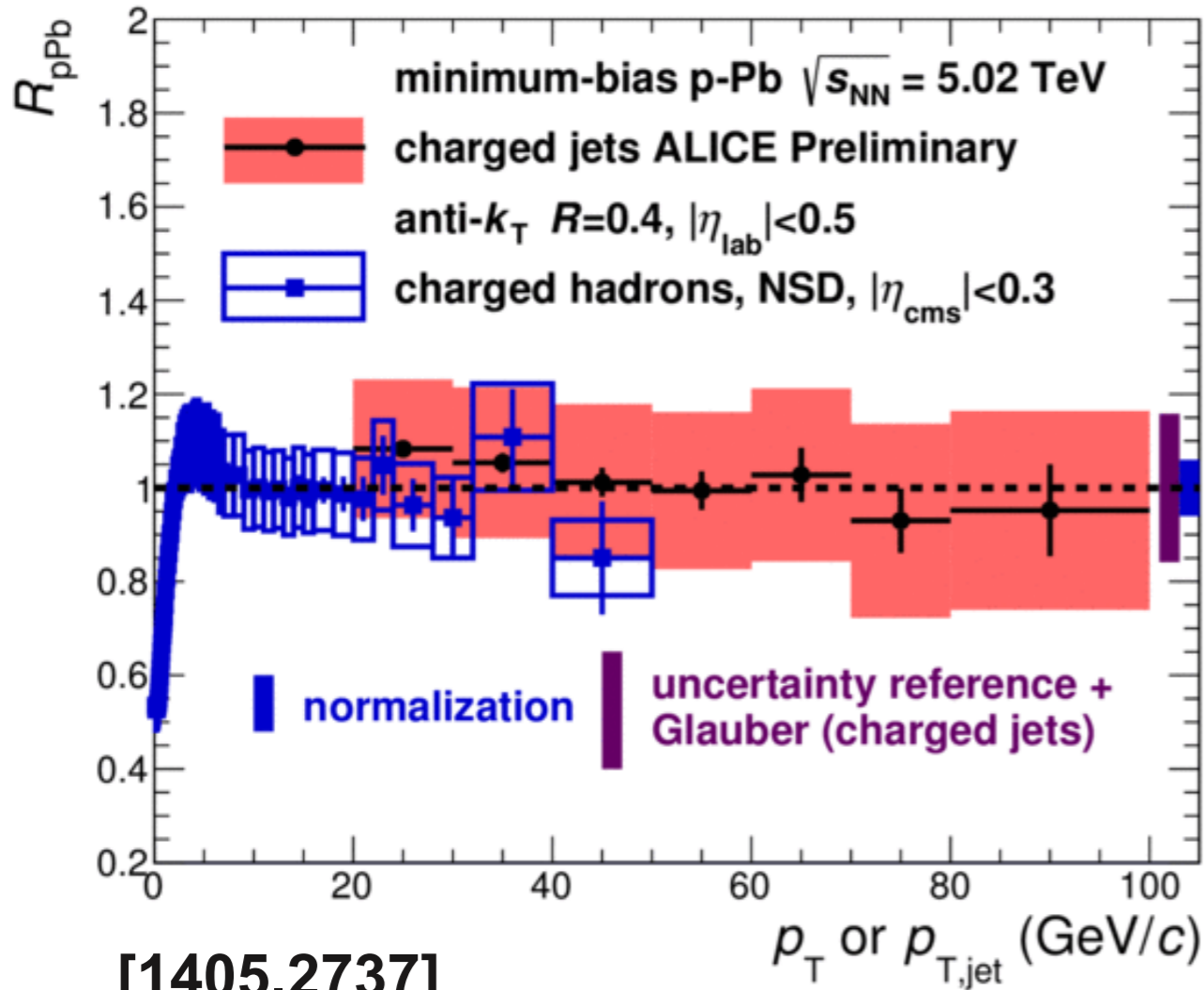
$$R_{pA} = \frac{dN_{pA} / dp_T}{\langle N_{coll} \rangle dN_{pp} / dp_T}$$



- Number of binary collisions is calculated in a Glauber model:
 $\langle N_{coll} \rangle = 6.9 \pm 0.6$
- For pQCD processes: if $R_{pA} \approx 1 \rightarrow$ p-Pb collision is approximately a superposition of independent proton-nucleon collisions and no nuclear effects are present.

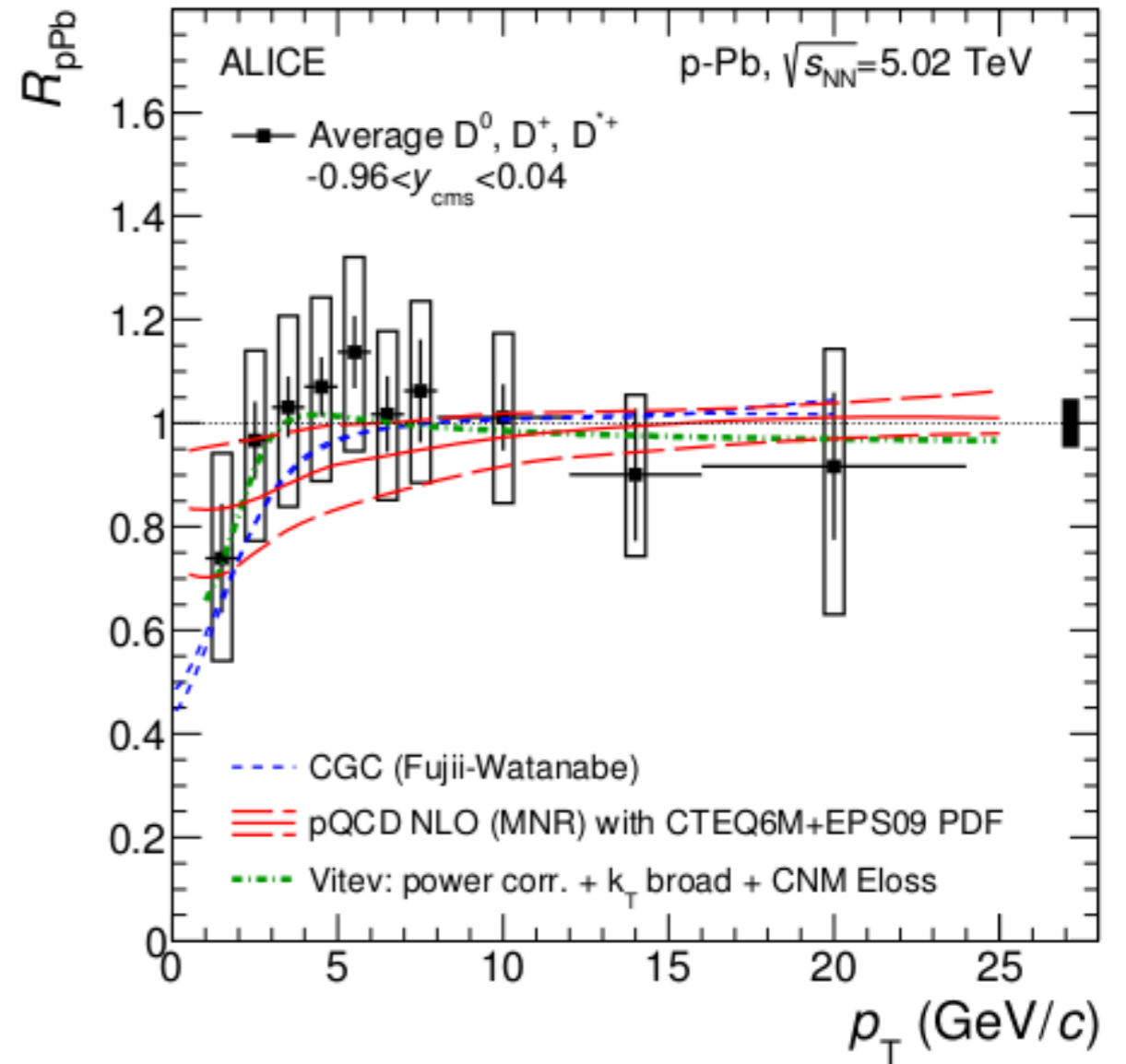
R_{pA} — examples

charged particles and jets



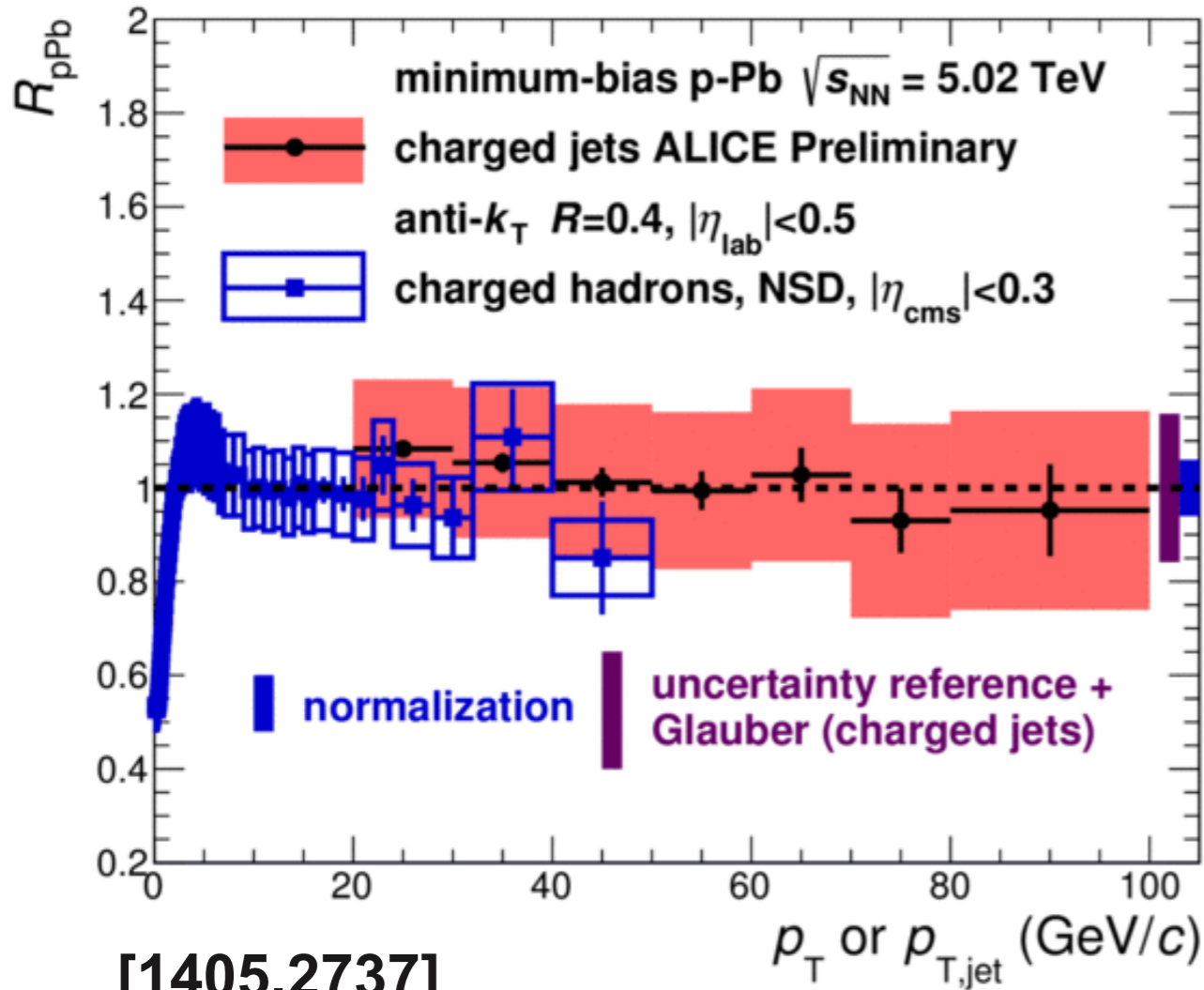
ALI-PREL-80555

D mesons (mid-rapidity) [1405.3452]



R_{pA} — examples

charged particles and jets

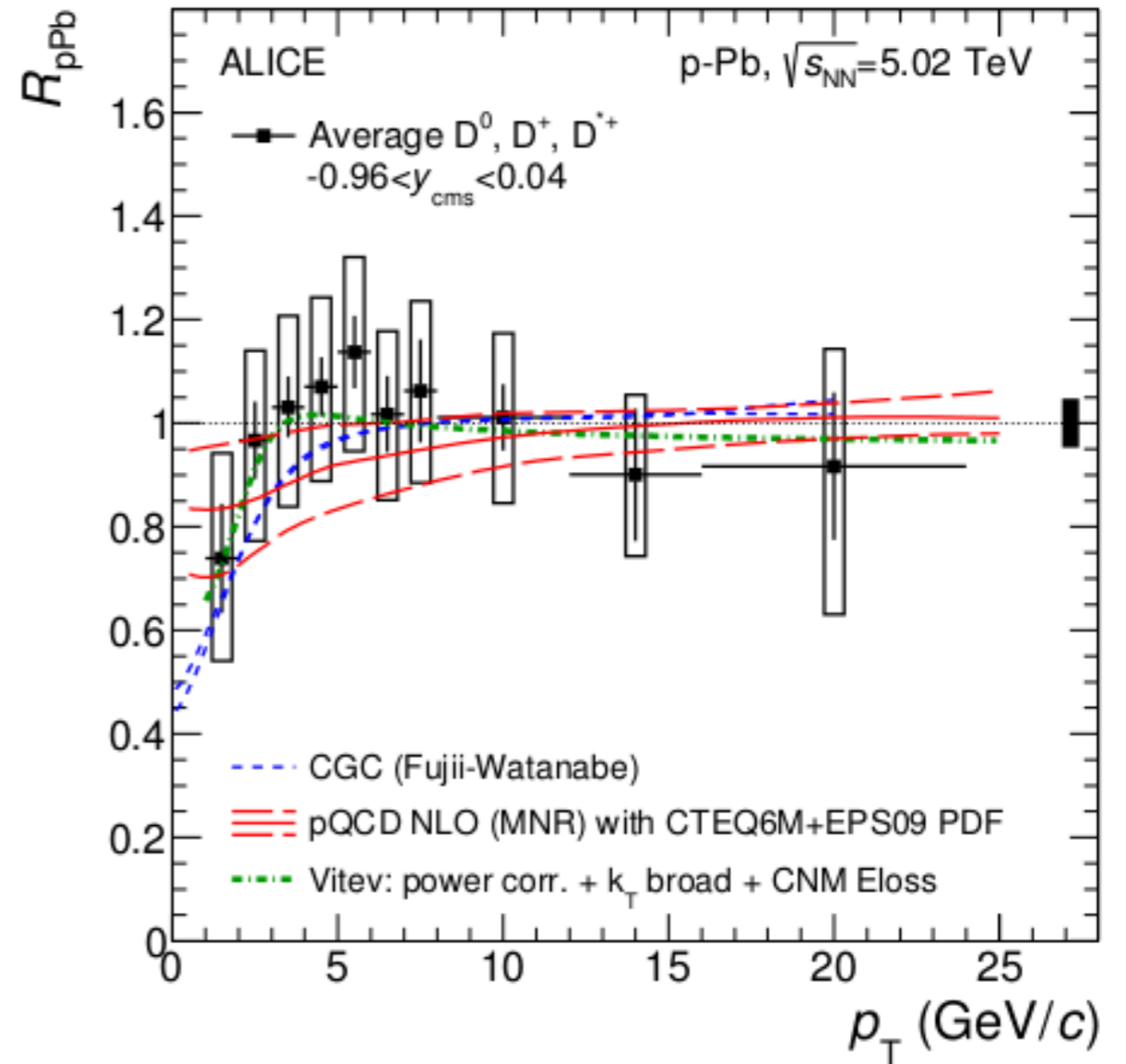


[1405.2737]

ALI-PREL-80555

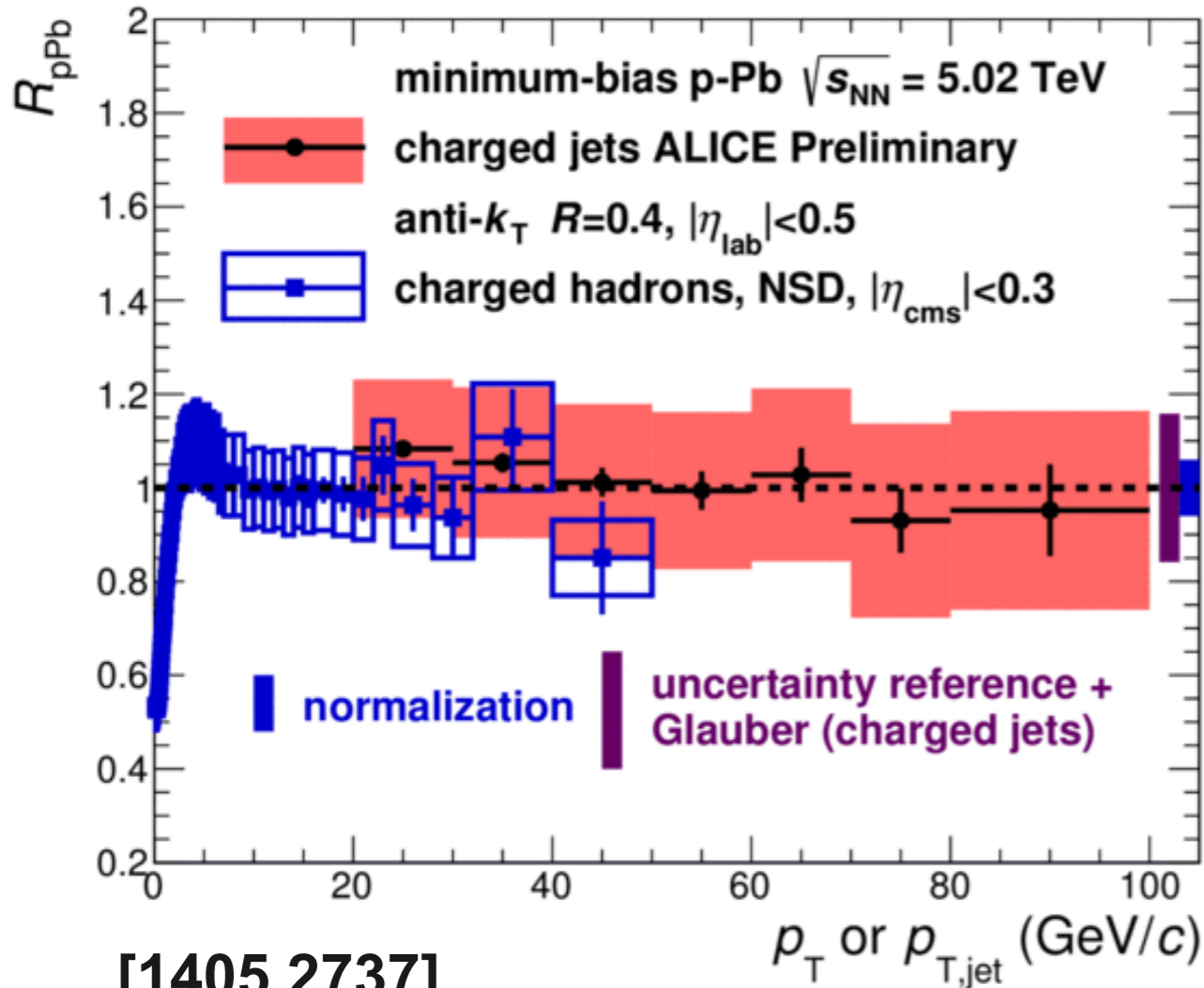
In general, no significant modification observed in the 10-30 GeV/c region.

D mesons (mid-rapidity) [1405.3452]



R_{pA} — examples

charged particles and jets

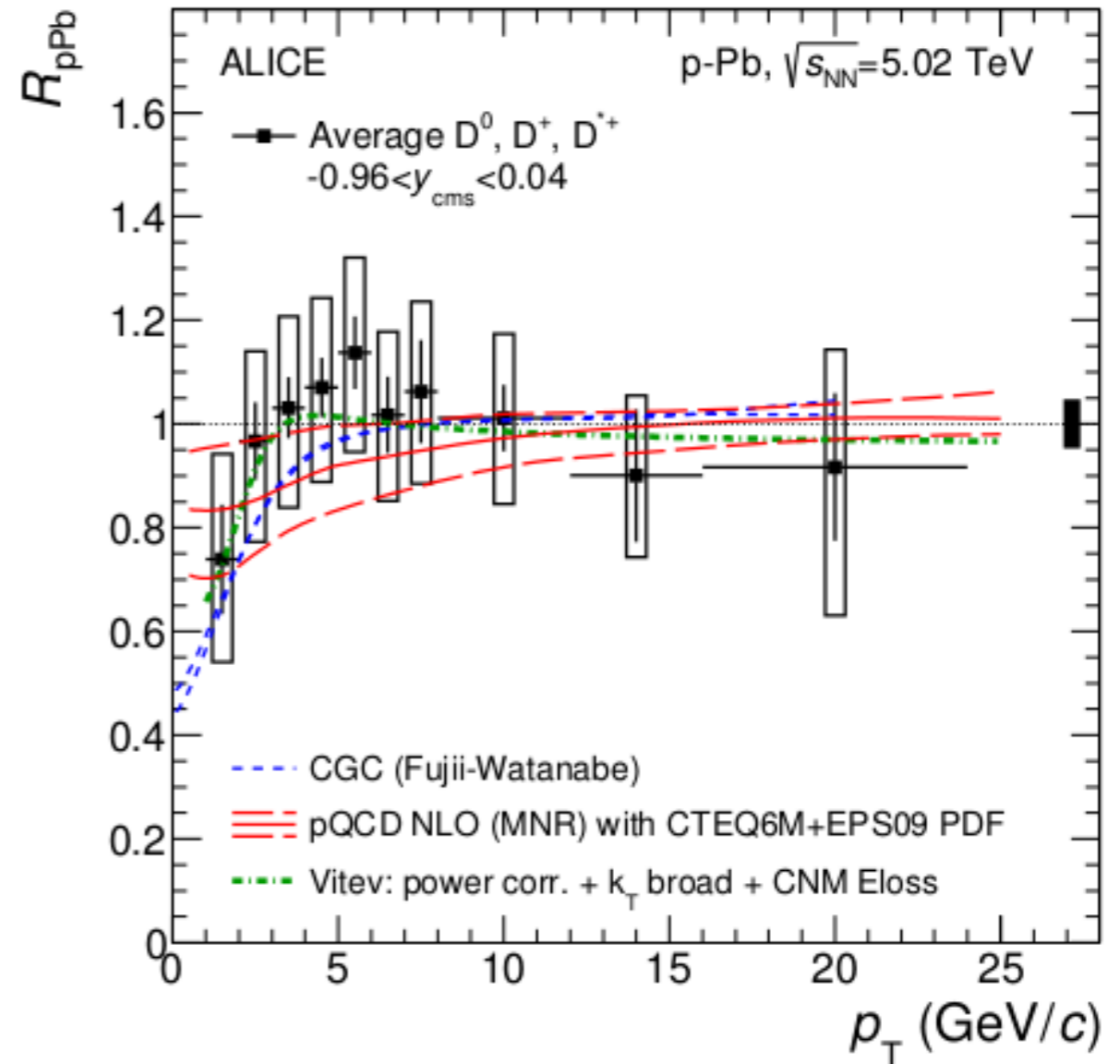


[1405.2737]

ALI-PREL-80555

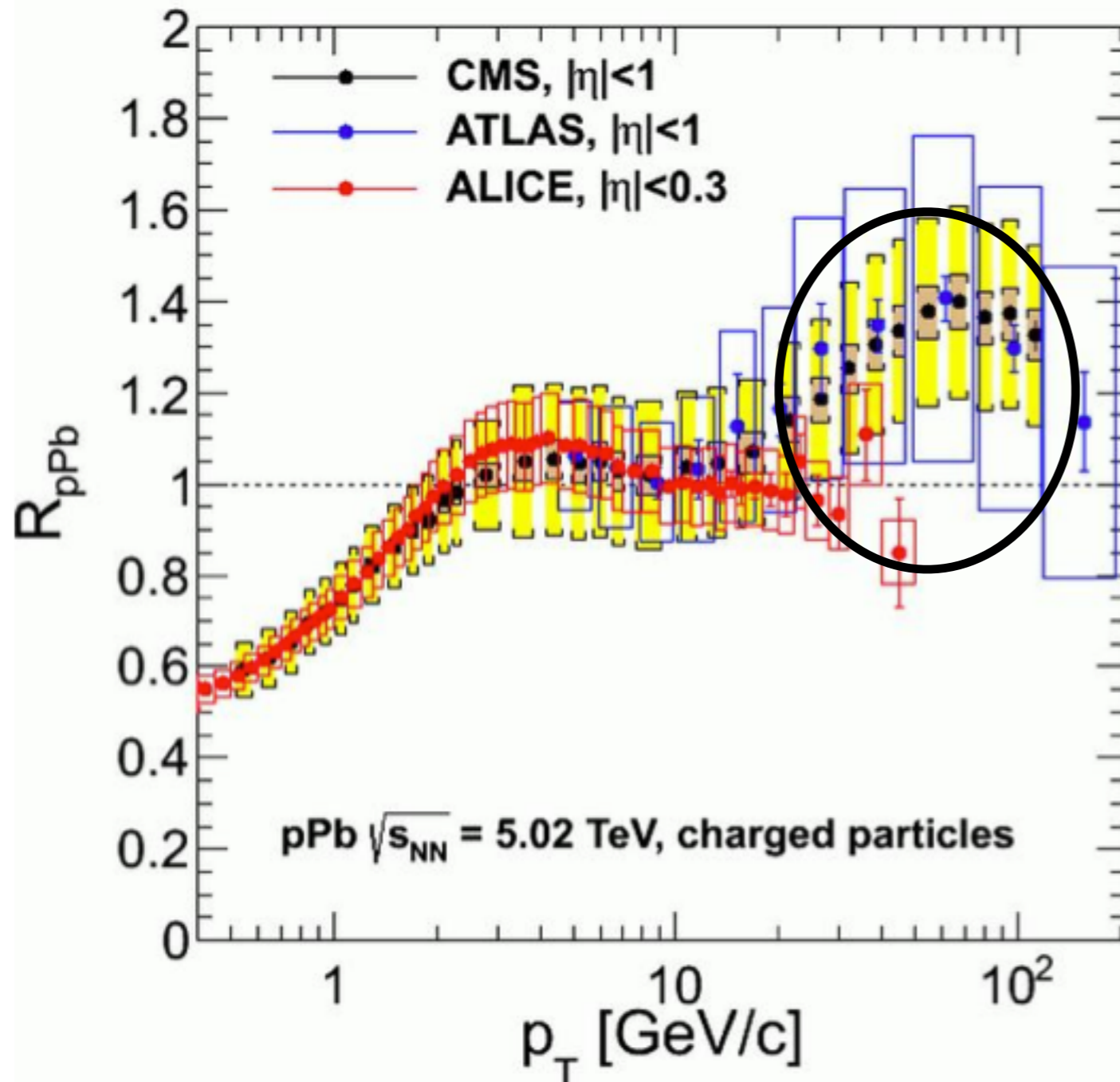
In general, no significant modification observed in the 10-30 GeV/c region.

D mesons (mid-rapidity) [1405.3452]



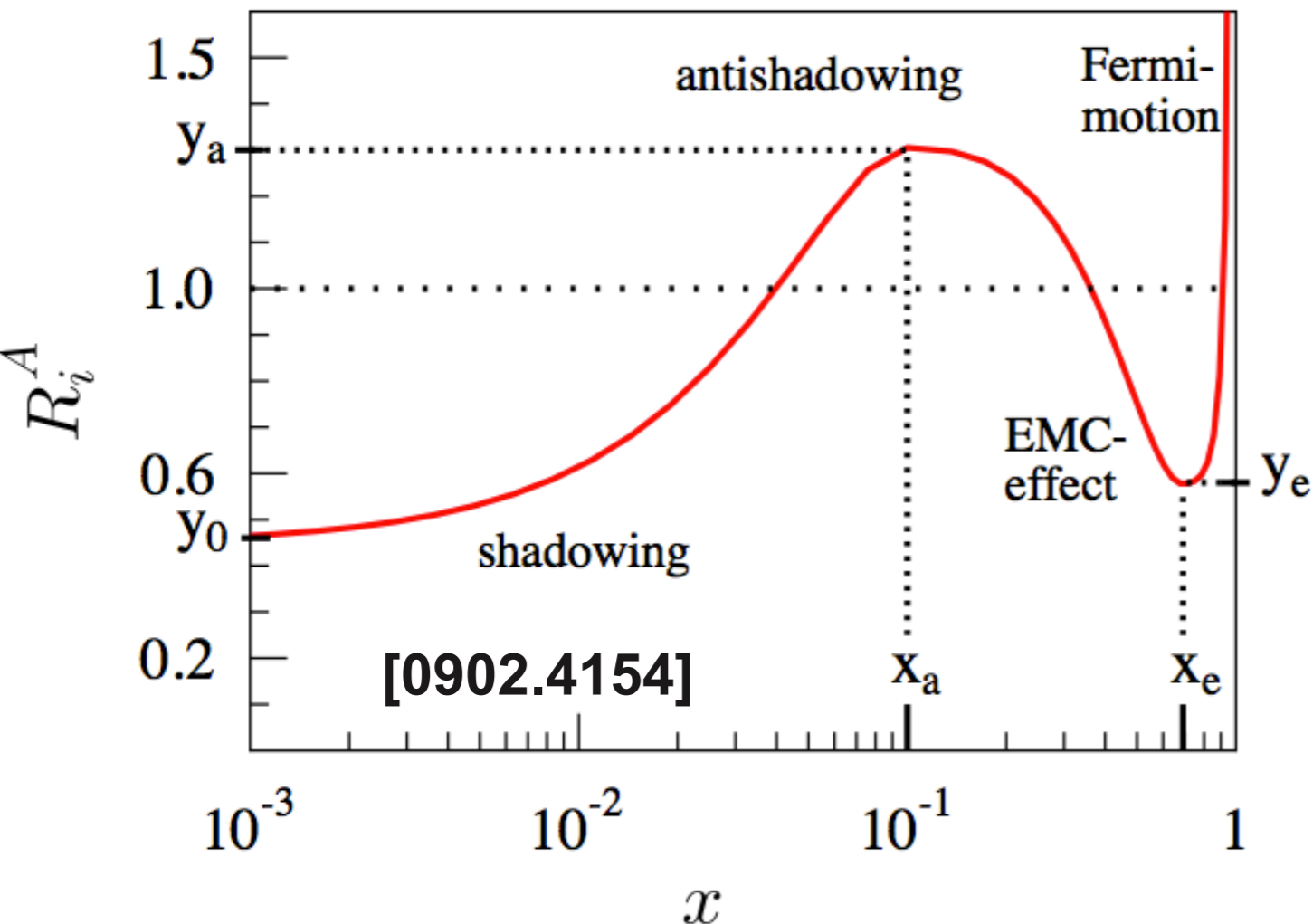
The suppression effects seen in AA collisions are not due to cold nuclear matter effects. They are final state effects in AA (energy lost in the medium).
 → see also talks by E. Scomparin and B. Cole

Charged particle R_{pA}



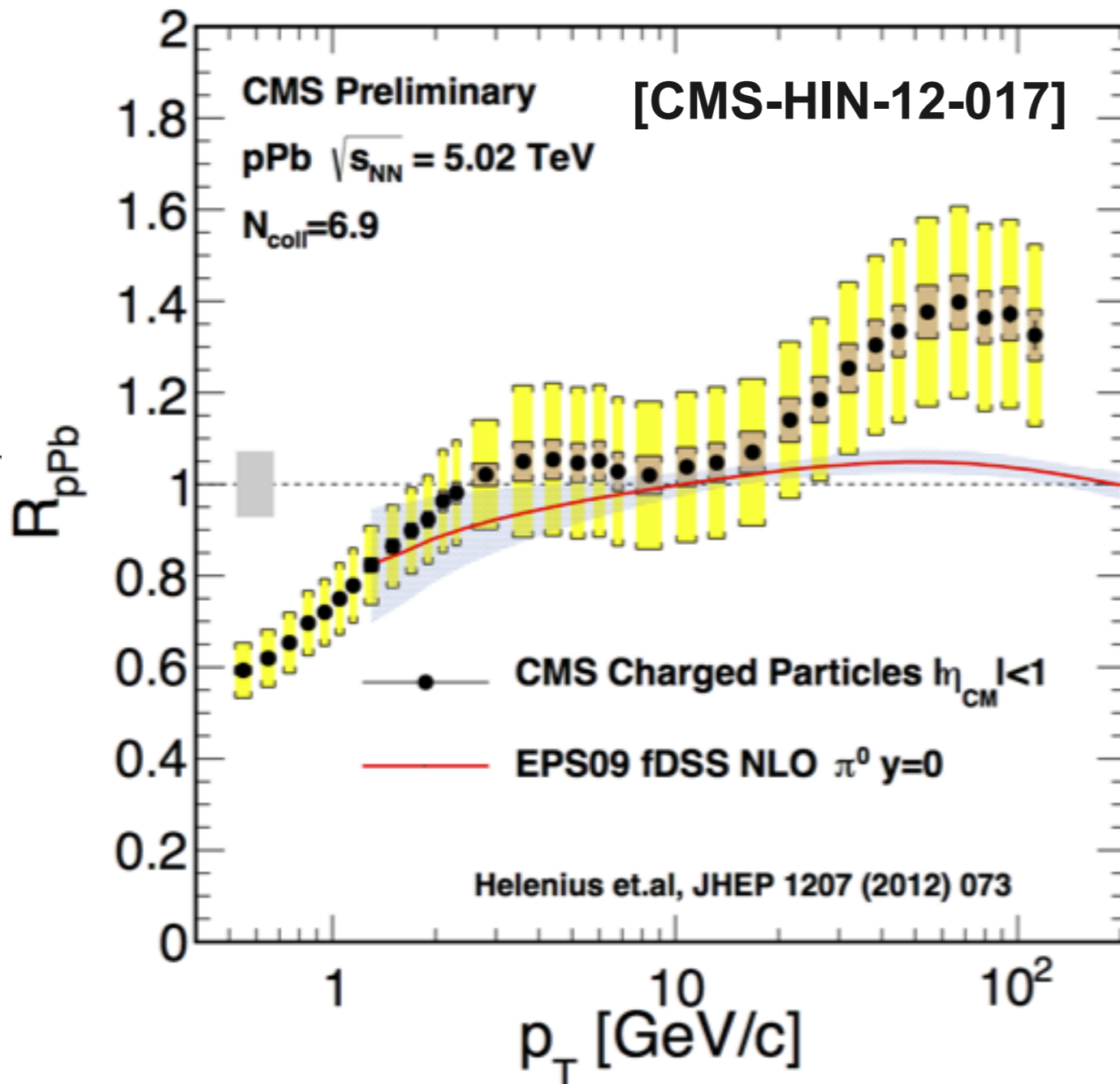
- Going to even higher p_T , CMS observed an *enhancement* in the charged particle R_{pA} . ATLAS now confirms this observation.
- No explanation yet for this phenomenon!
- PDFs are expected to be modified in the nucleus. However, *anti-shadowing* seems to be insufficient.
- Jet fragmentation needs to be checked, because the R_{pA} of jets is approximately equal to one in all three experiments.
- Different impression of CMS/ATLAS vs. ALICE data...

Charged particle R_{pA}



- Going to even higher p_T , CMS observed an *enhancement* in the charged particle R_{pA} . ATLAS now confirms this observation.
- No explanation yet for this phenomenon!
- PDFs are expected to be modified in the nucleus. However, *anti-shadowing* seems to be insufficient.
- Jet fragmentation needs to be checked, because the R_{pA} of jets is approximately equal to one in all three experiments.
- Different impression of CMS/ATLAS vs. ALICE data...

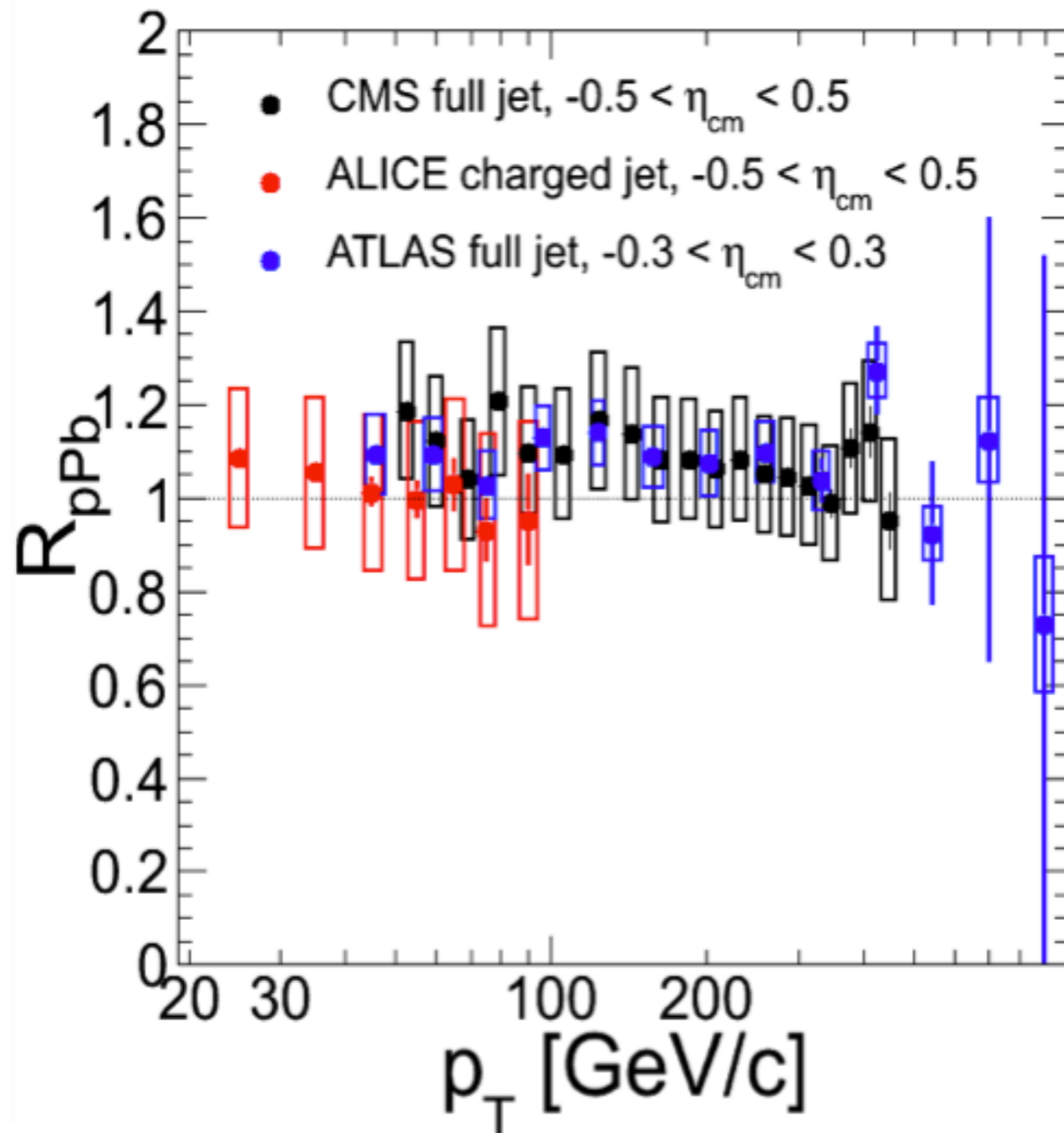
Charged particle R_{pA}



- Going to even higher p_T , CMS observed an *enhancement* in the charged particle R_{pA} . ATLAS now confirms this observation.
- No explanation yet for this phenomenon!
- PDFs are expected to be modified in the nucleus. However, *anti-shadowing* seems to be insufficient.
- Jet fragmentation needs to be checked, because the R_{pA} of jets is approximately equal to one in all three experiments.
- Different impression of CMS/ATLAS vs. ALICE data...

Charged particle R_{pA}

(Charged) Jet R_{pPb}

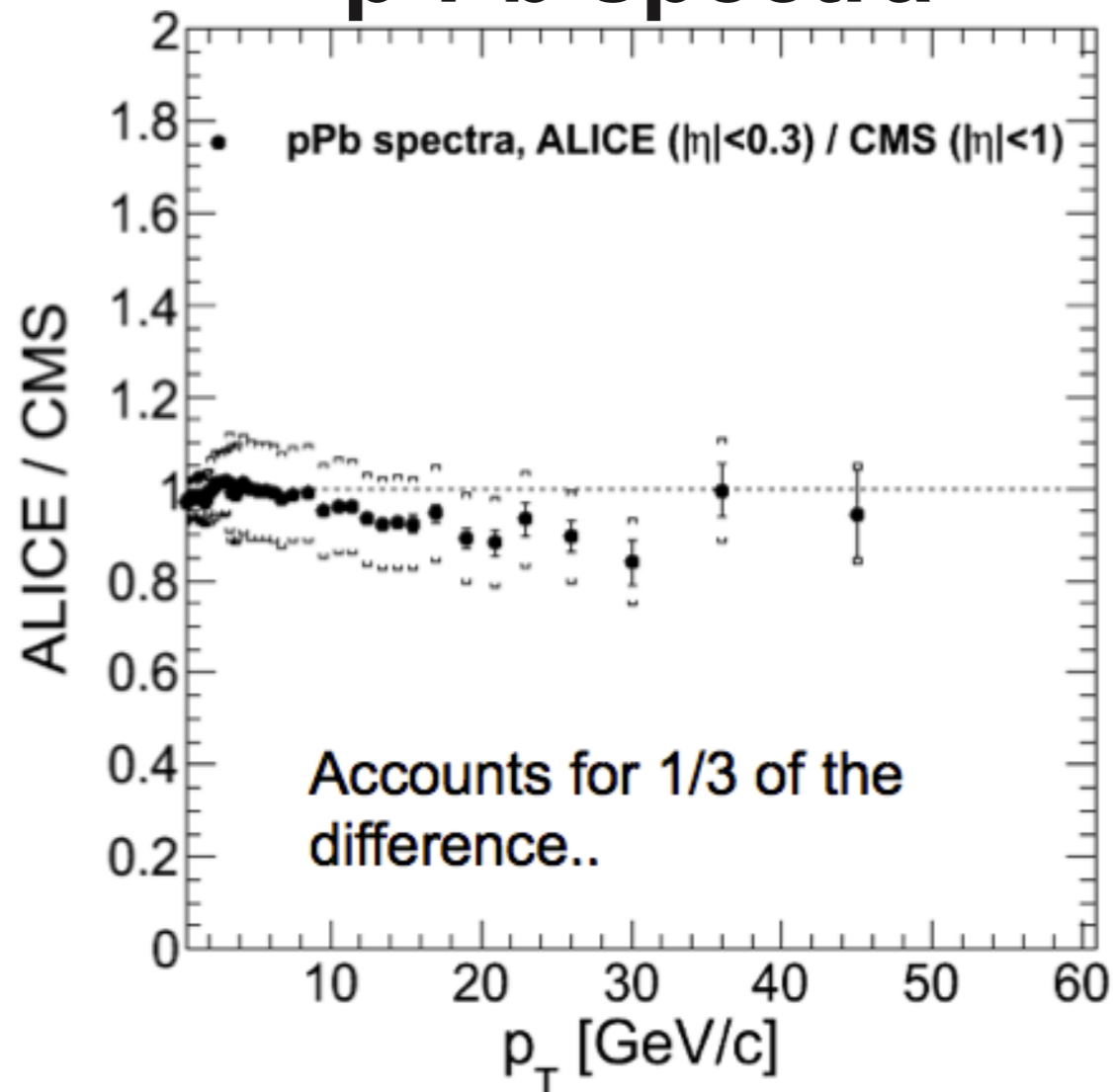


- Going to even higher p_T , CMS observed an *enhancement* in the charged particle R_{pA} . ATLAS now confirms this observation.
- No explanation yet for this phenomenon!
- PDFs are expected to be modified in the nucleus. However, *anti-shadowing* seems to be insufficient.
- Jet fragmentation needs to be checked, because the R_{pA} of jets is approximately equal to one in all three experiments.
- Different impression of CMS/ATLAS vs. ALICE data...

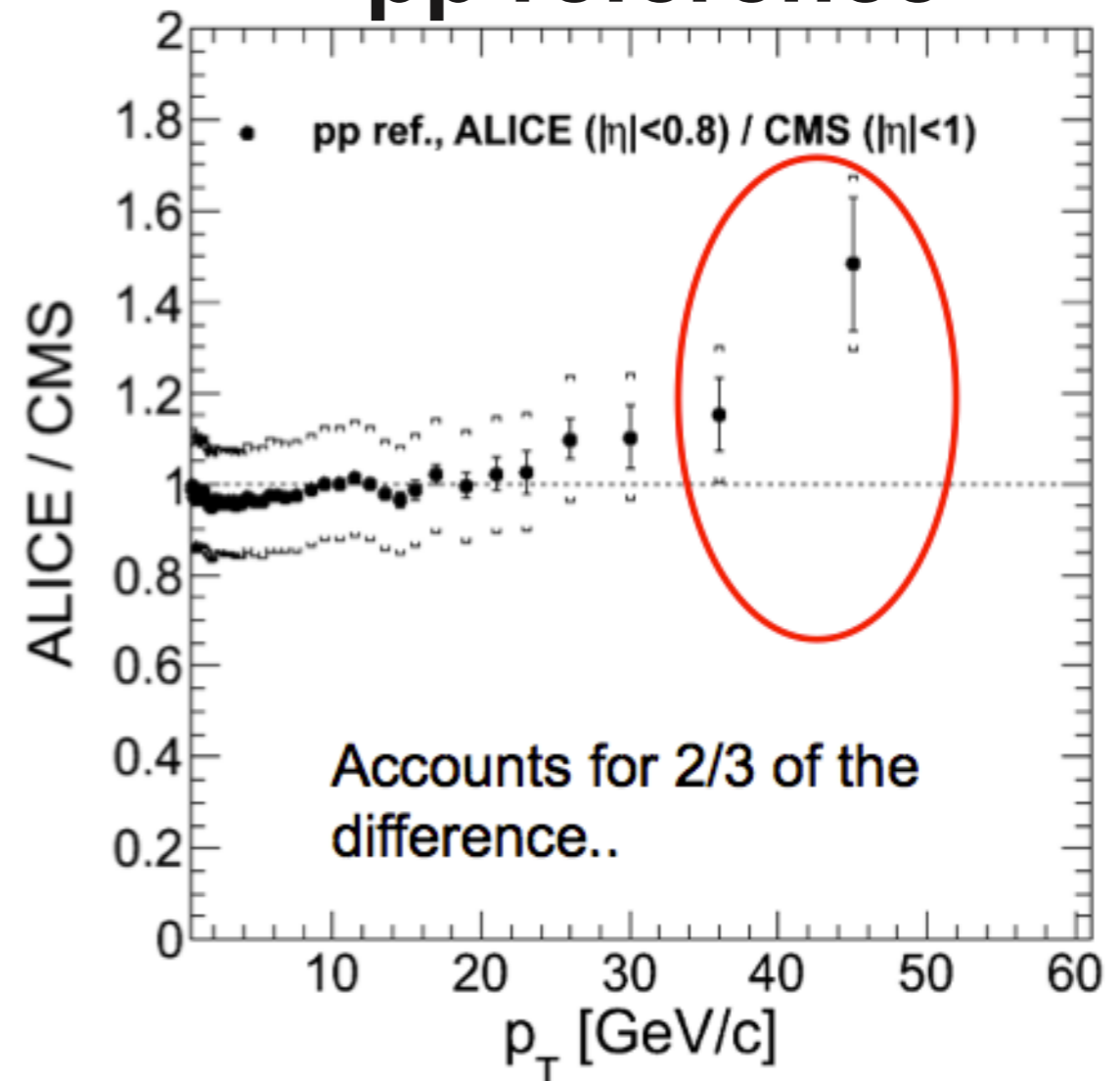
The need for 5 TeV pp reference data

- N.B.: There is no data at the reference energy! The proton spectrum is interpolated/extrapolated from 2.76 TeV and 7 TeV data...

p-Pb spectra



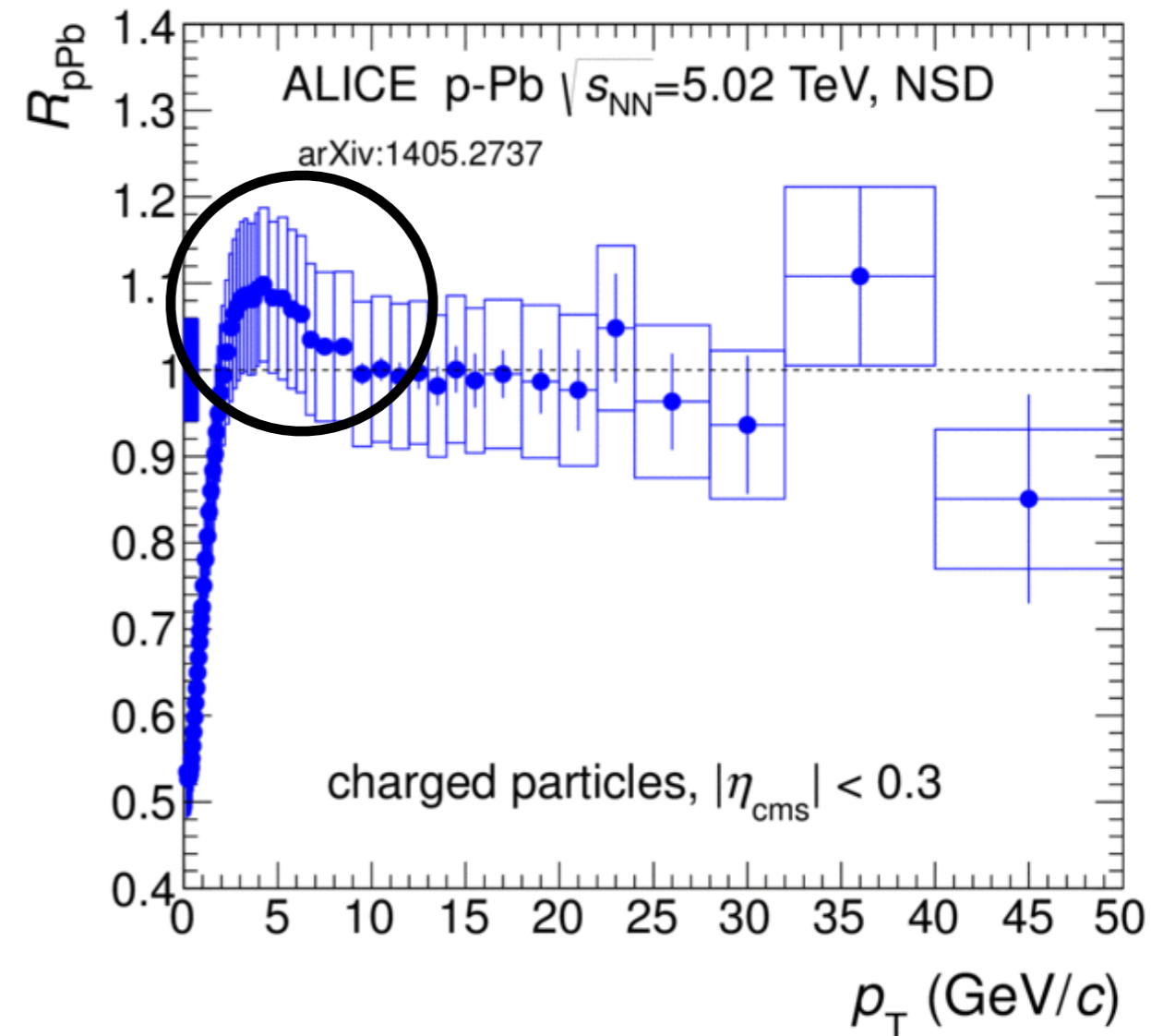
pp reference



- Also needed for: $13 \text{ TeV} * 82 / 208 = 5.125 \text{ TeV} !$

R_{pA} at intermediate p_T

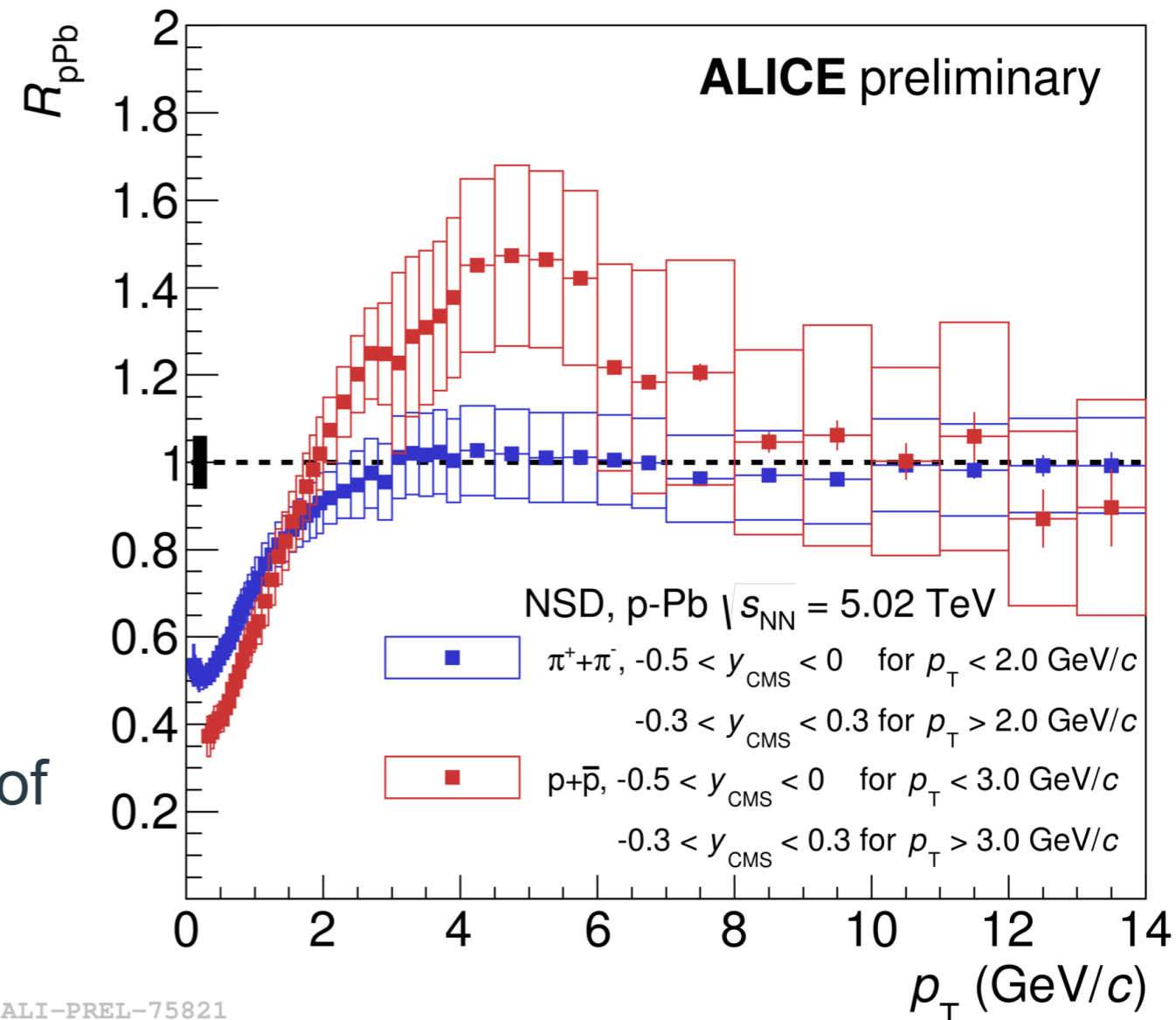
- The second interesting region is around 3-6 GeV/c \rightarrow Cronin peak
- Shows a strong dependence on particle type:
 - no peak for pions and kaons,
 - rather pronounced for protons..
- This could indicate that it is caused by the mass dependent hardening of the p_T -spectra as predicted by the radial flow picture.



ALI-DER-75525

R_{pA} at intermediate p_T

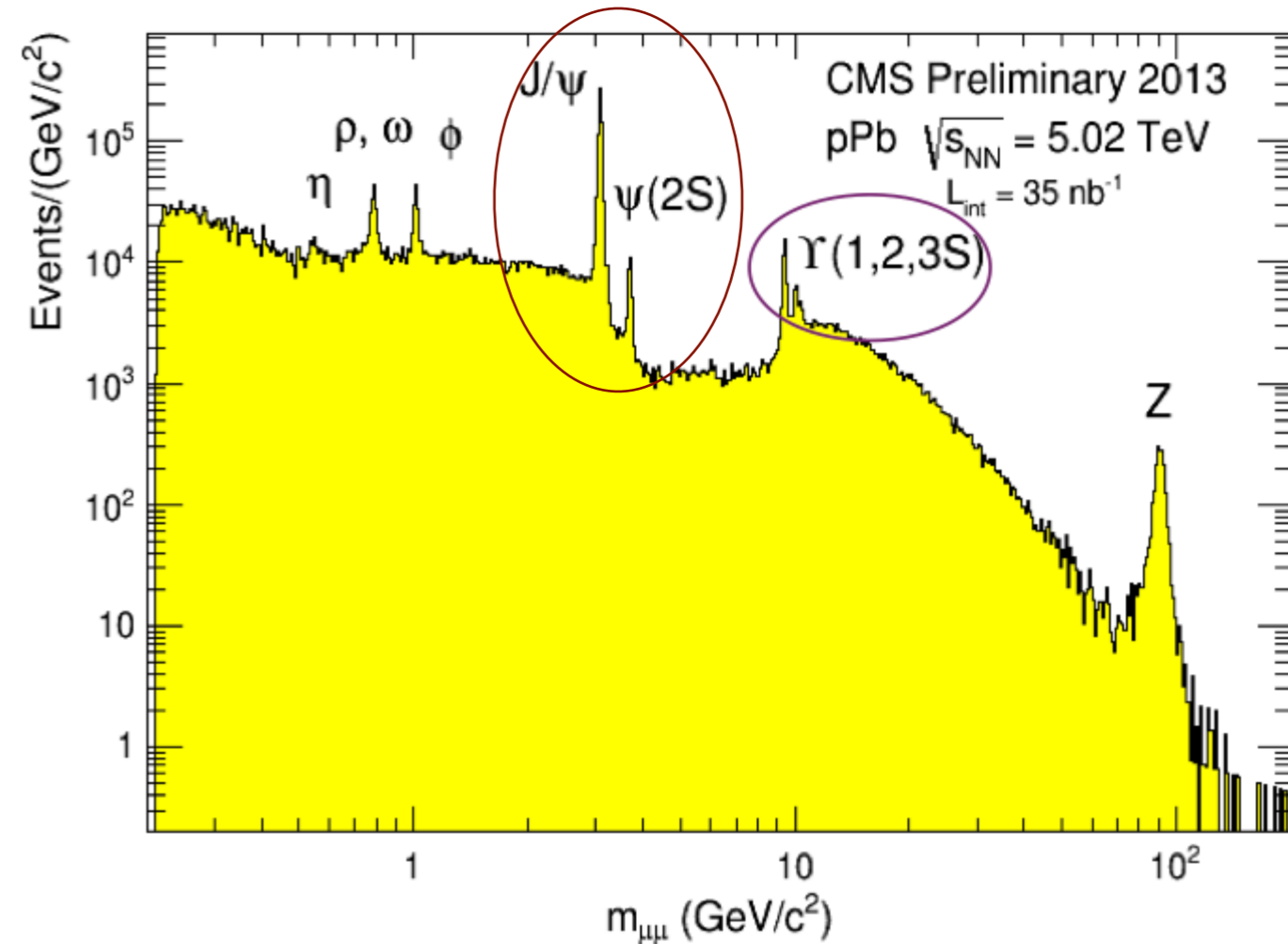
- The second interesting region is around 3-6 GeV/c \rightarrow Cronin peak
- Shows a strong dependence on particle type:
 - no peak for pions and kaons,
 - rather pronounced for protons..
- This could indicate that it is caused by the mass dependent hardening of the p_T -spectra as predicted by the radial flow picture.



Heavy flavor and electroweak bosons

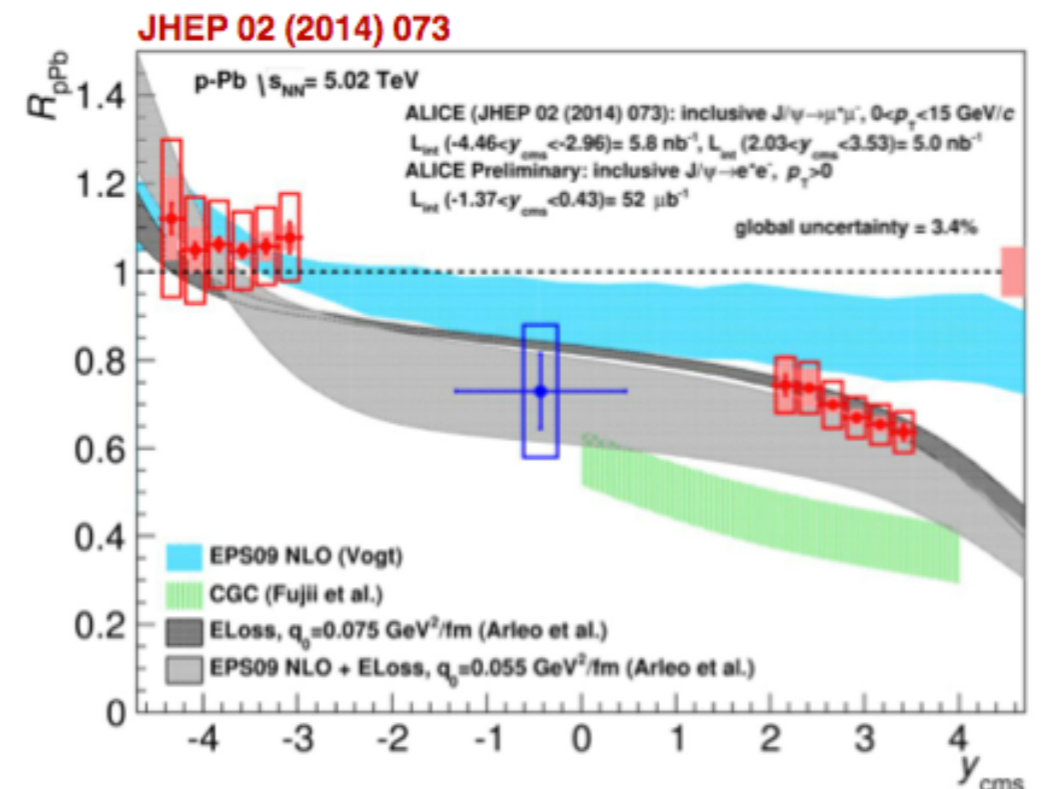
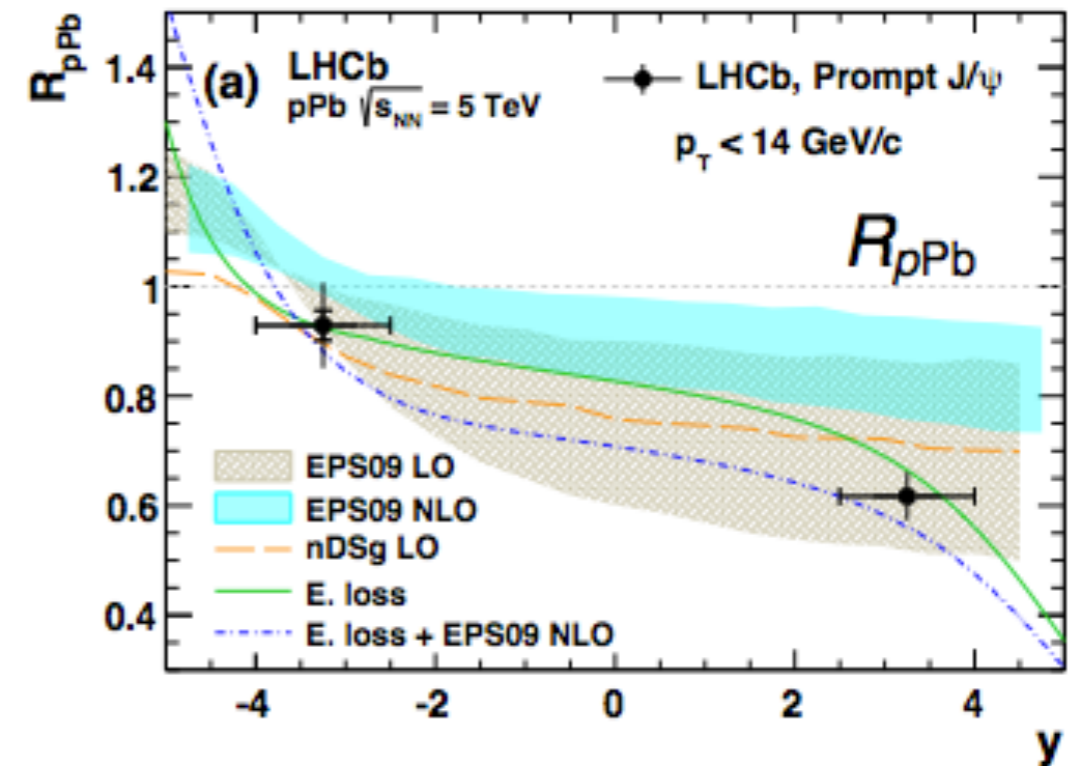
Quarkonia — Introduction

- A precise measurement of quarkonia is crucial for the understanding of *regeneration* effects in Pb-Pb collisions which probe de-confinement in PbPb.
- In addition, these measurements can help to constrain nuclear PDFs.
- More details in the next talk by E. Scomparin...



Quarkonia (1)

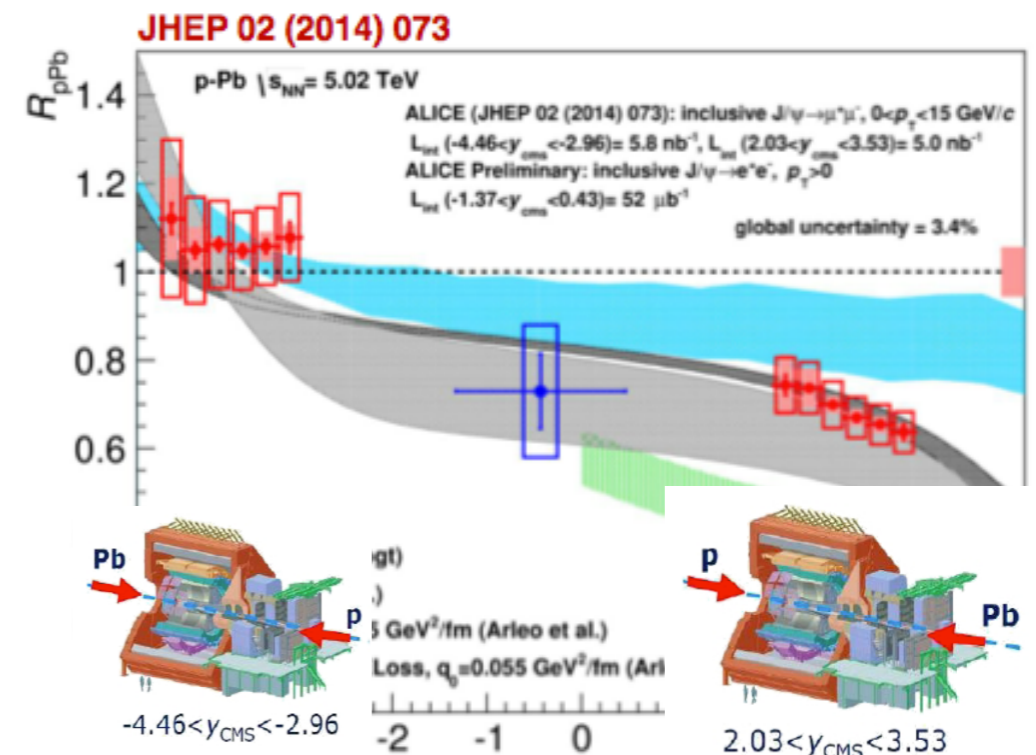
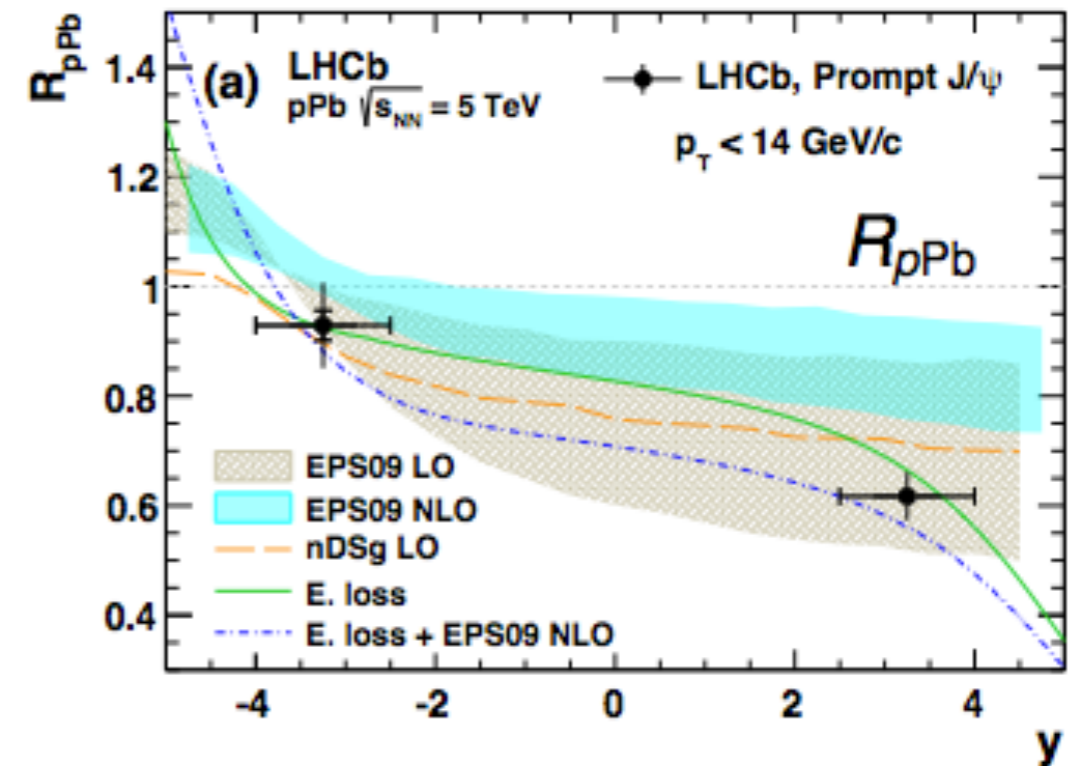
- In general, nuclear absorption effects are small at the LHC. Precision of the data allows for quantitative comparison with theory.
- Theoretical predictions based on nuclear shadowing (EPS09 + NLO) are in fair agreement with the J/ψ and data. Similarly for models including also partonic energy loss.
- Same picture for Y production.
- While models predict identical behavior for J/ψ and $\psi(2s)$, the data shows differences.
 - hint at final state effects
 - unexpected, because charmonia formation time is larger than $c\bar{c}$ crossing time in the nucleus
 - Suppression due to interaction with the (hadronic) medium created in the collision?



LLI-PREL-73492

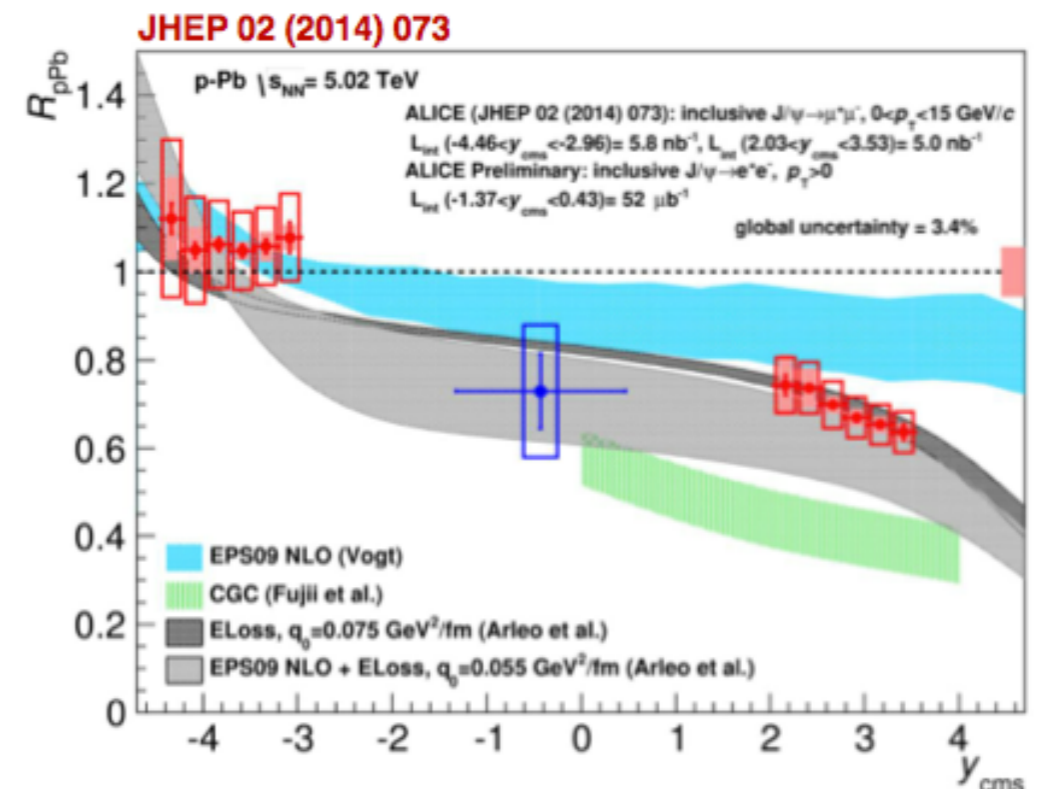
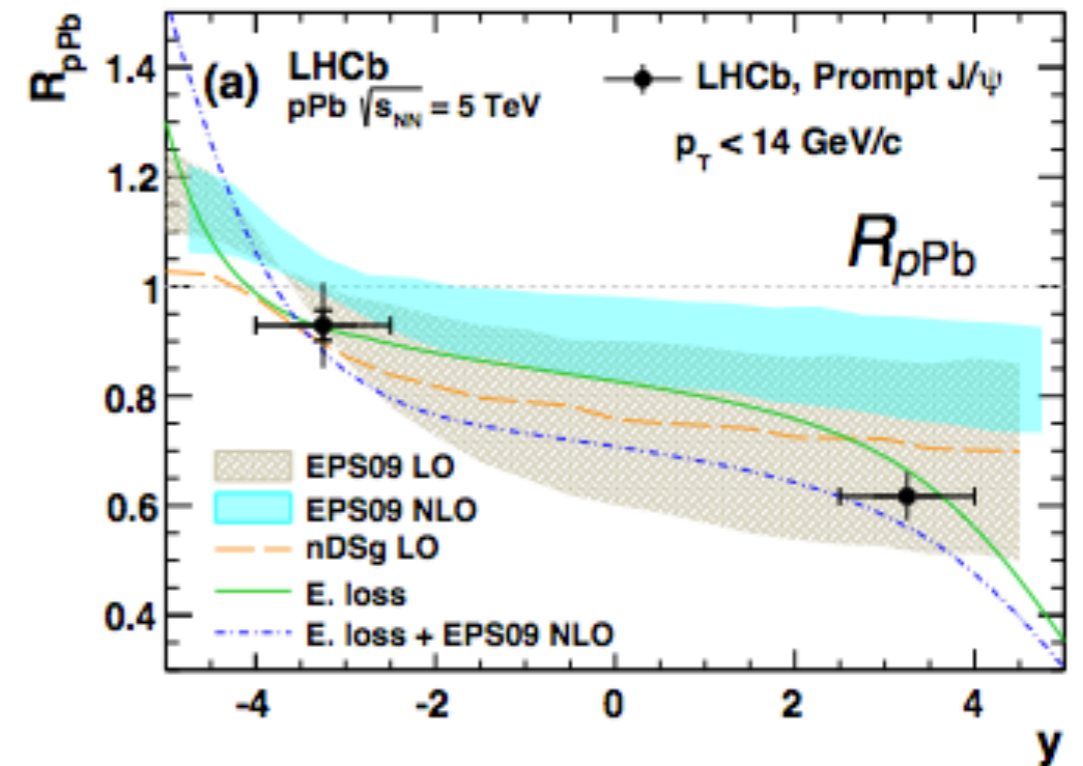
Quarkonia (1)

- In general, nuclear absorption effects are small at the LHC. Precision of the data allows for quantitative comparison with theory.
- Theoretical predictions based on nuclear shadowing (EPS09 + NLO) are in fair agreement with the J/ψ and data. Similarly for models including also partonic energy loss.
- Same picture for Y production.
- While models predict identical behavior for J/ψ and $\psi(2s)$, the data shows differences.
 - hint at final state effects
 - unexpected, because charmonia formation time is larger than $c\bar{c}$ crossing time in the nucleus
 - Suppression due to interaction with the (hadronic) medium created in the collision?



Quarkonia (1)

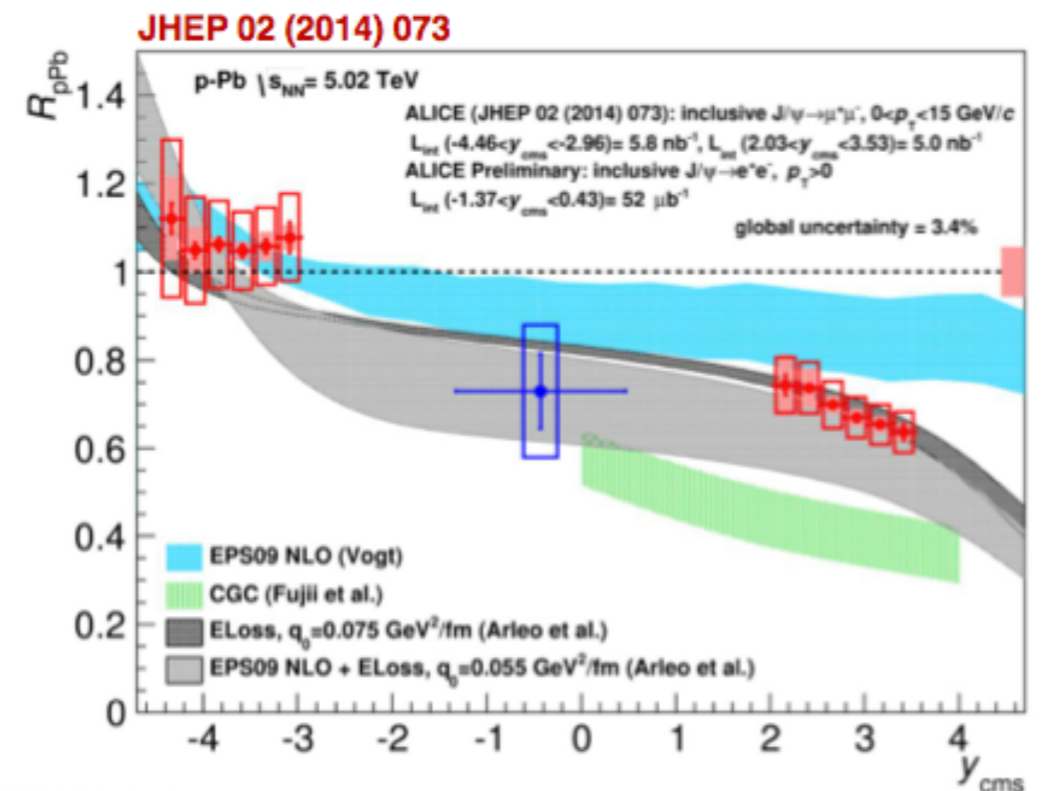
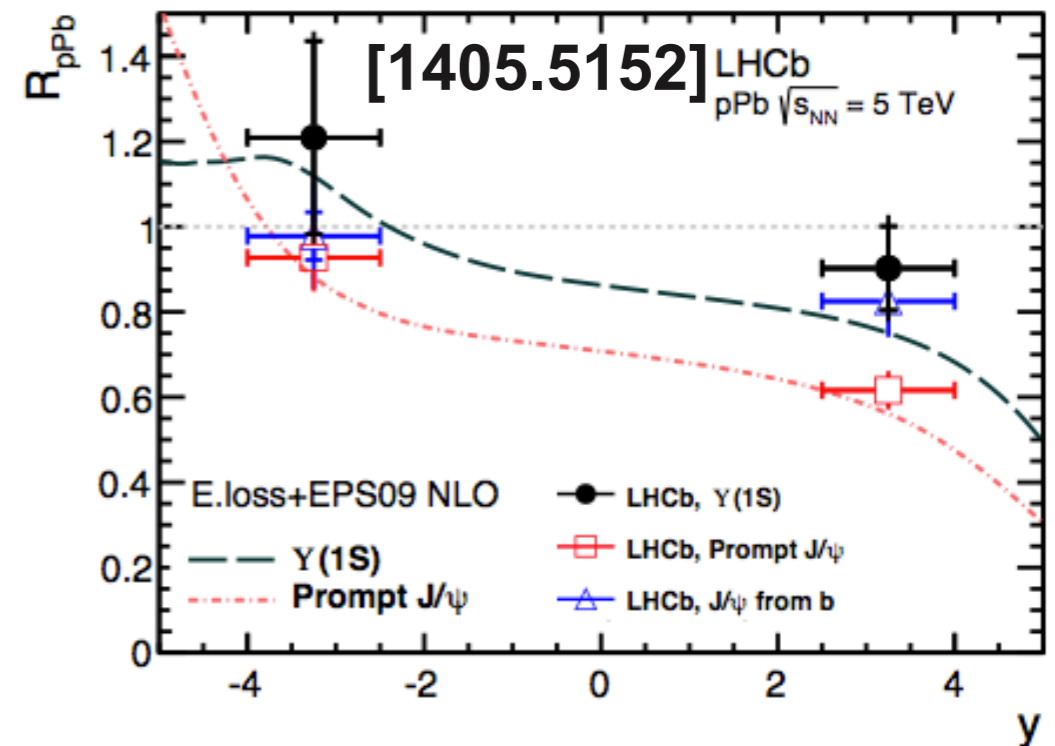
- In general, nuclear absorption effects are small at the LHC. Precision of the data allows for quantitative comparison with theory.
- Theoretical predictions based on nuclear shadowing (EPS09 + NLO) are in fair agreement with the J/ψ and data. Similarly for models including also partonic energy loss.
- Same picture for Y production.
- While models predict identical behavior for J/ψ and $\psi(2s)$, the data shows differences.
 - hint at final state effects
 - unexpected, because charmonia formation time is larger than $c\bar{c}$ crossing time in the nucleus
 - Suppression due to interaction with the (hadronic) medium created in the collision?



LLI-PREL-73492

Quarkonia (1)

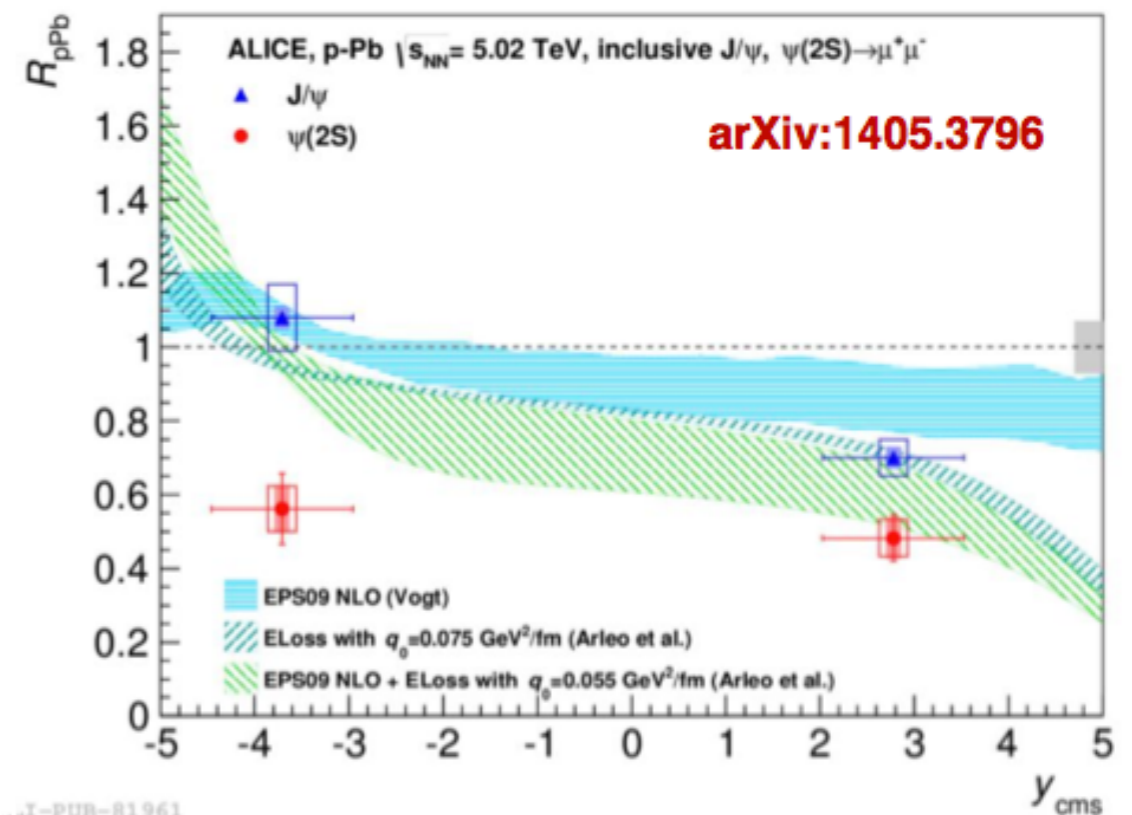
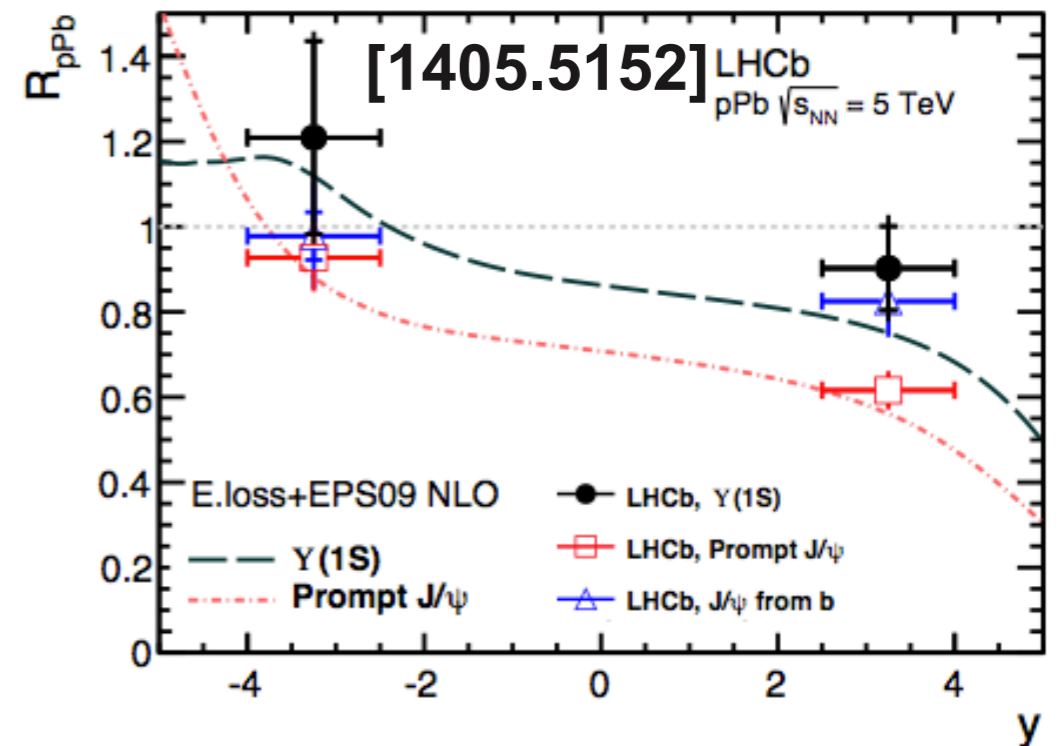
- In general, nuclear absorption effects are small at the LHC. Precision of the data allows for quantitative comparison with theory.
- Theoretical predictions based on nuclear shadowing (EPS09 + NLO) are in fair agreement with the J/ψ and data. Similarly for models including also partonic energy loss.
- Same picture for Y production.
- While models predict identical behavior for J/ψ and $\psi(2s)$, the data shows differences.
 - hint at final state effects
 - unexpected, because charmonia formation time is larger than $c\bar{c}$ crossing time in the nucleus
 - Suppression due to interaction with the (hadronic) medium created in the collision?



LLI-PREL-73492

Quarkonia (1)

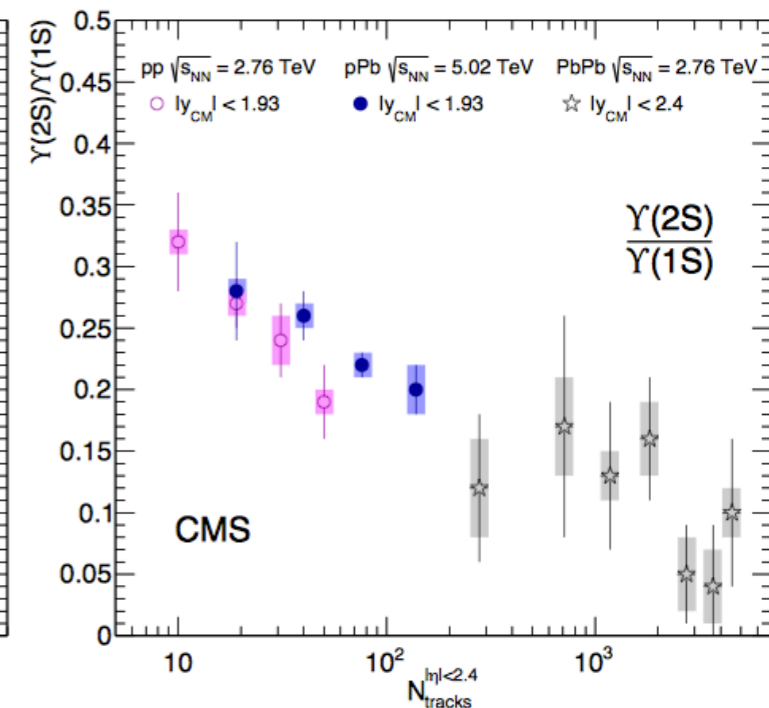
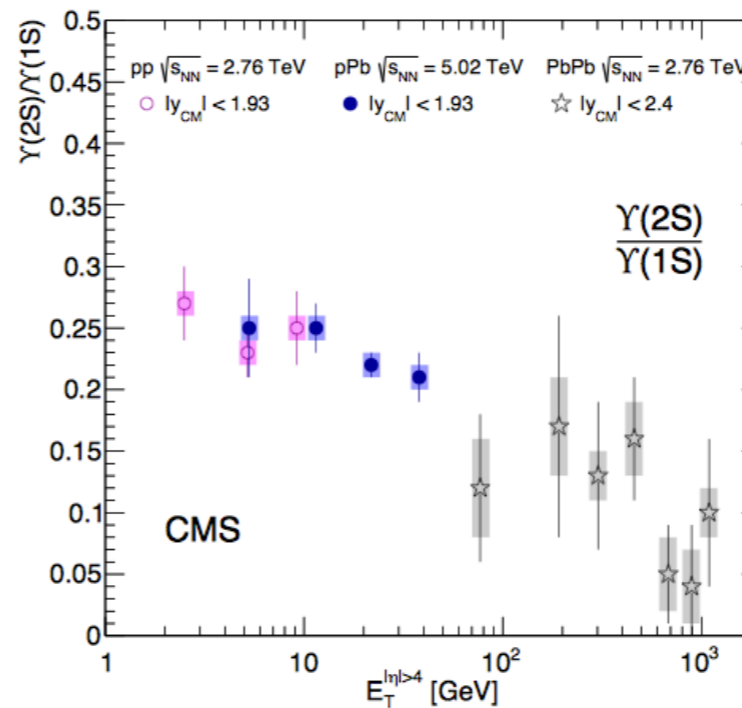
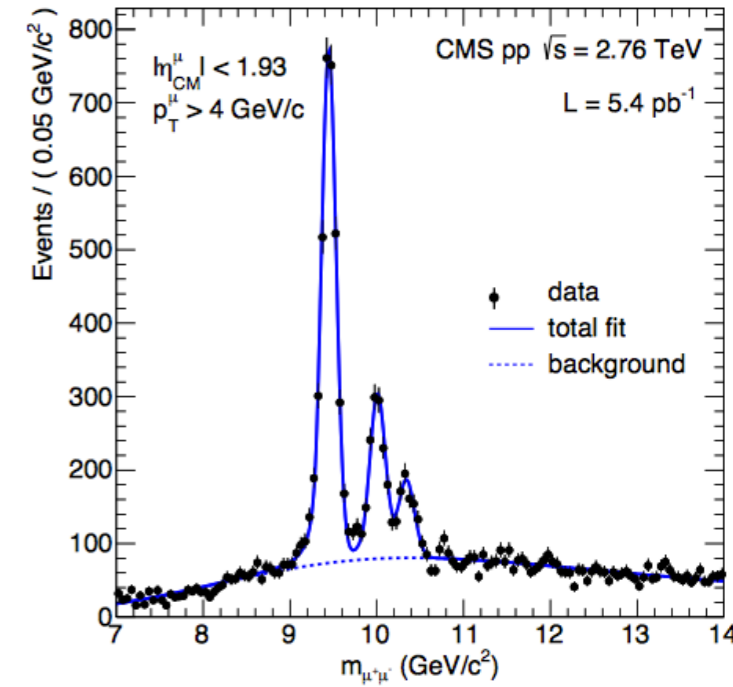
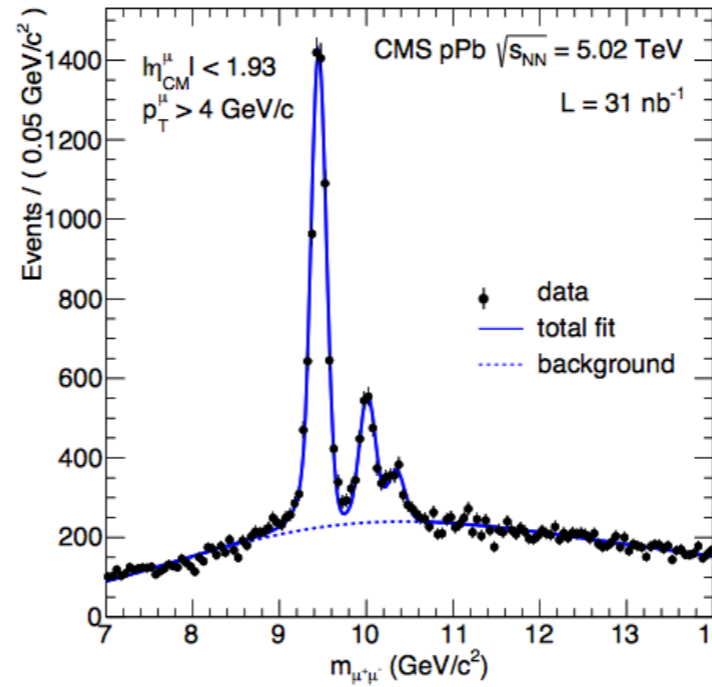
- In general, nuclear absorption effects are small at the LHC. Precision of the data allows for quantitative comparison with theory.
- Theoretical predictions based on nuclear shadowing (EPS09 + NLO) are in fair agreement with the J/ψ and data. Similarly for models including also partonic energy loss.
- Same picture for Y production.
- While models predict identical behavior for J/ψ and $\psi(2s)$, the data shows differences
 - hint at final state effects
 - unexpected, because charmonia formation time is larger than $c\bar{c}$ crossing time in the nucleus
 - Suppression due to interaction with the (hadronic) medium created in the collision?





Quarkonia (2)

- Excited Y states are less suppressed with respect to the ground states in min. bias p-Pb collisions than in Pb-Pb collisions.
- However, the suppression of excited states seems to vary with the event multiplicity (same in pp).
- It is an open question if excited states add multiplicity (event selection bias) or if the activity suppresses excited states (as in Pb-Pb collisions).

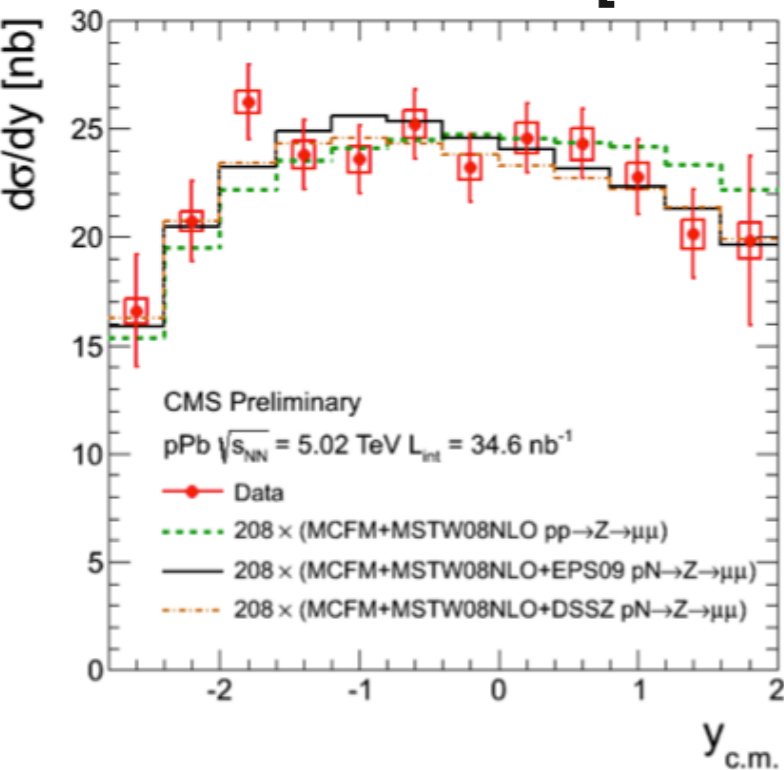


[1312.6300]

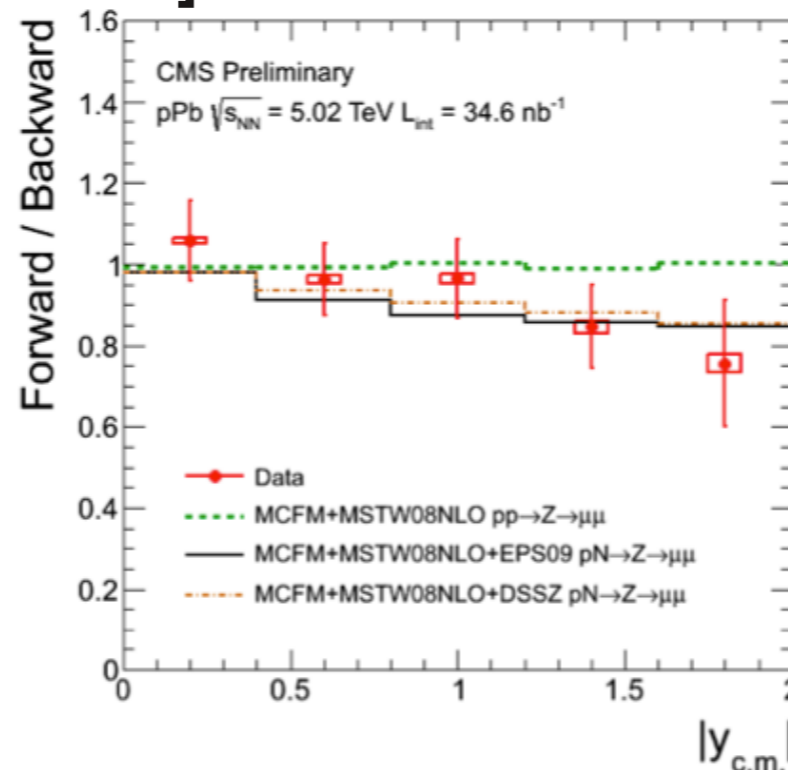
Z⁰ production in p-Pb collisions (1)

- New in the LHC energy regime... ≈ 2200 Z seen by CMS in $\mu^+\mu^-$ (similar for ATLAS). Also results from LHCb, but with much smaller statistics (≈ 15 candidates).
- Similar studies for W^+ and W^- (≈ 21000 $W \rightarrow \mu + \nu$, ≈ 16000 $W \rightarrow e + \nu$).
- Hints of forward-backward asymmetry might help to constrain nuclear PDFs...

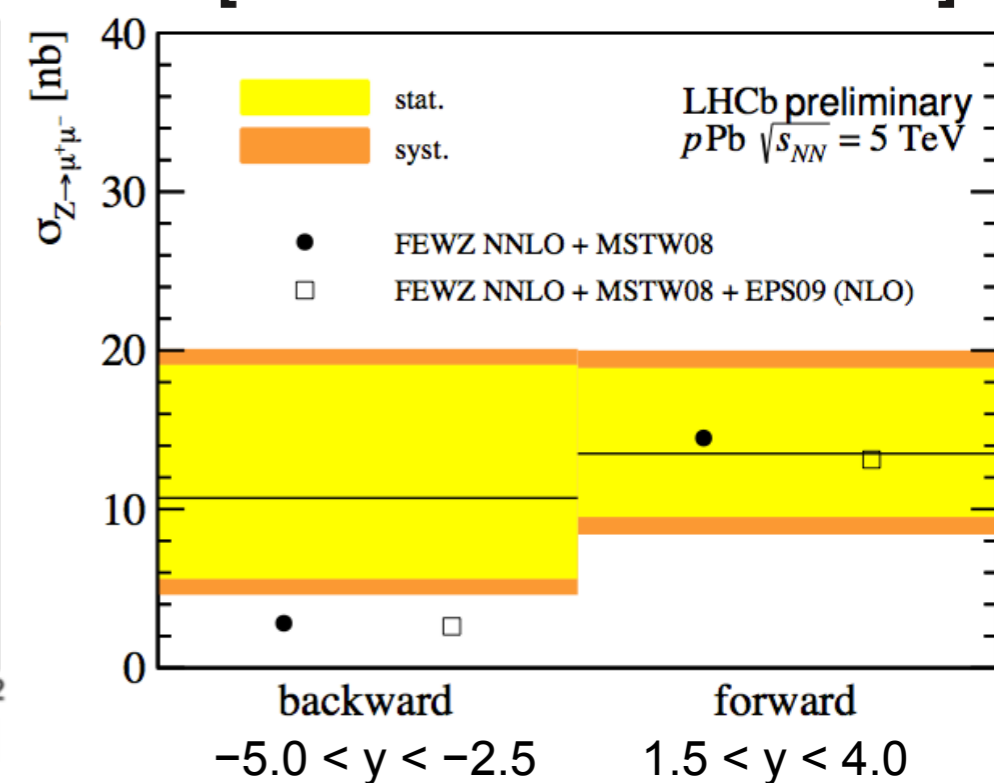
[CMS-HIN-14-003]



CMS



[LHCb-PAPER-2014-022]

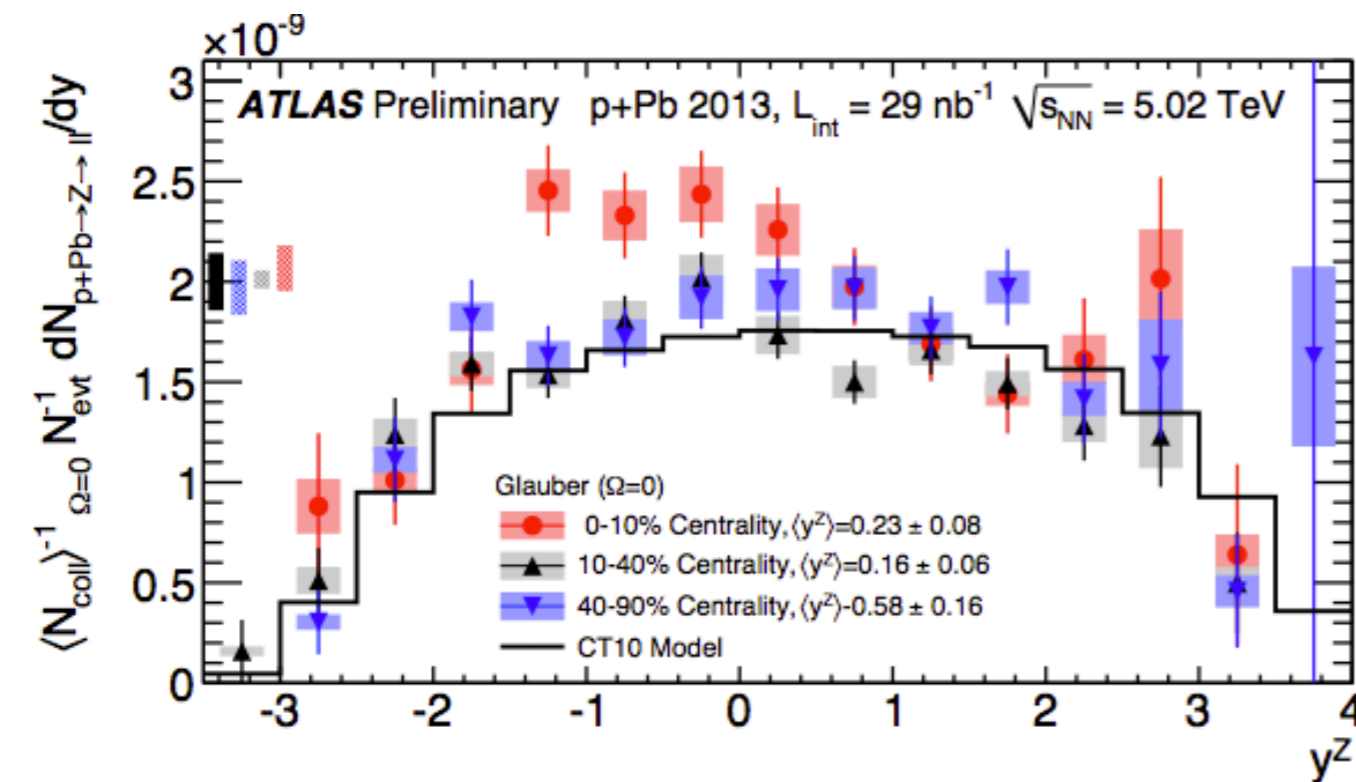


LHCb

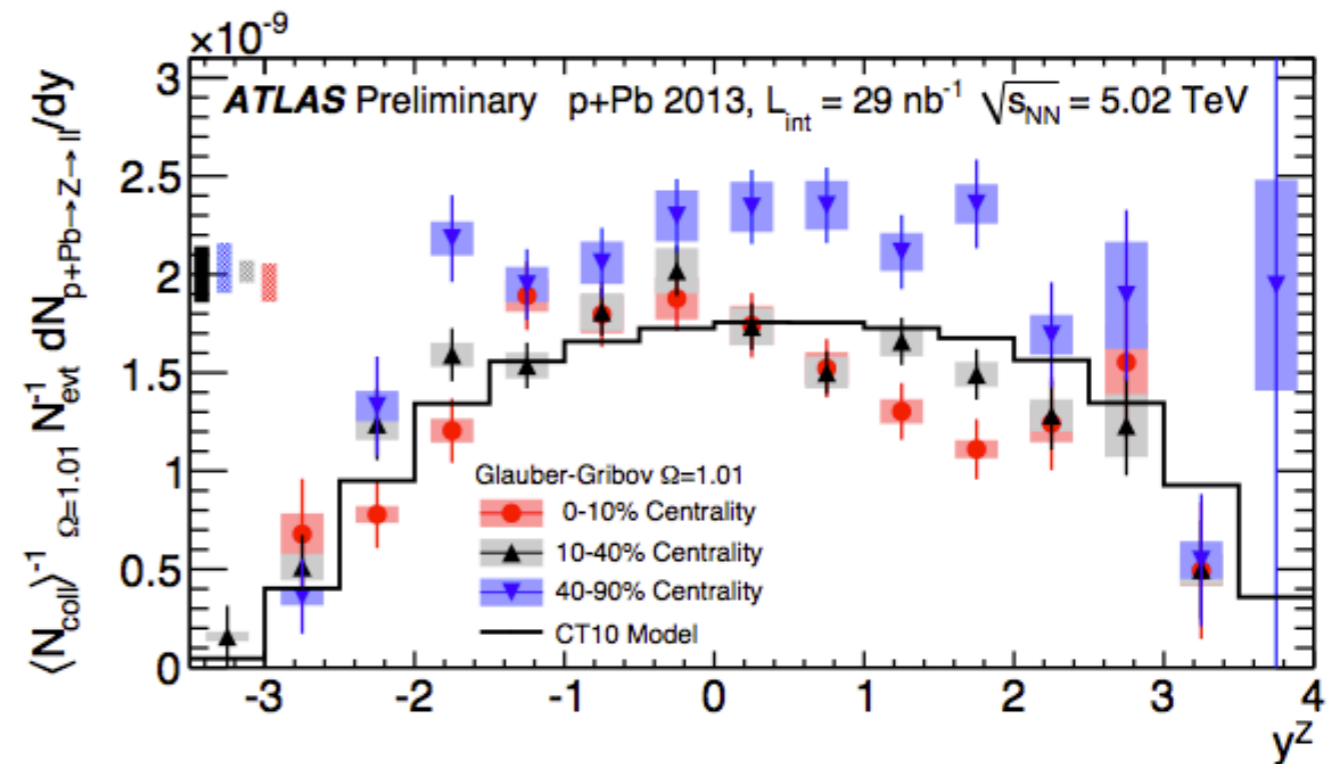
Z⁰ production in p-Pb collisions (2)

- Their production is expected to be unmodified by any medium effects and should just scale with the number of binary collisions.
- Therefore they can also help to constrain the centrality approaches.

Glauber



Glauber-Gribov



Summary and conclusion

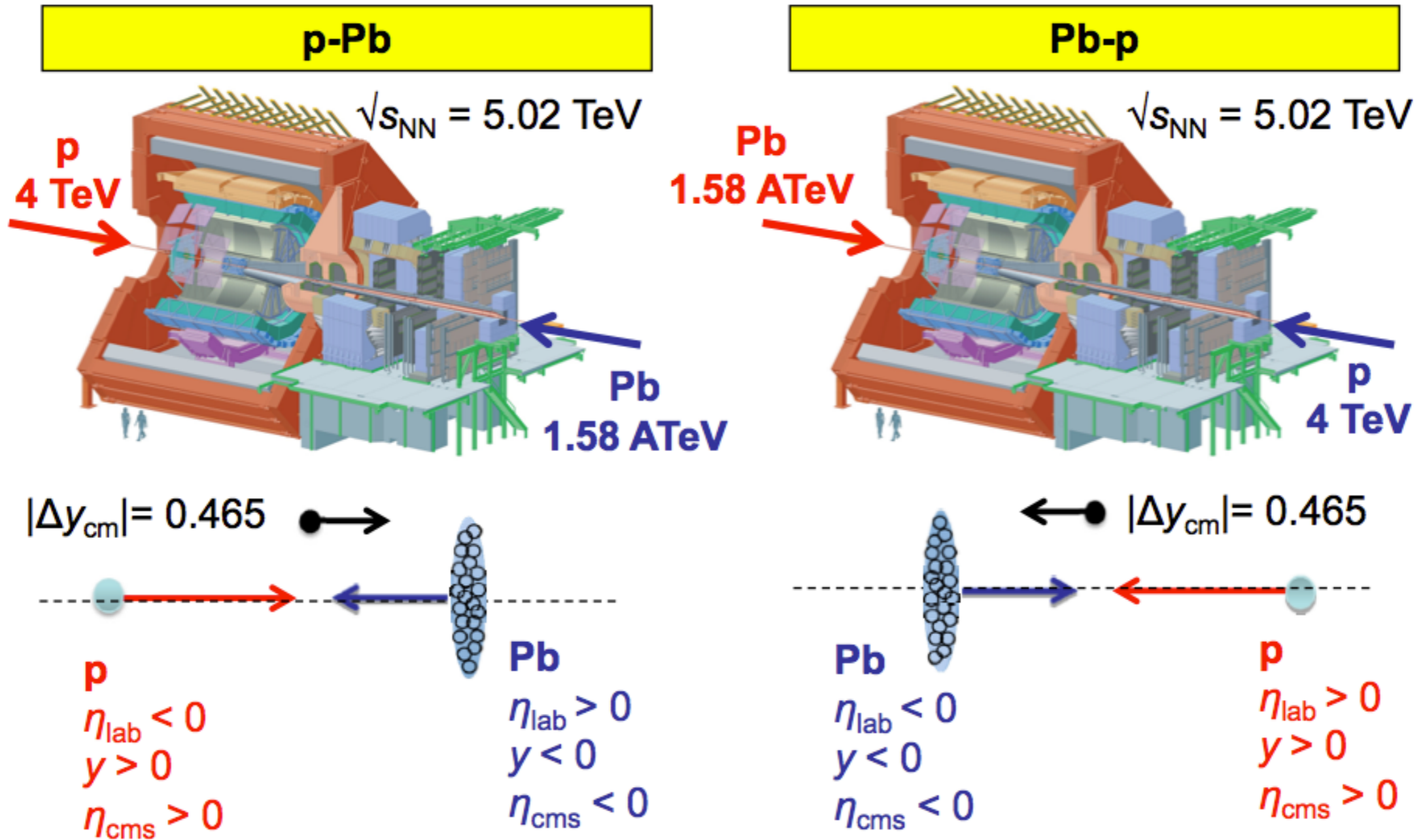


Summary and conclusion

- A lot of interesting physics results from this particular data set...
- Pb-Pb like features are observed for the bulk of the produced particles at **low p_T** : v_2 , radial flow, thermal fits..
- No indications of *quenching* at **high p_T** (charged hadrons, jets, open charm, heavy flavor, electrons, muons). However, CMS & ATLAS observe a yet unexplained *enhancement* at high p_T ...
- Quarkonia measurements provide an essential baseline for the understanding of the Pb-Pb results. Electroweak bosons can help to constrain nPDFs and centrality estimators.
- Very interesting times ahead of us...

Supporting slides

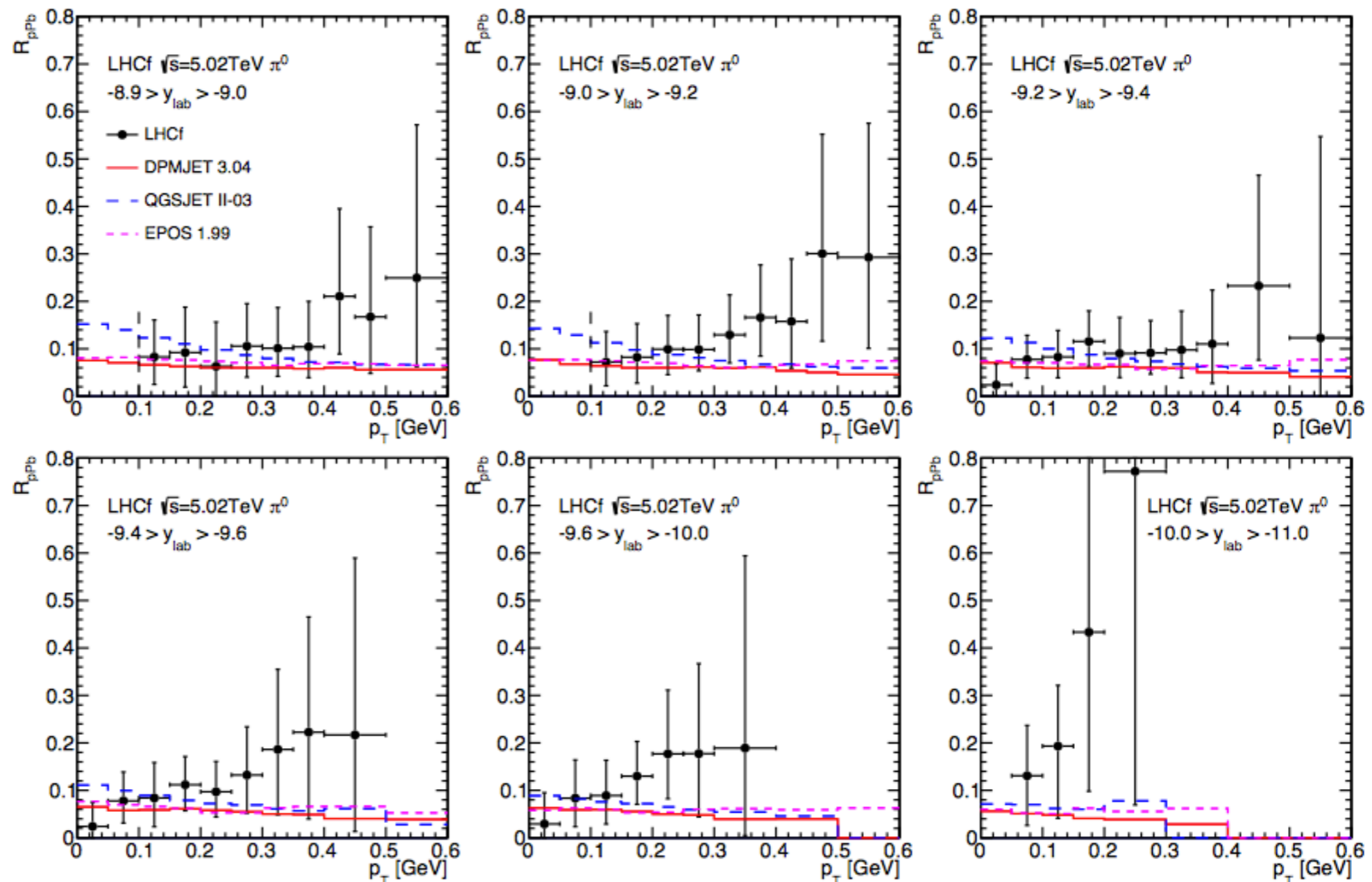
p-Pb collision geometry



the direction fo the proton is always at positive $y \equiv y_{cms}$ and positive η_{cms}

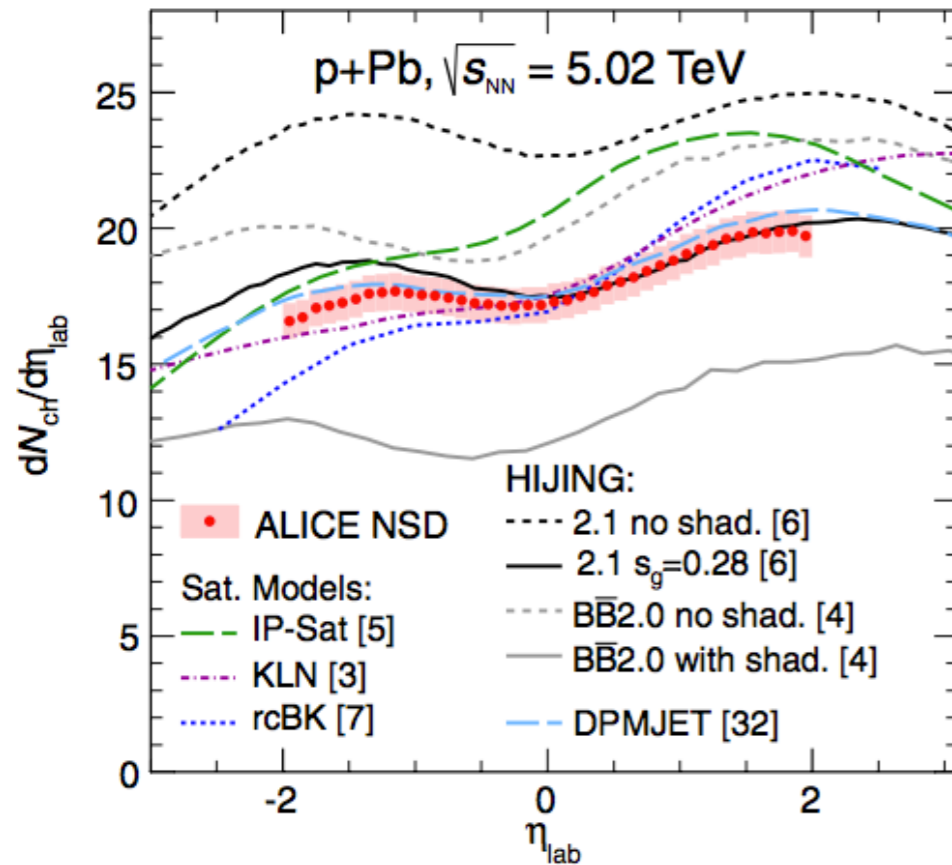
LHCf R_{pA} measurement

- R_{pA} measured at low p_T (< 0.6 GeV/c) and very forward ($y > 8.9$).
- Reproduced by models, helps to model nuclear effects in cosmic ray air showers.

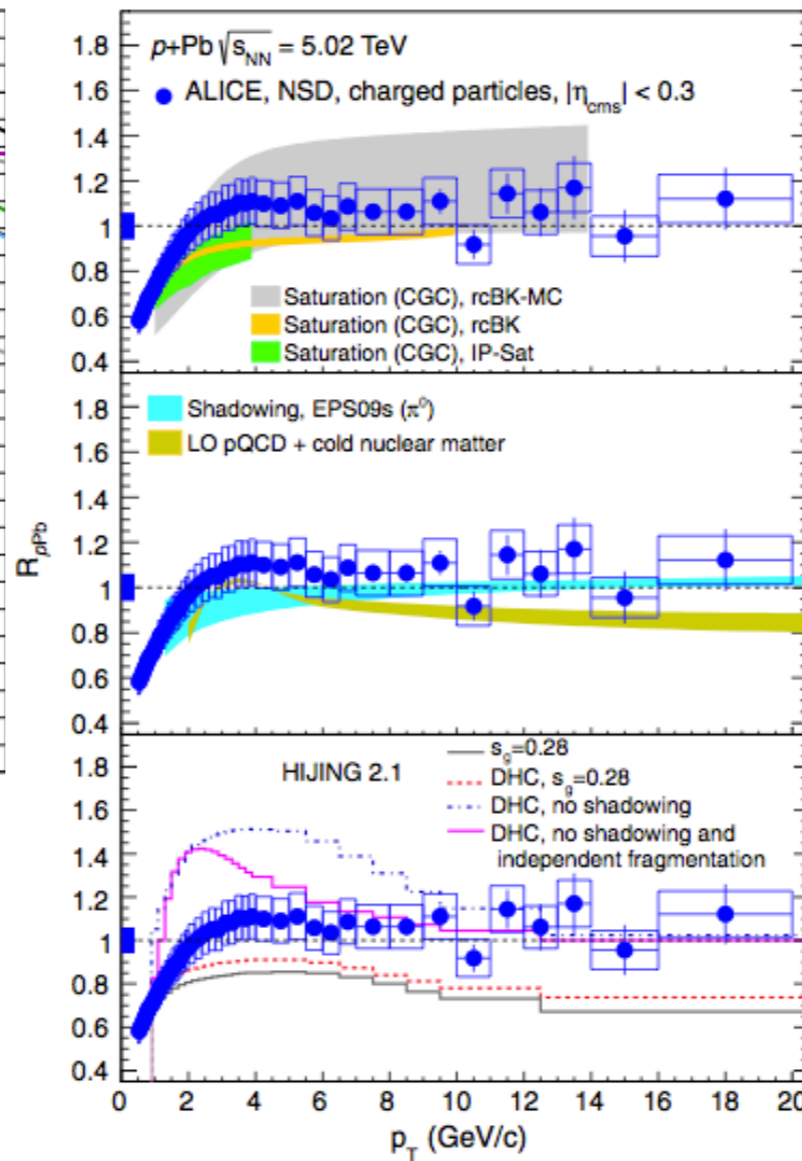


[1403.7845]

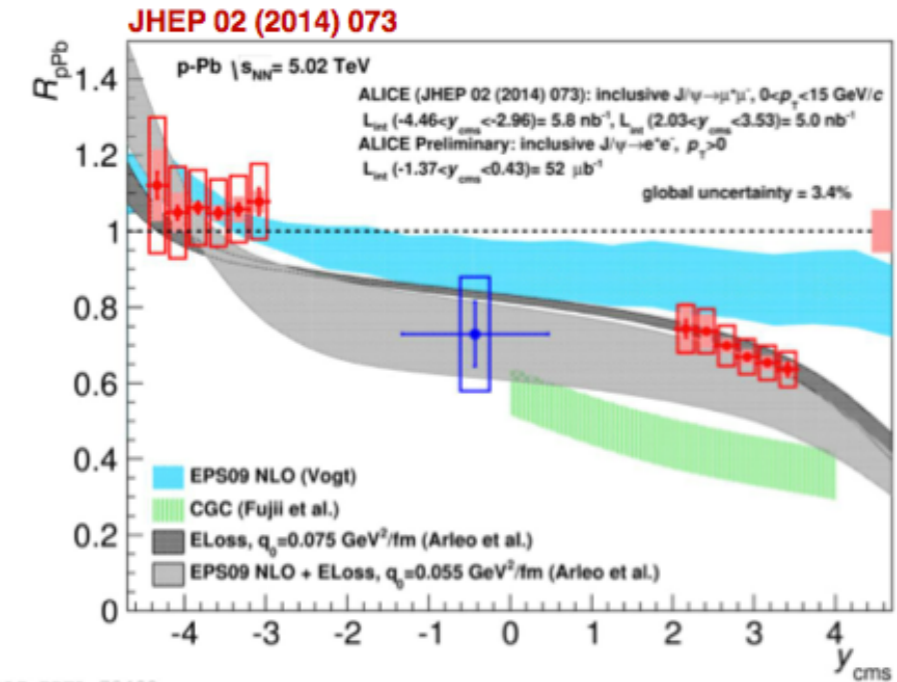
Comparisons with saturation models



[PRL 110, 032301 (2013)]



[PRL 110, 082302 (2013)]



LI-PREL-73492

Thermal model for heavy-ion collisions

- Starting point: grand-canonical partition function for an *relativistic ideal quantum gas of hadrons* of particle type i ($i = \text{pion, proton, ...} \rightarrow \text{full PDG!}$):

$$\ln Z_{GK_i} = \pm g_i \frac{V}{2\pi^2 \hbar^3} \int_0^\infty dp p^2 \ln (1 \pm e^{-\beta(\epsilon(p) - \mu_i)})$$

$$n = \frac{1}{V} \frac{\partial(T \ln Z)}{\partial \mu} \quad P = \frac{\partial(T \ln Z)}{\partial V} \quad s = \frac{1}{V} \frac{\partial(T \ln Z)}{\partial T}$$



Thermal model for heavy-ion collisions

- Starting point: grand-canonical partition function for an *relativistic ideal quantum gas of hadrons* of particle type i ($i = \text{pion, proton, ...} \rightarrow \text{full PDG!}$):

$$\ln Z_{GK_i} = \pm g_i \frac{V}{2\pi^2 \hbar^3} \int_0^\infty dp p^2 \ln (1 \pm e^{-\beta(\epsilon(p) - \mu_i)})$$

$\beta = \frac{1}{kT}$


$$n = \frac{1}{V} \frac{\partial(T \ln Z)}{\partial \mu} \quad P = \frac{\partial(T \ln Z)}{\partial V} \quad s = \frac{1}{V} \frac{\partial(T \ln Z)}{\partial T}$$

Thermal model for heavy-ion collisions

- Starting point: grand-canonical partition function for an *relativistic ideal quantum gas of hadrons* of particle type i ($i = \text{pion, proton, ...} \rightarrow \text{full PDG!}$):

(-) for bosons, (+) for fermions
(quantum gas)

$$\ln Z_{GK_i} = \pm g_i \frac{V}{2\pi^2 \hbar^3} \int_0^\infty dp p^2 \ln (1 \pm e^{-\beta(\epsilon(p) - \mu_i)})$$

$\beta = \frac{1}{kT}$ 

$$n = \frac{1}{V} \frac{\partial(T \ln Z)}{\partial \mu} \quad P = \frac{\partial(T \ln Z)}{\partial V} \quad s = \frac{1}{V} \frac{\partial(T \ln Z)}{\partial T}$$

Thermal model for heavy-ion collisions

- Starting point: grand-canonical partition function for an *relativistic ideal quantum gas of hadrons* of particle type i ($i = \text{pion, proton, ...} \rightarrow \text{full PDG!}$):

(-) for bosons, (+) for fermions
(quantum gas)

$$\ln Z_{GK_i} = \pm g_i \frac{V}{2\pi^2 \hbar^3} \int_0^\infty dp p^2 \ln (1 \pm e^{-\beta(\epsilon(p) - \mu_i)})$$

spin
degeneracy

$$\beta = \frac{1}{kT}$$

$$n = \frac{1}{V} \frac{\partial(T \ln Z)}{\partial \mu} \quad P = \frac{\partial(T \ln Z)}{\partial V} \quad s = \frac{1}{V} \frac{\partial(T \ln Z)}{\partial T}$$

Thermal model for heavy-ion collisions

- Starting point: grand-canonical partition function for an *relativistic ideal quantum gas of hadrons* of particle type i ($i = \text{pion, proton, ...} \rightarrow \text{full PDG!}$):

(-) for bosons, (+) for fermions
(quantum gas)

$$\ln Z_{GK_i} = \pm g_i \frac{V}{2\pi^2 \hbar^3} \int_0^\infty dp p^2 \ln (1 \pm e^{-\beta(\epsilon(p) - \mu_i)})$$

spin degeneracy \nearrow

$\beta = \frac{1}{kT}$ \searrow

$E_i = \sqrt{p^2 + m_i^2}$ \nwarrow dispersion relation (relativistic)

$$n = \frac{1}{V} \frac{\partial(T \ln Z)}{\partial \mu} \quad P = \frac{\partial(T \ln Z)}{\partial V} \quad s = \frac{1}{V} \frac{\partial(T \ln Z)}{\partial T}$$

Thermal model for heavy-ion collisions

- Starting point: grand-canonical partition function for an *relativistic ideal quantum gas of hadrons* of particle type i ($i = \text{pion, proton, ...} \rightarrow \text{full PDG!}$):

(-) for bosons, (+) for fermions
(quantum gas)

$$\ln Z_{GK_i} = \pm g_i \frac{V}{2\pi^2 \hbar^3} \int_0^\infty dp p^2 \ln (1 \pm e^{-\beta(\epsilon(p) - \mu_i)})$$

spin degeneracy \rightarrow g_i

$\beta = \frac{1}{kT}$ \rightarrow β

$E_i = \sqrt{p^2 + m_i^2}$ dispersion relation (relativistic) \rightarrow $\epsilon(p)$

$\mu_i = \mu_B B_i + \mu_S S_i + \mu_{I_3} I_{3_i} + \mu_C C_i$
chemical potential representing each conserved quantity \rightarrow μ_i

$$n = \frac{1}{V} \frac{\partial(T \ln Z)}{\partial \mu} \quad P = \frac{\partial(T \ln Z)}{\partial V} \quad s = \frac{1}{V} \frac{\partial(T \ln Z)}{\partial T}$$

Thermal model for heavy-ion collisions

- Starting point: grand-canonical partition function for an *relativistic ideal quantum gas of hadrons* of particle type i ($i = \text{pion, proton, ...} \rightarrow \text{full PDG!}$):

(-) for bosons, (+) for fermions
(quantum gas)

$$\ln Z_{GK_i} = \pm g_i \frac{V}{2\pi^2 \hbar^3} \int_0^\infty dp p^2 \ln (1 \pm e^{-\beta(\epsilon(p) - \mu_i)})$$

spin degeneracy

$\beta = \frac{1}{kT}$

$E_i = \sqrt{p^2 + m_i^2}$ dispersion relation (relativistic)

$\mu_i = \mu_B B_i + \mu_S S_i + \mu_{I_3} I_{3_i} + \mu_C C_i$
chemical potential representing each conserved quantity

$$n = \frac{1}{V} \frac{\partial(T \ln Z)}{\partial \mu} \quad P = \frac{\partial(T \ln Z)}{\partial V} \quad s = \frac{1}{V} \frac{\partial(T \ln Z)}{\partial T}$$

Only two free parameters are needed: (T, μ_B) . Volume cancels if particle ratios n_i/n_j are calculated. If yields are fitted, it acts as the third free parameter.

Thermal model for heavy-ion collisions

- Starting point: grand-canonical partition function for an *relativistic ideal quantum gas of hadrons* of particle type i ($i = \text{pion, proton, ...} \rightarrow \text{full PDG!}$):

(-) for bosons, (+) for fermions
(quantum gas)

$$\ln Z_{GK_i} = \pm g_i \frac{V}{2\pi^2 \hbar^3} \int_0^\infty dp p^2 \ln (1 \pm e^{-\beta(\epsilon(p) - \mu_i)})$$

spin degeneracy

$\beta = \frac{1}{kT}$

$E_i = \sqrt{p^2 + m_i^2}$ dispersion relation (relativistic)

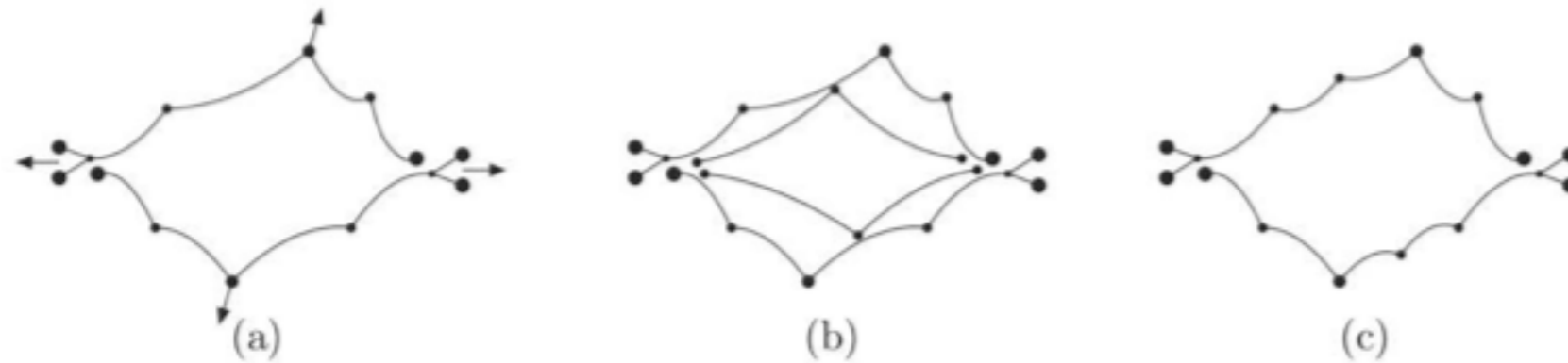
$\mu_i = \mu_B B_i + \mu_S S_i + \mu_{I_3} I_{3i} + \mu_C C_i$
chemical potential representing each conserved quantity

$$n = \frac{1}{V} \frac{\partial(T \ln Z)}{\partial \mu} \quad P = \frac{\partial(T \ln Z)}{\partial V} \quad s = \frac{1}{V} \frac{\partial(T \ln Z)}{\partial T}$$

Only two free parameters are needed: (T, μ_B) . Volume cancels if particle ratios n_i/n_j are calculated. If yields are fitted, it acts as the third free parameter.

Partition function shown here is only valid in the resonance gas limit (HRG), i.e. relevant interactions are mediated via resonances, and thus the non-interacting hadron resonance gas can be used as a good approximation for an interacting hadron gas.

Color reconnection

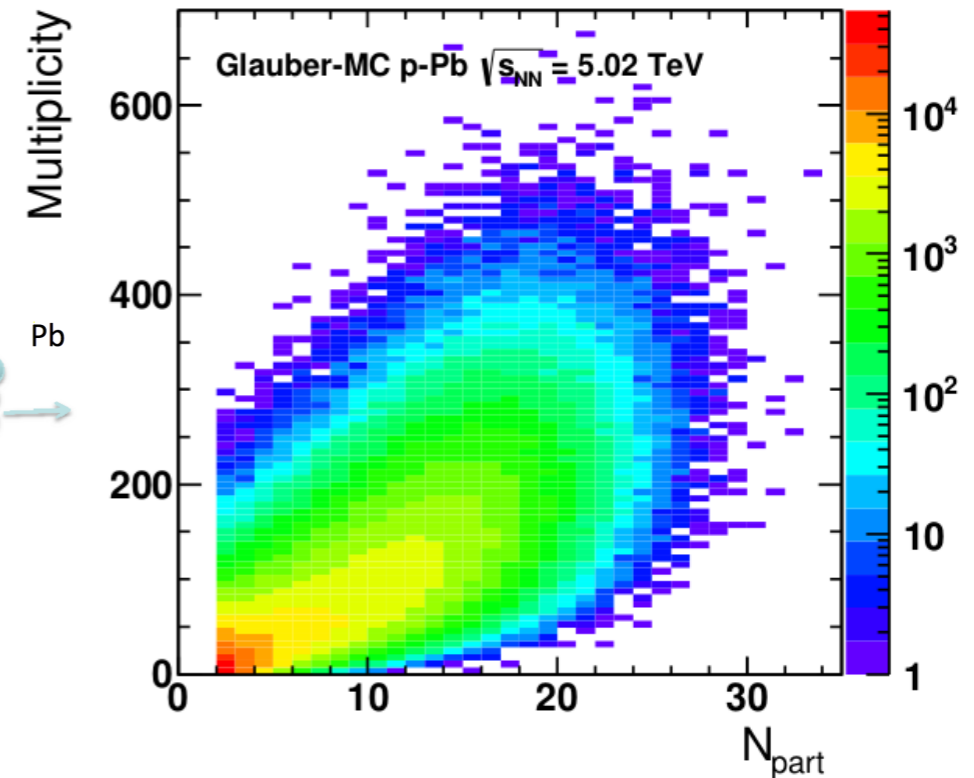
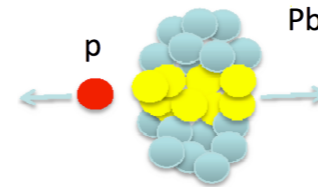


See also: A. Ortiz et al. Phys. Rev. Lett. 111, 042001 (2013)

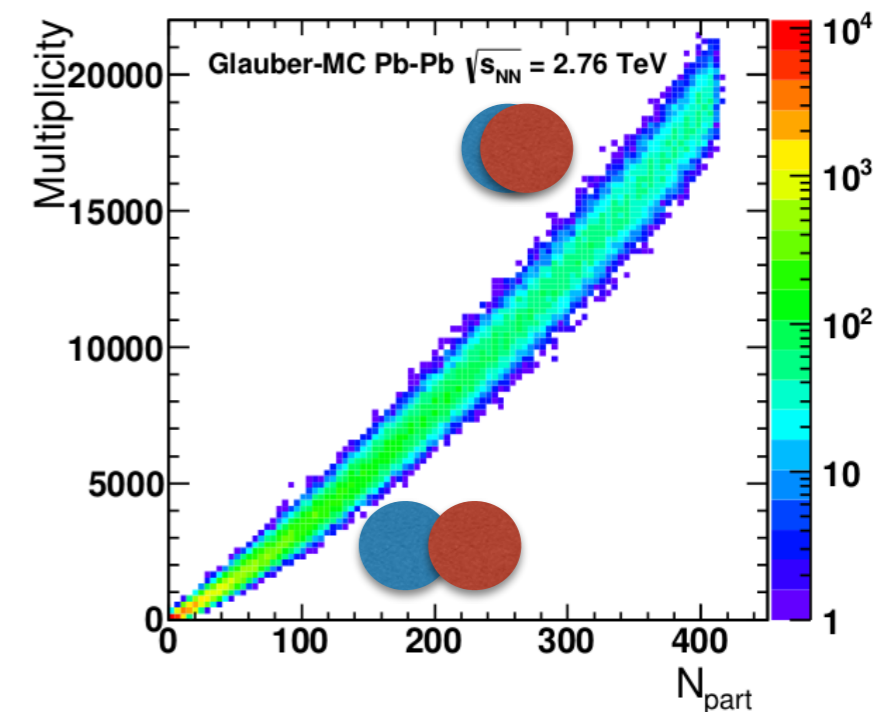
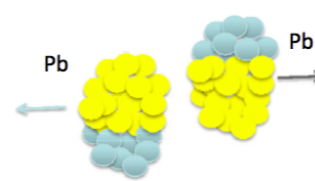
Centrality

Centrality — Introduction

- In contrast to Pb-Pb collisions, it is not straightforward to relate experimental quantities to the collision geometry, i.e. the number of participants N_{part} and binary collisions N_{coll} .
→ in p-Pb collisions: $N_{\text{coll}} = N_{\text{part}} - 1$



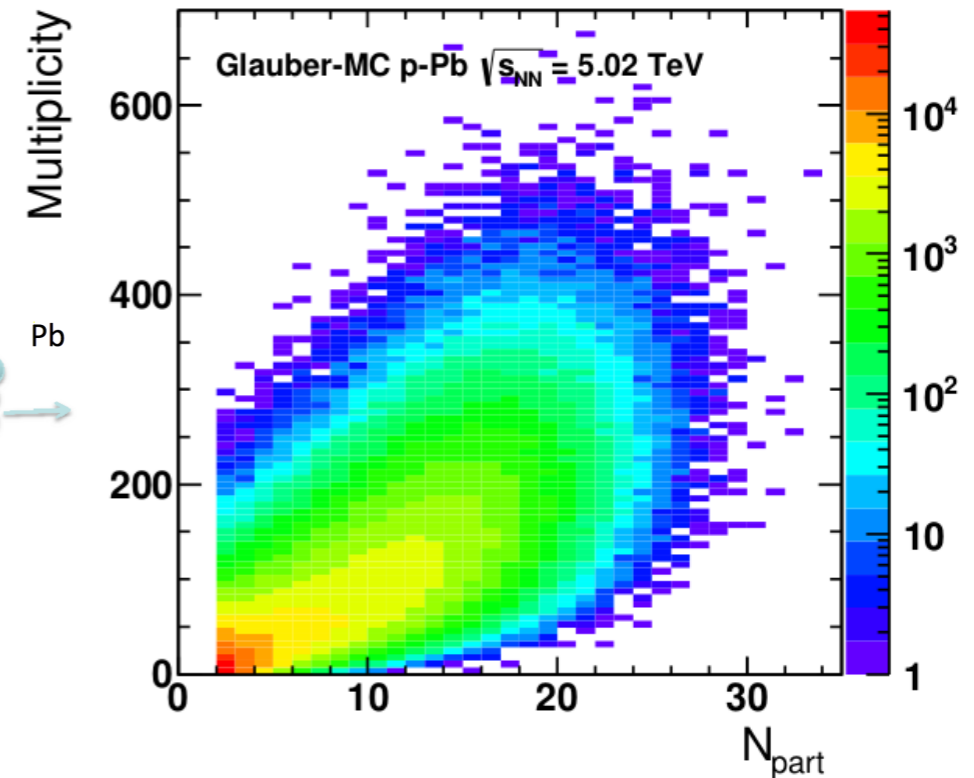
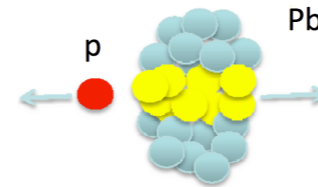
- Large biases present in the system:
 - Multiplicity fluctuations
 - Jet-veto bias
 - Geometric bias
- Most simple approach: only multiplicity classes instead of centrality, but more can be done...



Centrality — Introduction

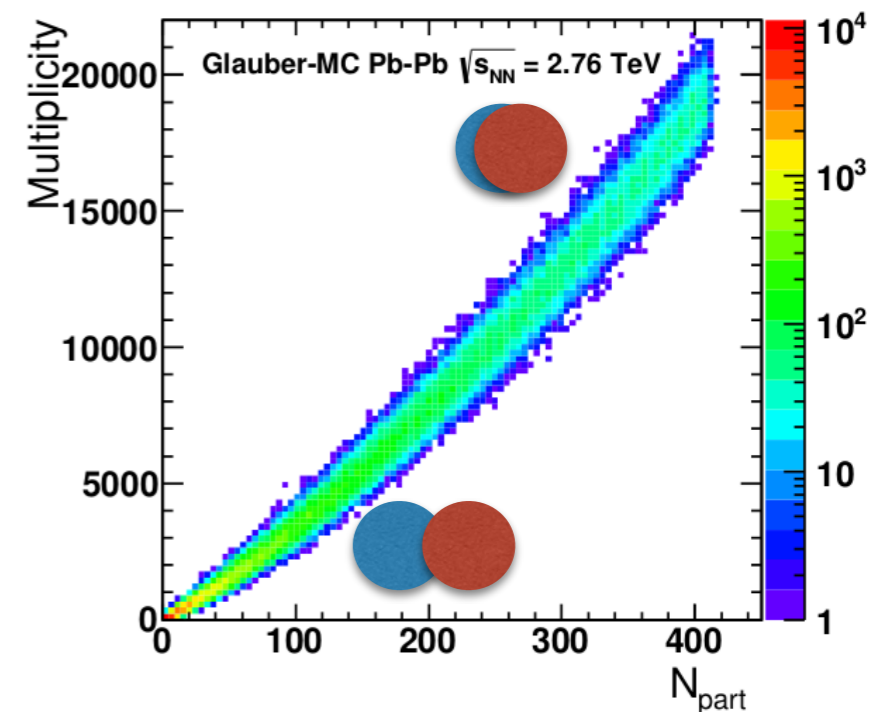
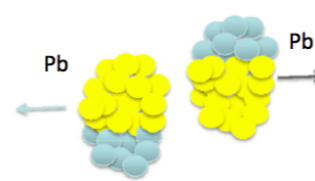
- In contrast to Pb-Pb collisions, it is not straightforward to relate experimental quantities to the collision geometry, i.e. the number of participants N_{part} and binary collisions N_{coll} .

→ in p-Pb collisions: $N_{\text{coll}} = N_{\text{part}} - 1$



- Large biases present in the system:

- Multiplicity fluctuations
- Jet-veto bias
- Geometric bias



- Most simple approach: only multiplicity classes instead of centrality, but more can be done...

Different experiments employ different approaches in order to deal with biases. One needs to be careful in comparisons.

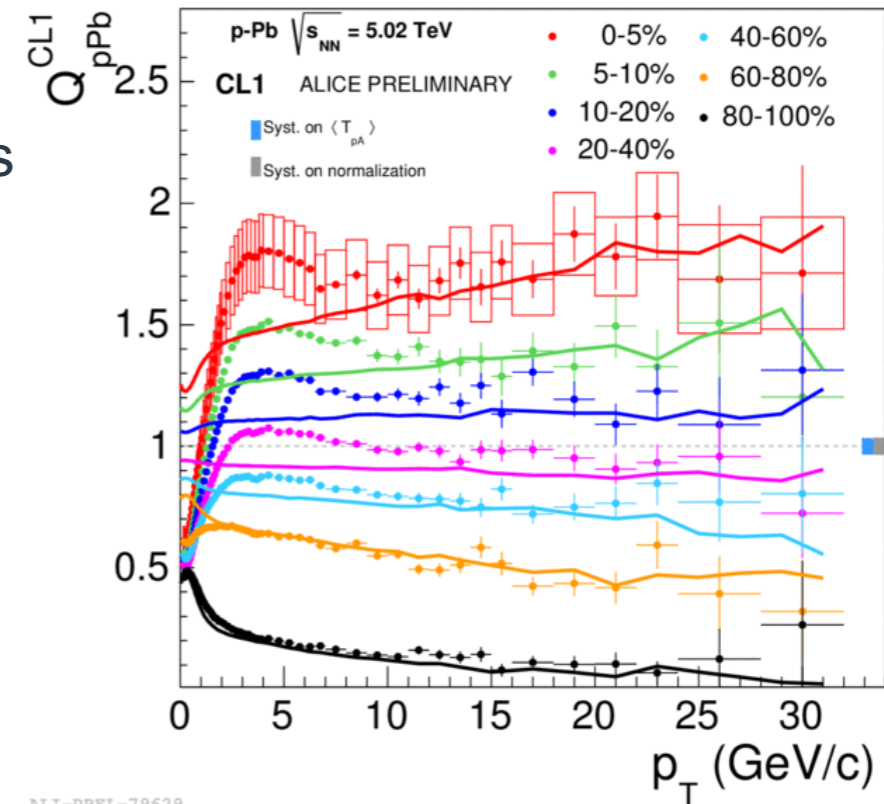
Centrality — ALICE

- Standard Glauber fit+event selection (a la AA) leads to results which depends on the η -region of the centrality estimator.
- Example Q_{pA} (not called R_{pA} , because collision geometry is not properly reflected):

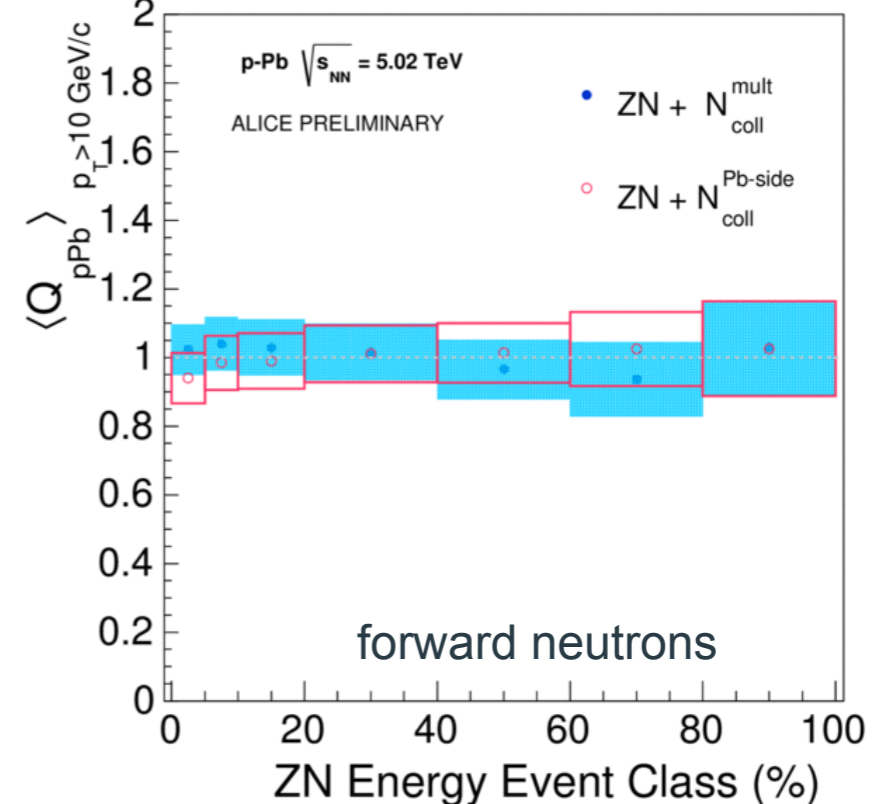
$$Q_{pA}^i = \frac{dN_{pA} / dp_T}{\langle N_{coll} \rangle_i dN_{pp} / dp_T}$$

- Forward neutrons (measured in Zero Degree calorimeter) cause no selection bias on mid-rapidity bulk production
-> used to bin events in classes
- Determine N_{coll}/N_{part} by assuming one out of:
 - Mid-rapidity $dN_{ch}/d\eta \sim N_{part}$
 - Forward $dN_{ch}/d\eta \sim N_{part}^{Pb} = N_{part} - 1$
 - High p_T yield $\sim N_{coll}$
- Methods reach consistent results:
 - N_{coll} consistent within 5-10%
 - High p_T Q_{pA} flat ($> 10\text{GeV}/c$)

Standard Glauber fit+event selection



ALI-PREL-79629



ALI-PREL-80800

Centrality — ATLAS

- A different approach is used:
 - The underlying model is changed from a Glauber model to a Glauber-Gribov.
 - NN cross-section is subject to quantum fluctuations in the proton configuration (controlled by fluctuation parameter Ω).
 - Model can be constrained by pp diffraction data.

